What can continuum QCD tell us about heavy ion collisions and the hadron spectrum?

Jan M. Pawlowski

Universität Heidelberg & ExtreMe Matter Institute

GSI, April 15^{th} 2015

Outline

- Vacuum QCD & the hadron spectrum

- Phase structure of QCD

- Spectral Functions & Transport Coefficients

- Outlook

Continuum Methods for QCD

quark-gluon correlations

$$\langle q(x_1)\cdots\bar{q}(x_{2n})\,A_\mu(y_1)\cdots A_\mu(y_m)\rangle$$

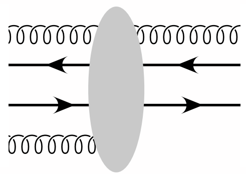

functional relations

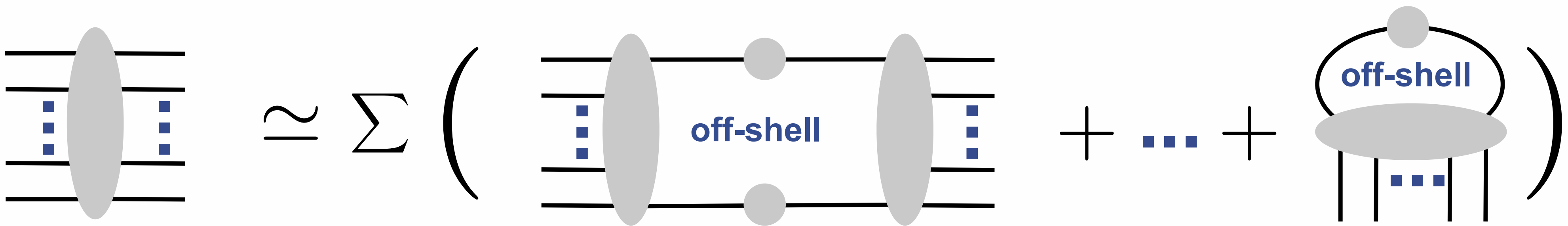

scattering amplitude/
vertex functions

Continuum Methods for QCD

quark-gluon-hadron correlations

$$\langle q(x_1)\cdots \bar{q}(x_{2n})\, A_\mu(y_1)\cdots A_\mu(y_m)\, h(z_1)\cdots h(z_l)\rangle$$

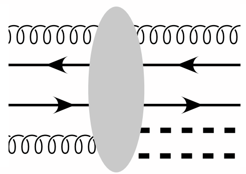

functional relations

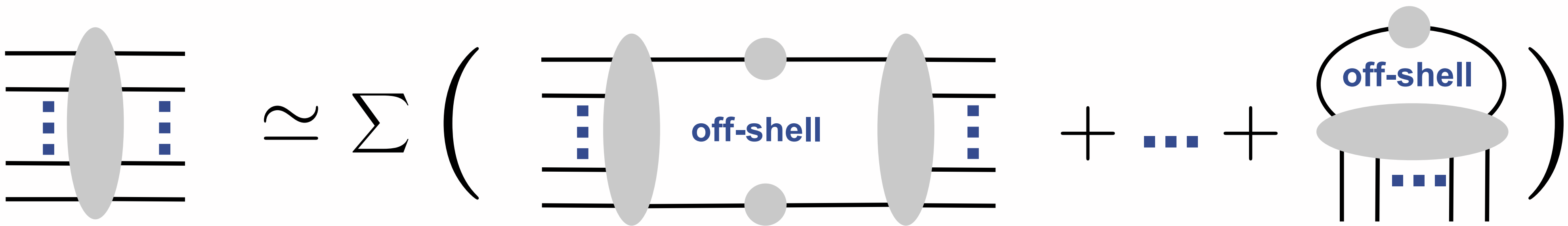

scattering amplitude/
vertex functions

Functional renormalisation group equations

Dyson-Schwinger equations

2PI/nPI hierarchies

Bethe-Salpeter equations

⋮

Continuum Methods for QCD

quark-gluon-hadron correlations

$$\langle q(x_1)\cdots\bar{q}(x_{2n})\,A_\mu(y_1)\cdots A_\mu(y_m)\,h(z_1)\cdots h(z_l)\rangle$$

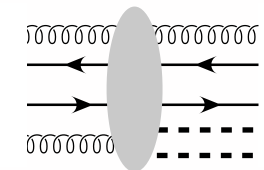

functional relations

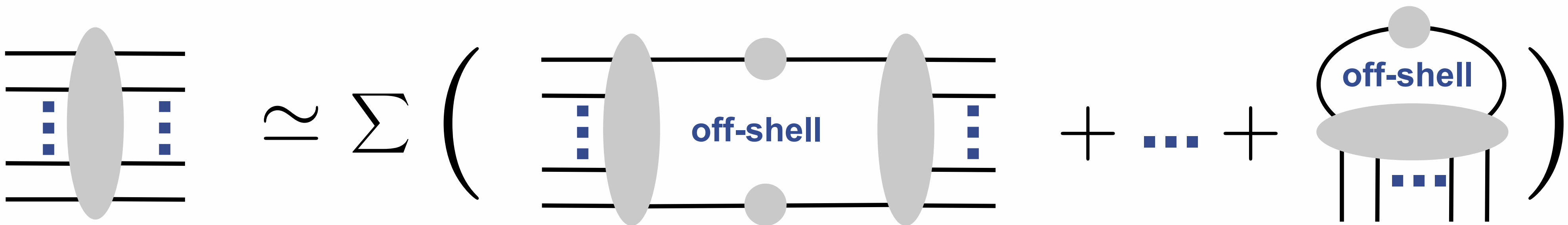

scattering amplitude/
vertex functions

properties

- access to physics mechanisms
- numerically tractable
  no sign problem
  systematic error control via closed form
- low energy models naturally encorporated

Continuum Methods for QCD

quark-gluon-hadron correlations

$$\langle q(x_1) \cdots \bar{q}(x_{2n})\, A_\mu(y_1) \cdots A_\mu(y_m)\, h(z_1) \cdots h(z_l) \rangle$$

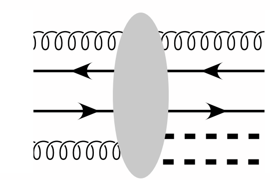

functional relations

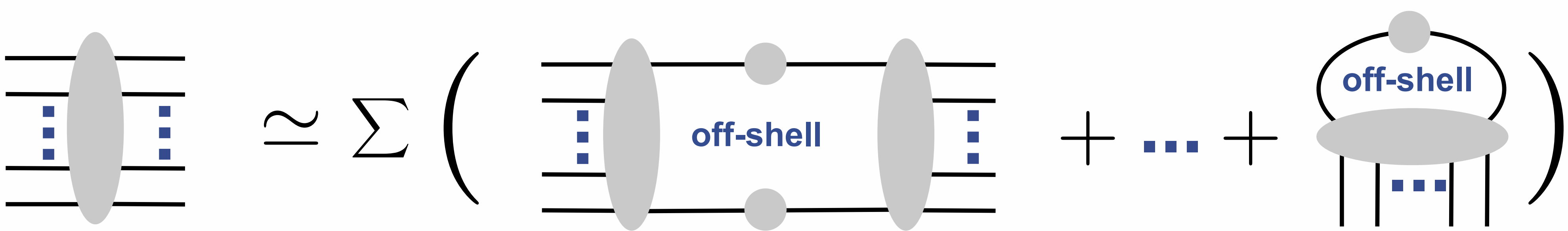

scattering amplitude/
vertex functions

properties

- access to physics mechanisms
- numerically tractable
  no sign problem
  systematic error control via closed form
- low energy models naturally encorporated

Continuum Methods for QCD

quark-gluon-hadron correlations

$$\langle q(x_1)\cdots\bar{q}(x_{2n})\,A_\mu(y_1)\cdots A_\mu(y_m)\,h(z_1)\cdots h(z_l)\rangle$$

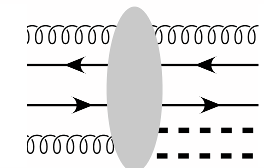

functional relations

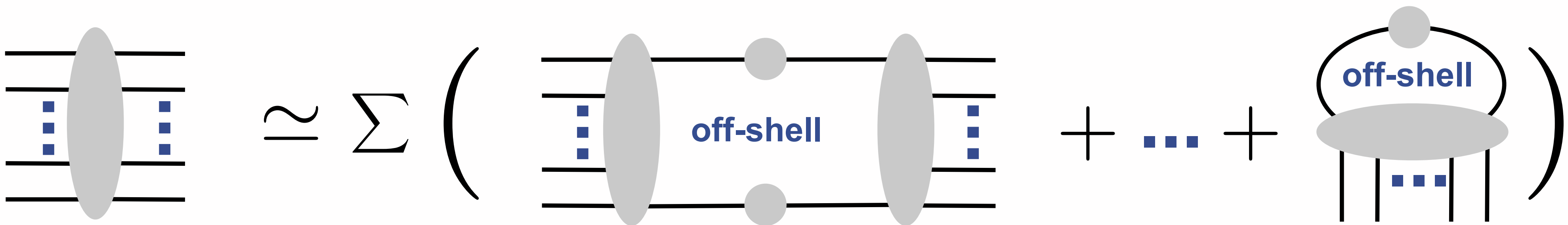

scattering amplitude/
vertex functions

e.g. lattice input on rhs

e.g. volume flucs., finite density,
dynamics, ...

properties

- access to physics mechanisms
- numerically tractable
  no sign problem
  systematic error control via closed form
- low energy models naturally encorporated

FunMethods complementary to lattice

‘Local’ expertise in functional continuum methods

J. Berges (Heidelberg)
J. Braun (Darmstadt)
M. Buballa (Darmstadt)
C.S. Fischer (Gießen)
B. Friman (GSI)
M. Lutz (GSI)
JMP (Heidelberg)
D. Rischke (Frankfurt)
B.-J. Schaefer (Gießen)
L. von Smekal (Darmstadt)
J. Wambach (Darmstadt)
C. Wetterich (Heidelberg)

N. Christiansen
A. Cyrol
N. Khan
N. Müller
F. Rennecke

Young guns (PostDocs)

T. Herbst (Heidelberg)
G. Eichmann (Giessen)
W.-j. Fu (Heidelberg)
M. Mitter (Heidelberg)
S. Rechenberger (Darmstadt)
H. Sanchis-Alepuz (Gießen)
N. Strodthoff (Heidelberg)
R. Stiele (Gießen)
R. Williams (Gießen)

unique concentration

Functional RG for QCD

JMP, AIP Conf.Proc. 1343 (2011)
Nucl.Phys. A931 (2014) 113-124

free energy at momentum scale k

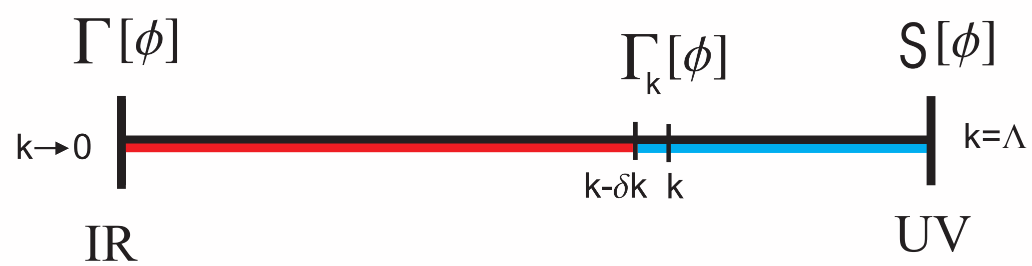

ab initio

glue quantum fluctuations

hadronic quantum fluctuations

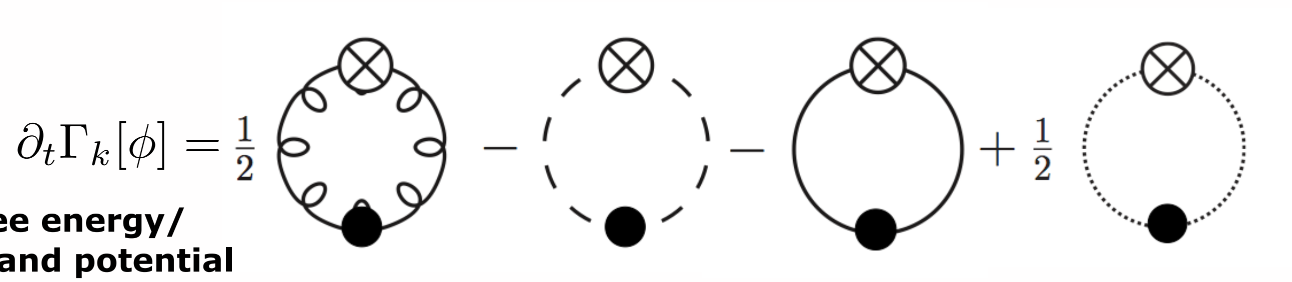

free energy/ grand potential

quark quantum fluctuations

RG-scale k: $t = \ln k$

Functional RG for QCD

JMP, AIP Conf.Proc. 1343 (2011)
Nucl.Phys. A931 (2014) 113-124

free energy at momentum scale k

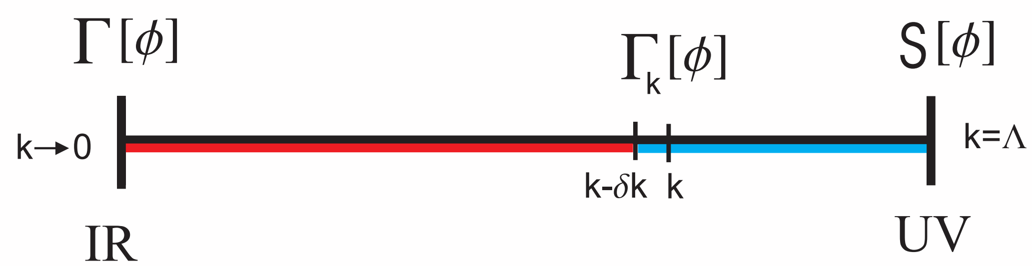

ab initio

$\partial_t \Gamma_k[\phi] = \frac{1}{2}$ 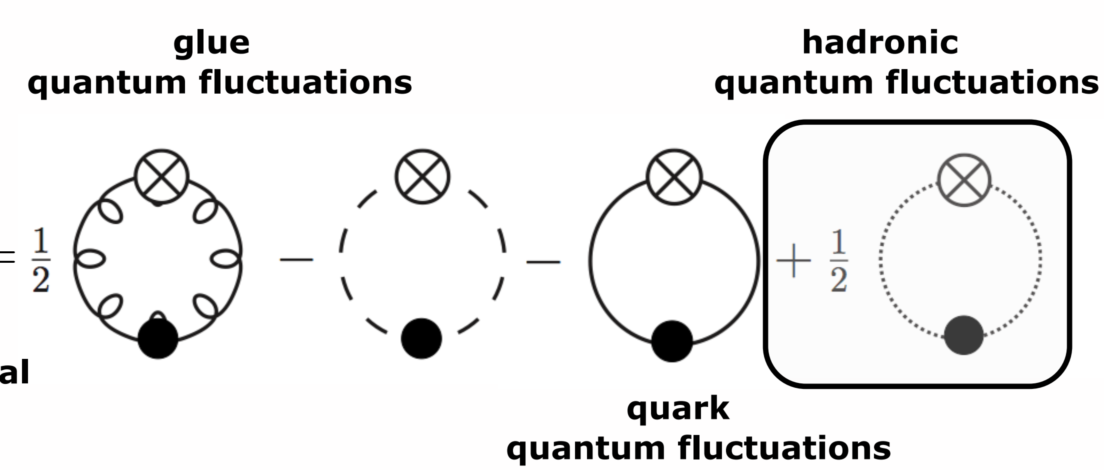

free energy/ grand potential

$\text{RG-scale k: } t = \ln k$

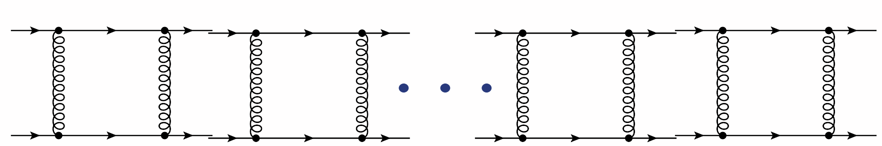

Dynamical hadronisation

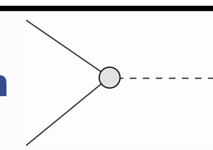

dynamical

Gies, Wetterich '01
JMP '05
Flörchinger, Wetterich '09

Functional RG for QCD

fQCD collaboration: J. Braun, A. Cyrol, L. Fister, W.-j. Fu, T.K. Herbst, M. Mitter, N. Mueller, JMP, S. Rechenberger, F. Rennecke, N. Strodthoff

TARDIS, ERGE, DoFun2.0

DoFun

Braun, Huber, Comput.Phys.Commun. 183 (2012) 1290-1320

Mitter, JMP, Strodthoff, Phys.Rev. D91 (2015) 054035

Braun, Fister, Haas, JMP, Rennecke, arXiv:1412.1045

Outline

- **Vacuum QCD & the hadron spectrum**
- **Phase structure of QCD**
- **Spectral Functions & Transport Coefficients**
- **Outlook**

Glue sector

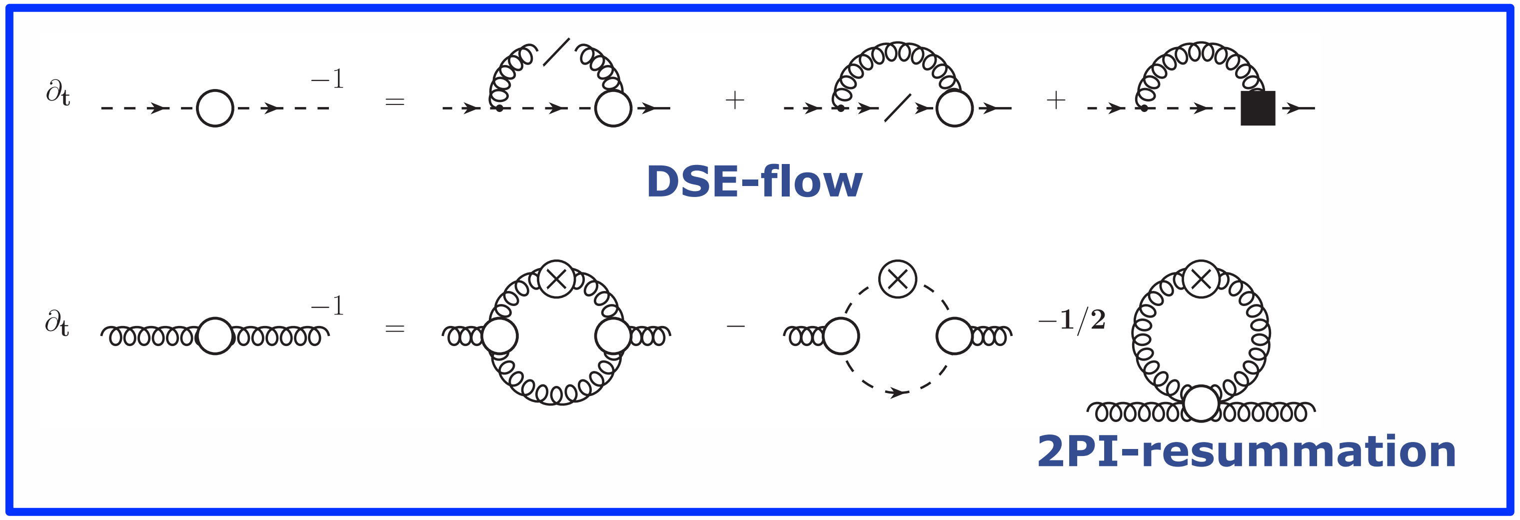

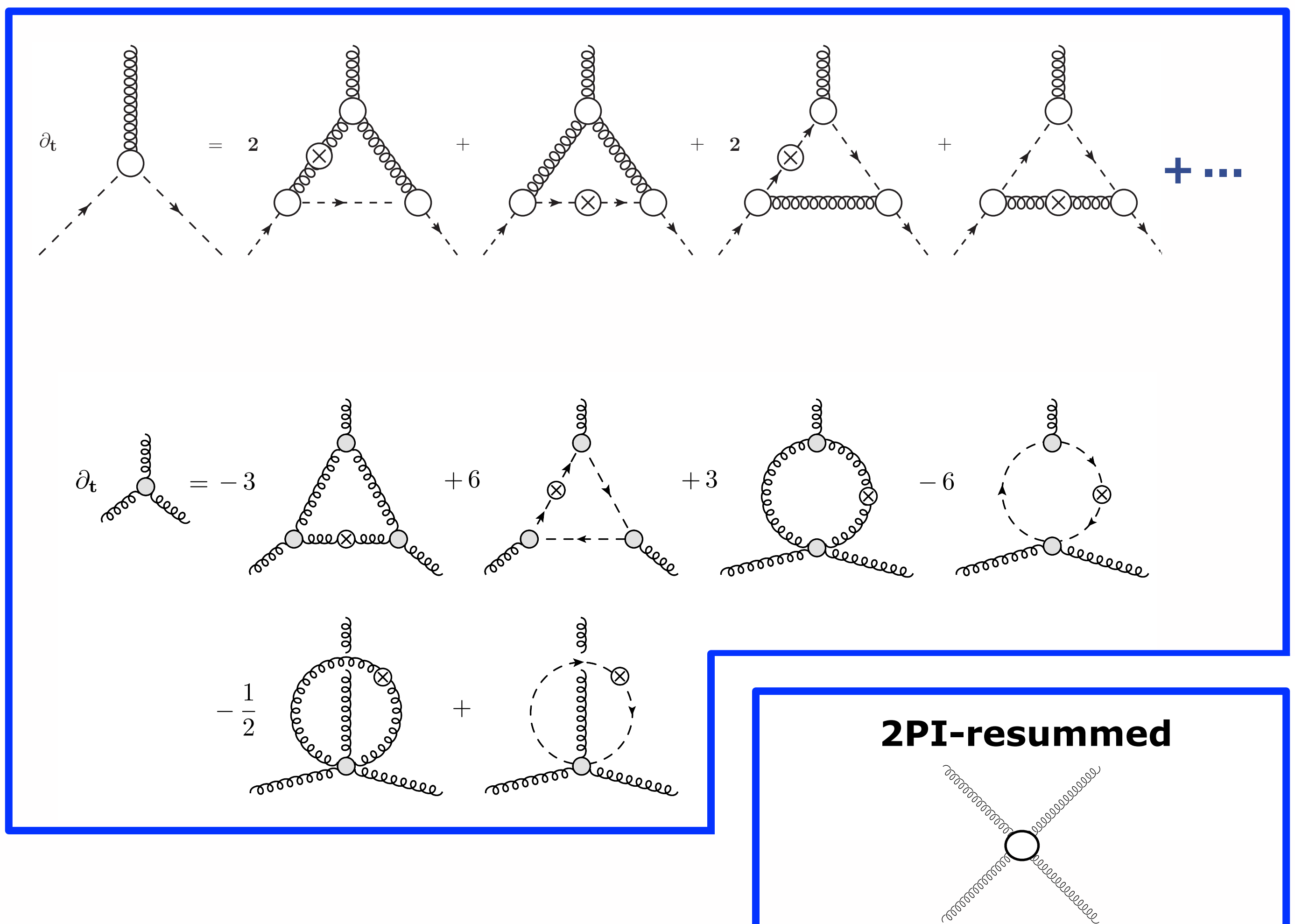

Glue sector

Yang-Mills propagators, T=0

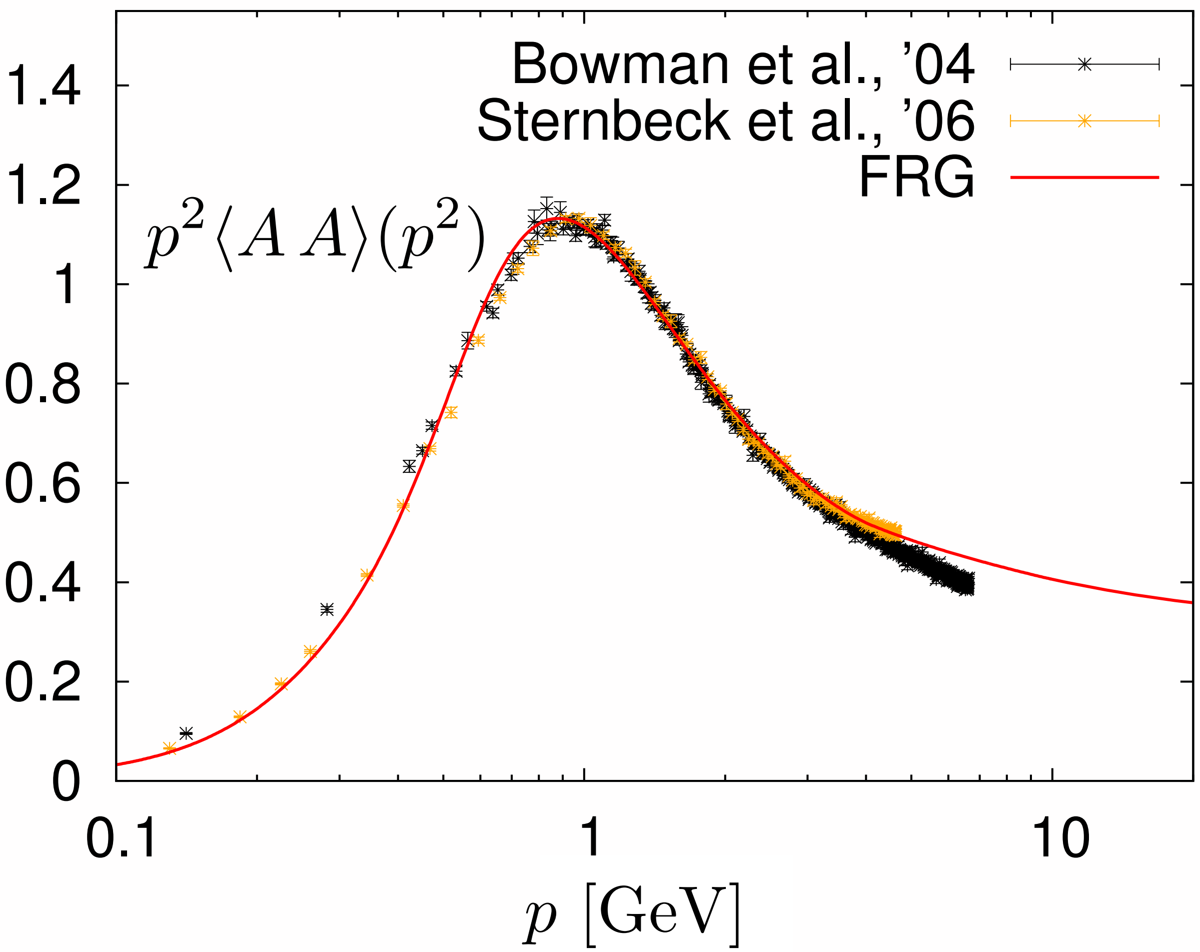

Fischer, Maas, JMP, Annals Phys. 324 (2009) 2408

Fister, JMP '14

Yang-Mills propagators, finite T

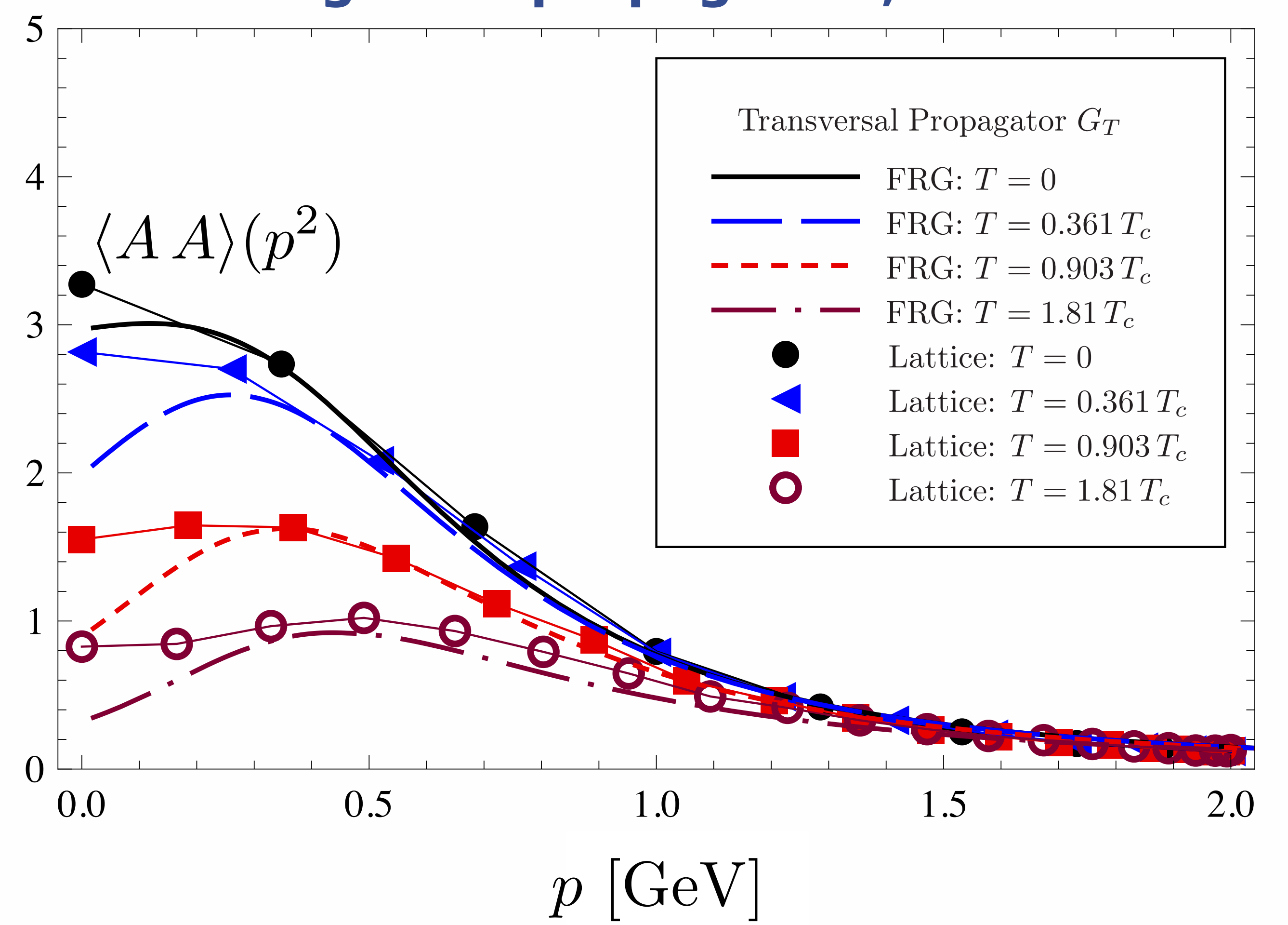

Fister, JMP, arXiv:1112.5440

Chiral symmetry breaking

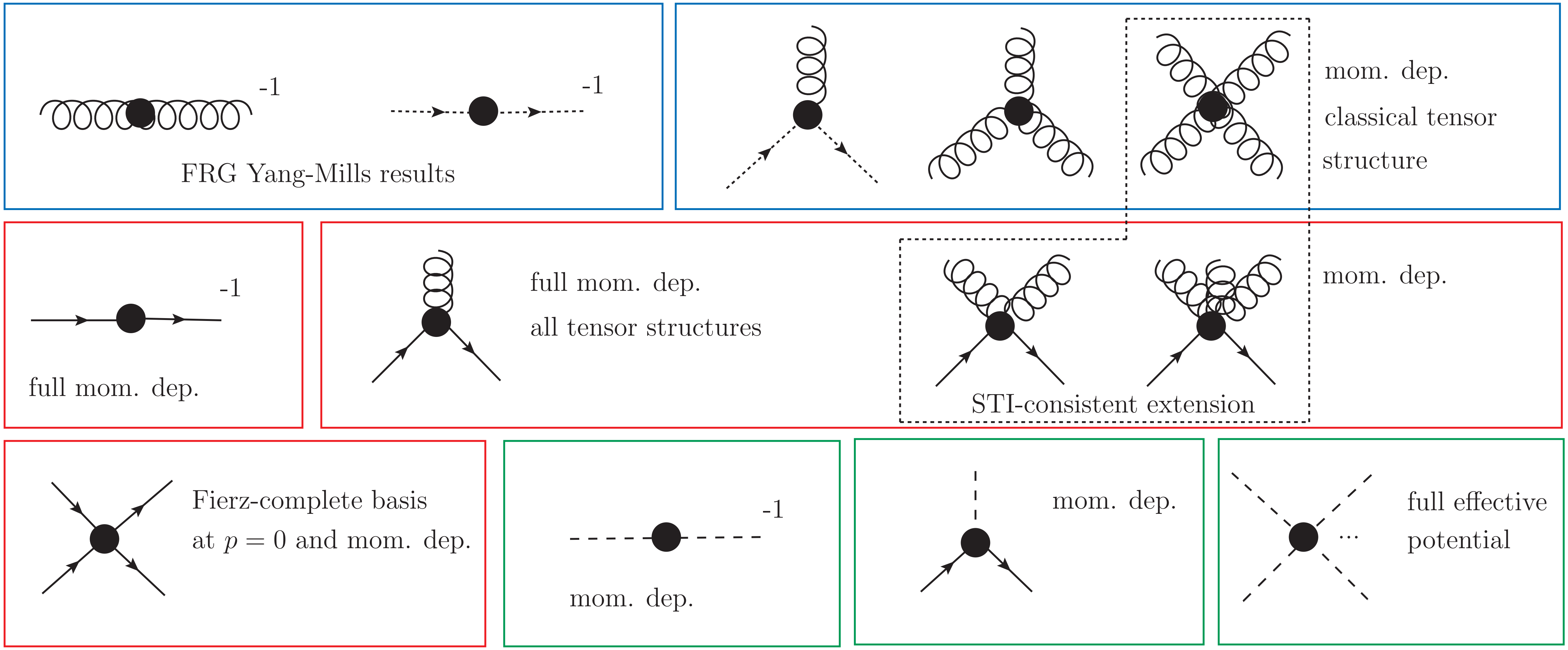

fQCD

Mitter, JMP, Strodthoff, PRD 91 (2015) 054035

see also Williams, arXiv:1404.2545

Chiral symmetry breaking

FRG-quenched QCD vs lattice-quenced QCD

quenched gluon dressing

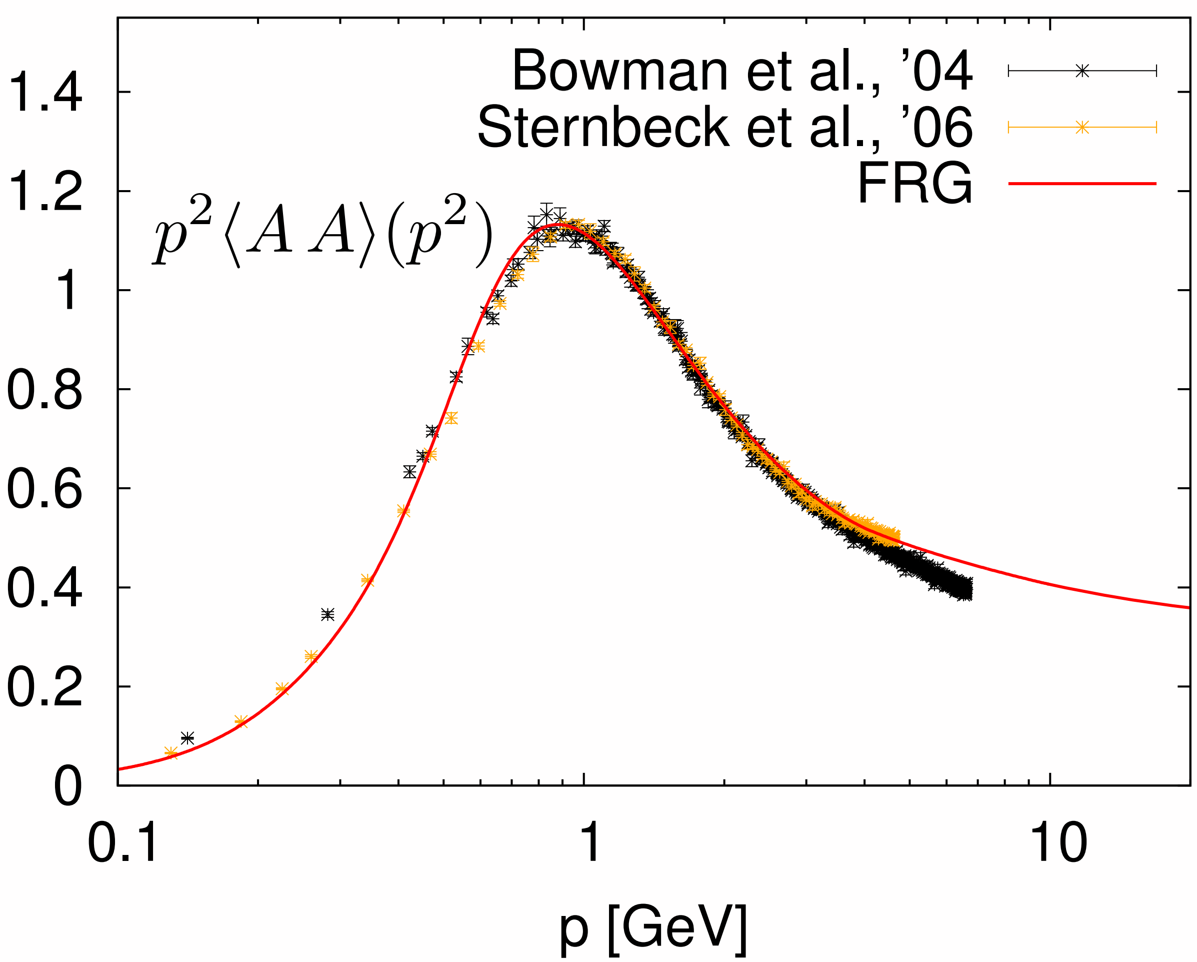

quark propagator

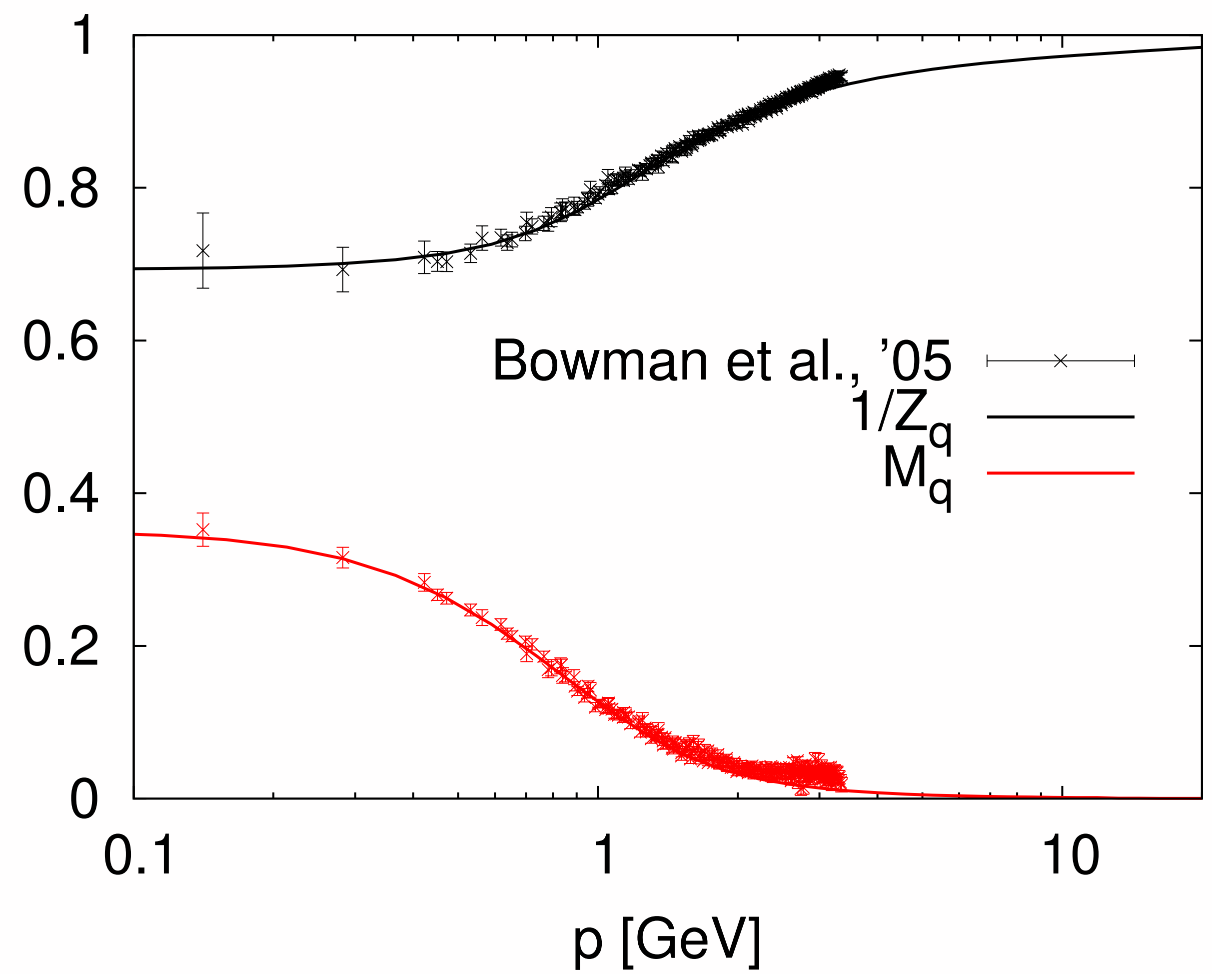

$$\mathbf{N_f = 2}$$

Mitter, JMP, Strodthoff, PRD 91 (2015) 054035

Chiral symmetry breaking

FRG-quenched QCD vs lattice-quenced QCD

quenched gluon dressing

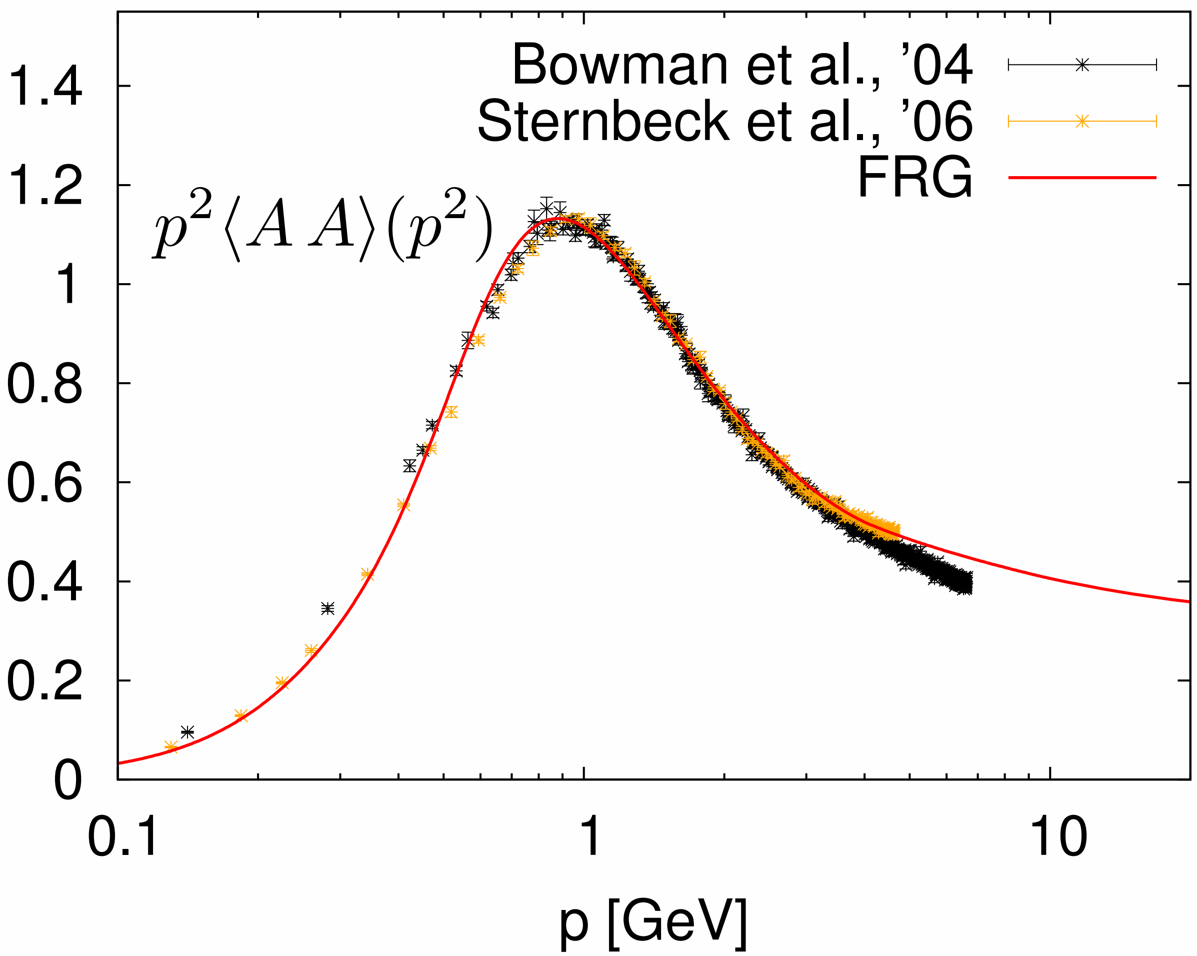

quark propagator

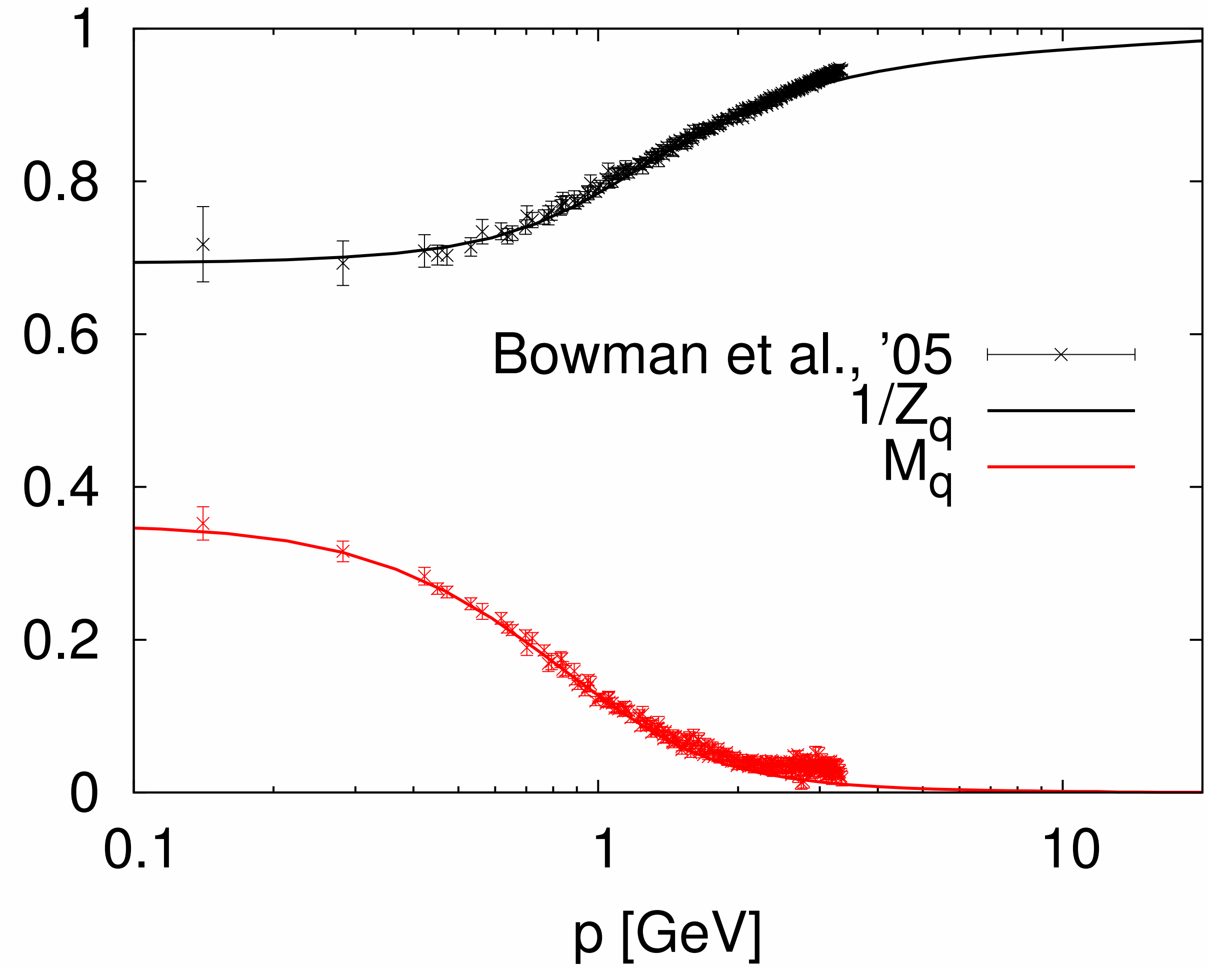

JMP, Rennecke, PRD 90, 076002

Helmboldt, JMP, Strodthoff, PRD 91 (2015) 5, 054010

Braun, Fister, Haas, JMP, Rennecke, arXiv:1412.1045

$$N_f = 2$$

systematic error estimate: ~10%

JMP

Mitter, JMP, Strodthoff, PRD 91 (2015) 054035

Chiral symmetry breaking

FRG-quenched QCD vs lattice-quenced QCD

unquenched gluon dressing

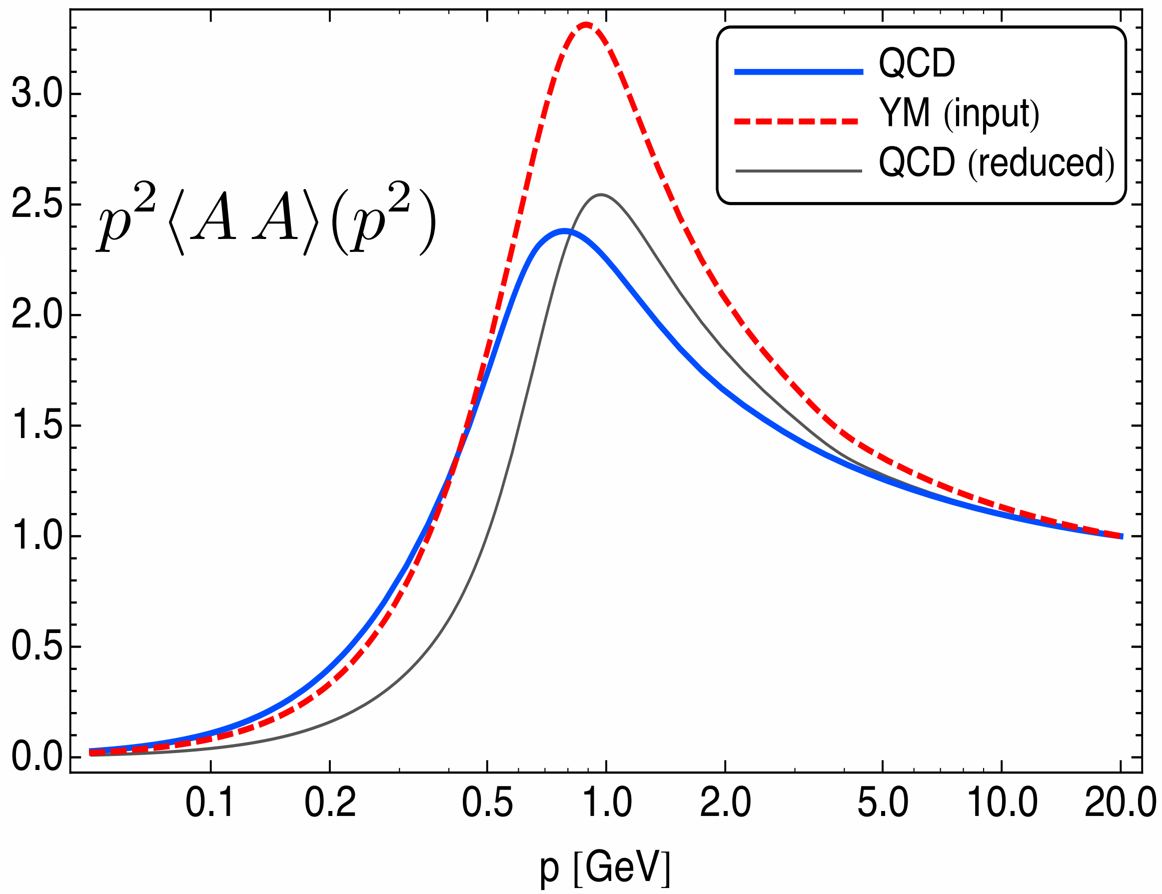

Braun, Fister, Haas, JMP, Rennecke, arXiv:1412.1045

Rennecke, arXive:1504.03585

quark propagator

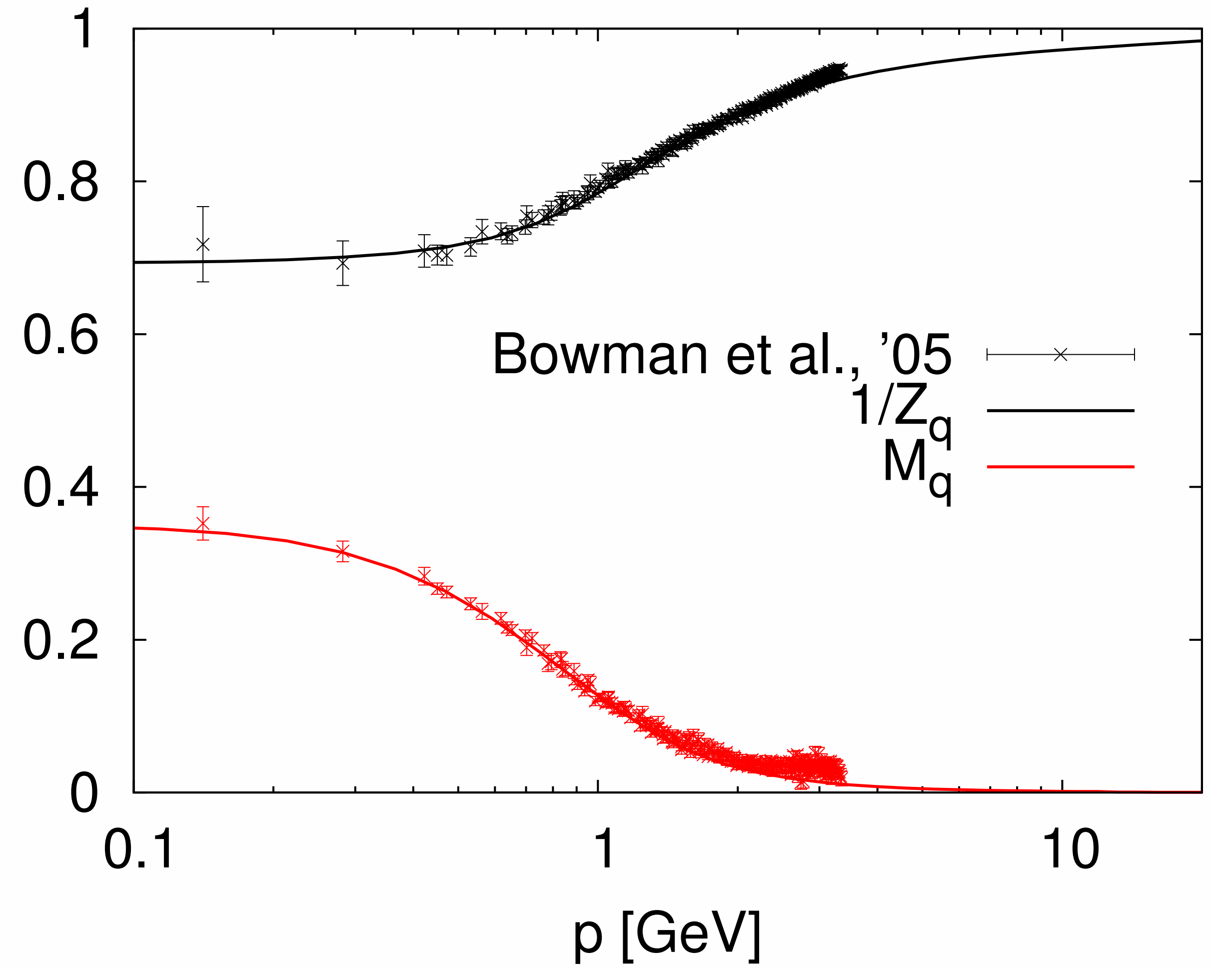

$\mathbf{N_f = 2}$

systematic error estimate: ~10%

Mitter, JMP, Strodthoff, PRD 91 (2015) 054035

A glimpse at the hadron spectrum

quenched QCD

four-fermi scattering amplitude at pion pole

$$\langle \bar{q}\vec{\sigma}\gamma_5 q(p) \quad \bar{q}\vec{\sigma}\gamma_5 q(-p)\rangle \quad \to \quad \frac{\chi_{\bar{q}\pi q}\bar{\chi}_{\bar{q}\pi q}}{p^2 - m_\pi^2} \quad + \quad \text{finite terms}$$

$$\Gamma^{(4)}(p_1, p_2, p_3, p_4)$$

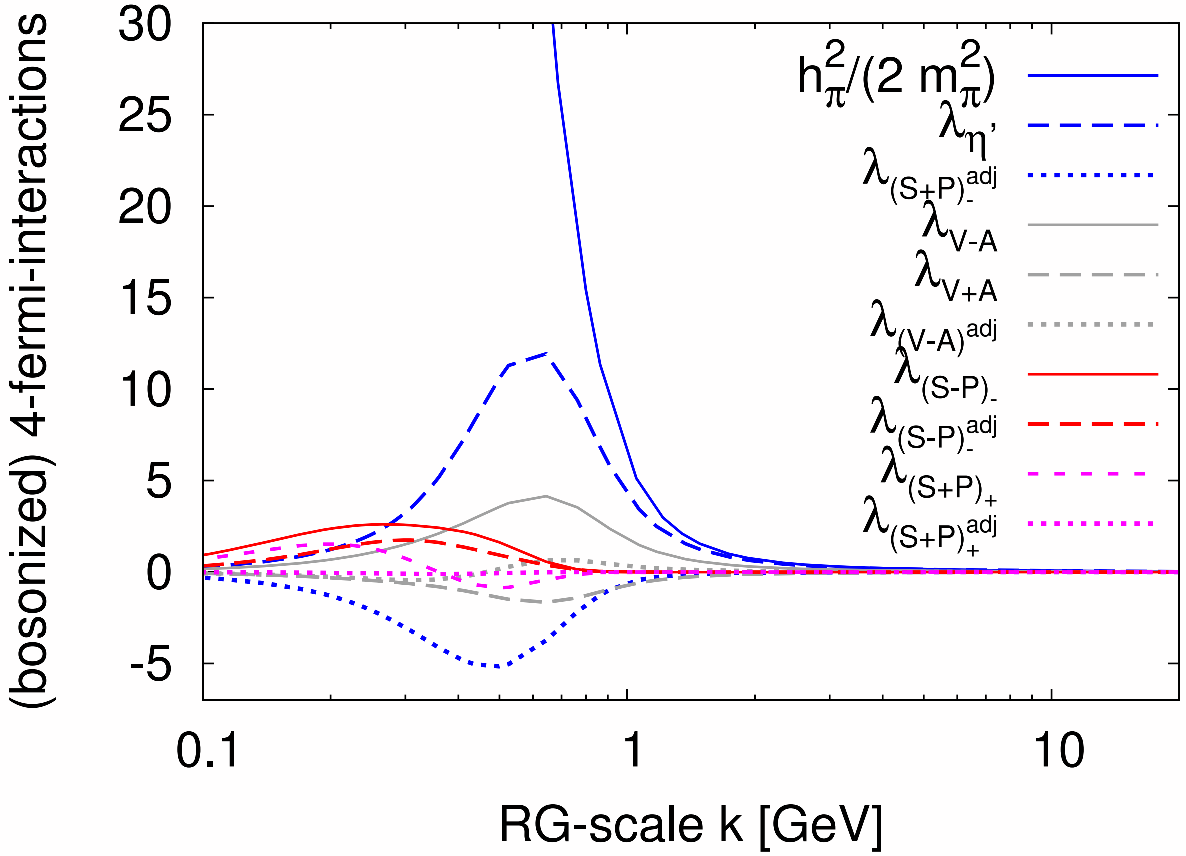

Mitter, JMP, Strodthoff, in preparation

A glimpse at the hadron spectrum

quenched QCD

four-fermi scattering amplitude at pion pole

$$\langle \bar{q}\vec{\sigma}\gamma_5 q(p) \quad \bar{q}\vec{\sigma}\gamma_5 q(-p)\rangle \to \frac{\chi_{\bar{q}\pi q}\bar{\chi}_{\bar{q}\pi q}}{p^2 - m_\pi^2} + \quad \text{finite terms}$$

$$\Gamma^{(4)}_{(\bar{q}\gamma_5\vec{\sigma}q)^2}(p,p,-p,-p) \qquad \frac{\Gamma^{(3)}_{\bar{q}\pi q}\Gamma^{(3)}_{\bar{q}\pi q}}{p^2 - m_\pi^2}$$

Mitter, JMP, Strodthoff, in preparation

A glimpse at the hadron spectrum

quenched QCD

four-fermi scattering amplitude at pion pole

$$\langle \bar{q}\vec{\sigma}\gamma_5 q(p) \quad \bar{q}\vec{\sigma}\gamma_5 q(-p)\rangle \to \frac{\chi_{\bar{q}\pi q}\bar{\chi}_{\bar{q}\pi q}}{p^2 - m_\pi^2} + \text{finite terms}$$

$$\Gamma^{(4)}_{(\bar{q}\gamma_5\vec{\sigma}q)^2}(p,p,-p,-p) \qquad \frac{\Gamma^{(3)}_{\bar{q}\pi q}\Gamma^{(3)}_{\bar{q}\pi q}}{p^2 - m_\pi^2}$$

pion decay constant f_π **via normalisation of** $\boldsymbol{\Gamma^{(3)}_{\bar{q}\pi q}}$

aka BSE wave function

recent mini-review on DSE-BSE
Sanchis-Alepuz, Williams, arXiv:1503.05896

Hadron DSE-BSE center Gießen

Mitter, JMP, Strodthoff, in preparation

A glimpse at the hadron spectrum

quenched QCD

four-fermi scattering amplitude at pion pole

$$\langle \bar{q}\vec{\sigma}\gamma_5 q(p) \quad \bar{q}\vec{\sigma}\gamma_5 q(-p)\rangle \to \frac{\chi_{\bar{q}\pi q}\bar{\chi}_{\bar{q}\pi q}}{p^2 - m_\pi^2} + \text{finite terms}$$

$$\downarrow \qquad\qquad \downarrow$$

$$\Gamma^{(4)}_{(\bar{q}\gamma_5\vec{\sigma}q)^2}(p,p,-p,-p) \qquad \frac{\Gamma^{(3)}_{\bar{q}\pi q}\Gamma^{(3)}_{\bar{q}\pi q}}{p^2 - m_\pi^2}$$

pion decay constant f_π **via normalisation of** $\Gamma^{(3)}_{\bar{q}\pi q}$

$$\mathrm{f}_\pi = 88\,\mathrm{MeV}$$

continuum QCD

$$\mathrm{f}_\pi = 89\,\mathrm{MeV}$$

lattice **Aoki et al, PRD 62 (2000) 094501**

Mitter, JMP, Strodthoff, in preparation

A glimpse at the hadron spectrum

quenched QCD

four-fermi scattering amplitude at pion pole

$$\langle \bar{q}\vec{\sigma}\gamma_5 q(p) \quad \bar{q}\vec{\sigma}\gamma_5 q(-p)\rangle \to \frac{\chi_{\bar{q}\pi q}\bar{\chi}_{\bar{q}\pi q}}{p^2 - m_\pi^2} + \quad \text{finite terms}$$

$$\Gamma^{(4)}_{(\bar{q}\gamma_5\vec{\sigma}q)^2}(p,p,-p,-p) \qquad \frac{\Gamma^{(3)}_{\bar{q}\pi q}\Gamma^{(3)}_{\bar{q}\pi q}}{p^2 - m_\pi^2}$$

pion decay constant f_π **via normalisation of** $\Gamma^{(3)}_{\bar{q}\pi q}$

real-time:

- **Spectral Fcts & Transport Coeffs**

$f_\pi = 88\,\text{MeV}$
continuum QCD

$f_\pi = 89\,\text{MeV}$
lattice **Aoki et al, PRD 62 (2000) 094501**

Mitter, JMP, Strodthoff, in preparation

Outline

- Vacuum QCD & the hadron spectrum
- Phase structure of QCD
- Spectral Functions & Transport Coefficients
- Outlook

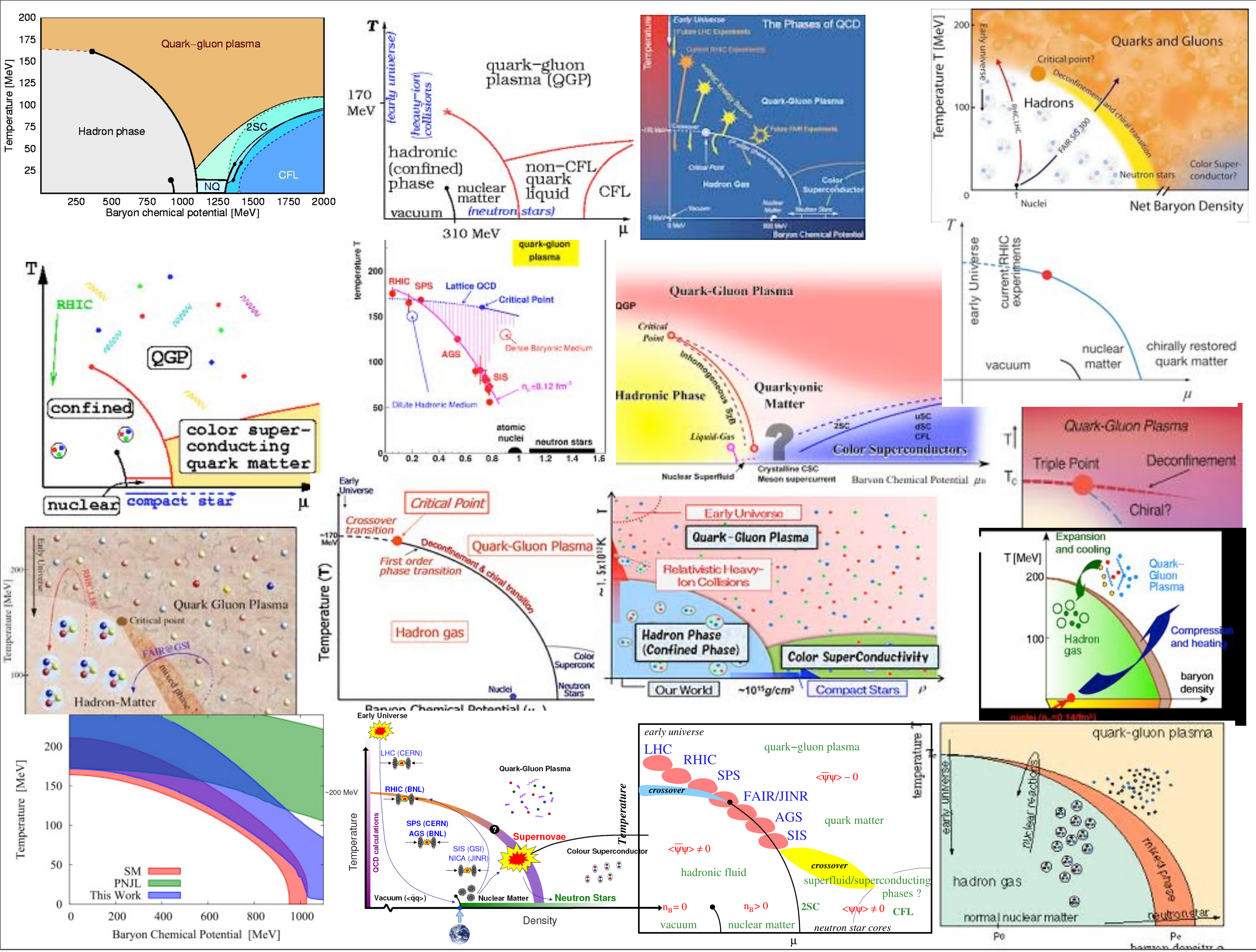
Quark–gluon plasma
Hadron phase
2SC
CFL
NQ
Temperature [MeV]
Baryon chemical potential [MeV]
quark–gluon plasma (QGP)
hadronic (confined) phase
nuclear matter
(neutron stars)
non-CFL quark liquid
vacuum
170 MeV
310 MeV
early universe
heavy-ion collisions
The Phases of QCD
Quark-Gluon Plasma
Hadron Gas
Color Superconductor
Critical Point
Baryon Chemical Potential
Quarks and Gluons
Hadrons
Critical point?
Deconfinement and chiral transition
Neutron stars
Color Super-conductor?
Nuclei
Net Baryon Density
Temperature T [MeV]
RHIC
QGP
confined
color super-conducting quark matter
nuclear
compact star
quark-gluon plasma
RHIC
SPS
Lattice QCD
Critical Point
AGS
SIS
Dense Baryonic Medium
Dilute Hadronic Medium
atomic nuclei
neutron stars
Quark-Gluon Plasma
Hadronic Phase
Quarkyonic Matter
Color Superconductors
Nuclear Superfluid
Crystalline CSC
Meson supercurrent
Baryon Chemical Potential
vacuum
nuclear matter
chirally restored quark matter
current RHIC experiments
Quark-Gluon Plasma
Triple Point
Deconfinement
Chiral?
Quark Gluon Plasma
Critical point
Hadron-Matter
mixed phase
Early Universe
Critical Point
Crossover transition
First order phase transition
Deconfinement & chiral transition
Quark-Gluon Plasma
Hadron gas
Temperature (T)
Color Superconductor
Nuclei
Neutron Stars
Baryon Chemical Potential
Early Universe
Quark - Gluon Plasma
Relativistic Heavy-Ion Collisions
Hadron Phase (Confined Phase)
Color SuperConductivity
Our World
Compact Stars
Expansion and cooling
Quark-Gluon Plasma
Hadron gas
Compression and heating
baryon density
T [MeV]
SM
PNJL
This Work
Temperature [MeV]
Baryon Chemical Potential [MeV]
Early Universe
LHC (CERN)
RHIC (BNL)
SPS (CERN)
AGS (BNL)
SIS (GSI)
NICA (JINR)
Quark-Gluon Plasma
Supernovae
Colour Superconductor
QCD calculations
Vacuum
Nuclear Matter
Neutron Stars
Temperature
Density
early universe
LHC
RHIC
SPS
FAIR/JINR
AGS
SIS
quark–gluon plasma
crossover
quark matter
hadronic fluid
superfluid/superconducting phases ?
2SC
CFL
vacuum
nuclear matter
neutron star cores
quark-gluon plasma
early universe
nuclear reactions
hadron gas
mixed phase
normal nuclear matter
neutron star

QCD

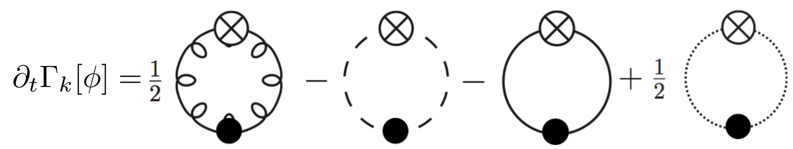

Sequential decoupling of gluon, quark, sigma, pion fluctuations

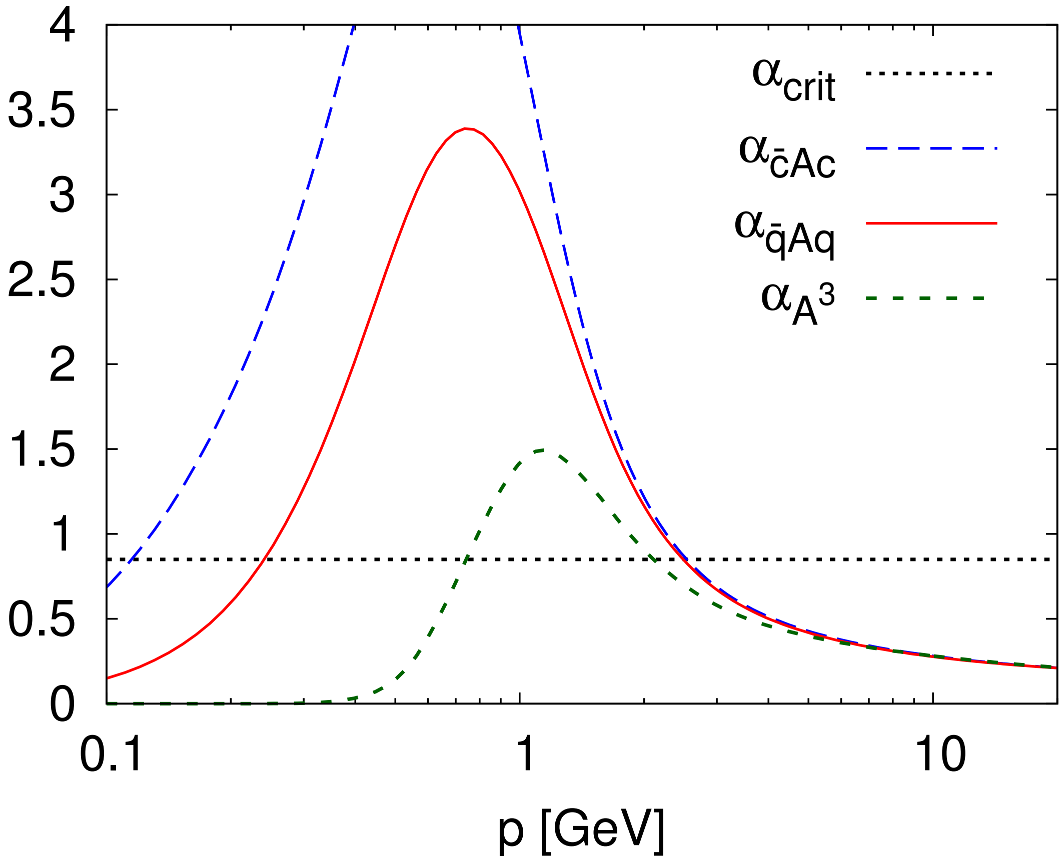

Mitter, JMP, Strodthoff, PRD 91 (2015) 054035

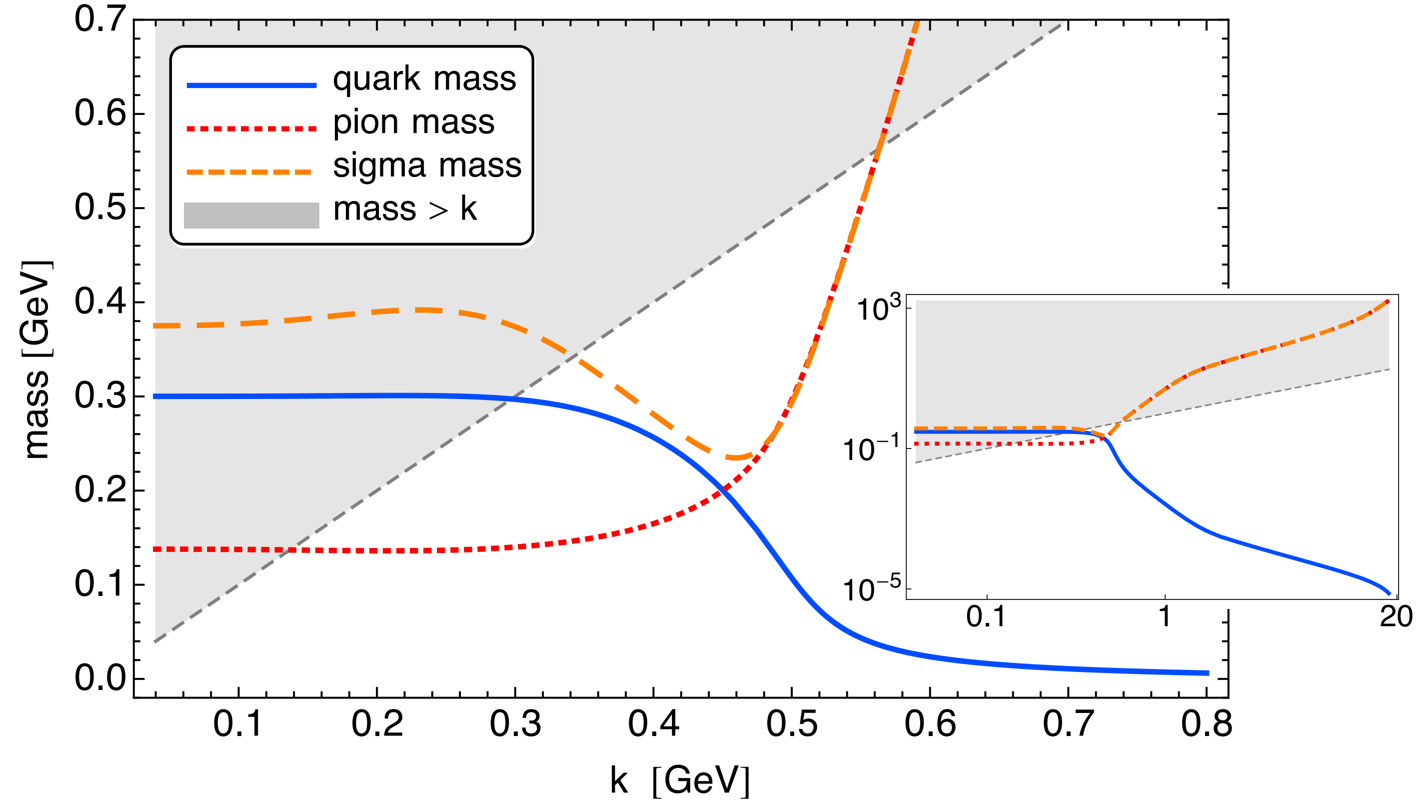

Braun, Fister, Haas, JMP, Rennecke, arXiv:1412.1045

Rennecke, arXive:1504.03585

QCD

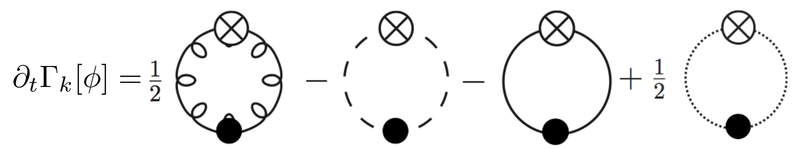

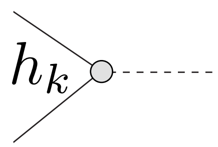

quark-meson coupling

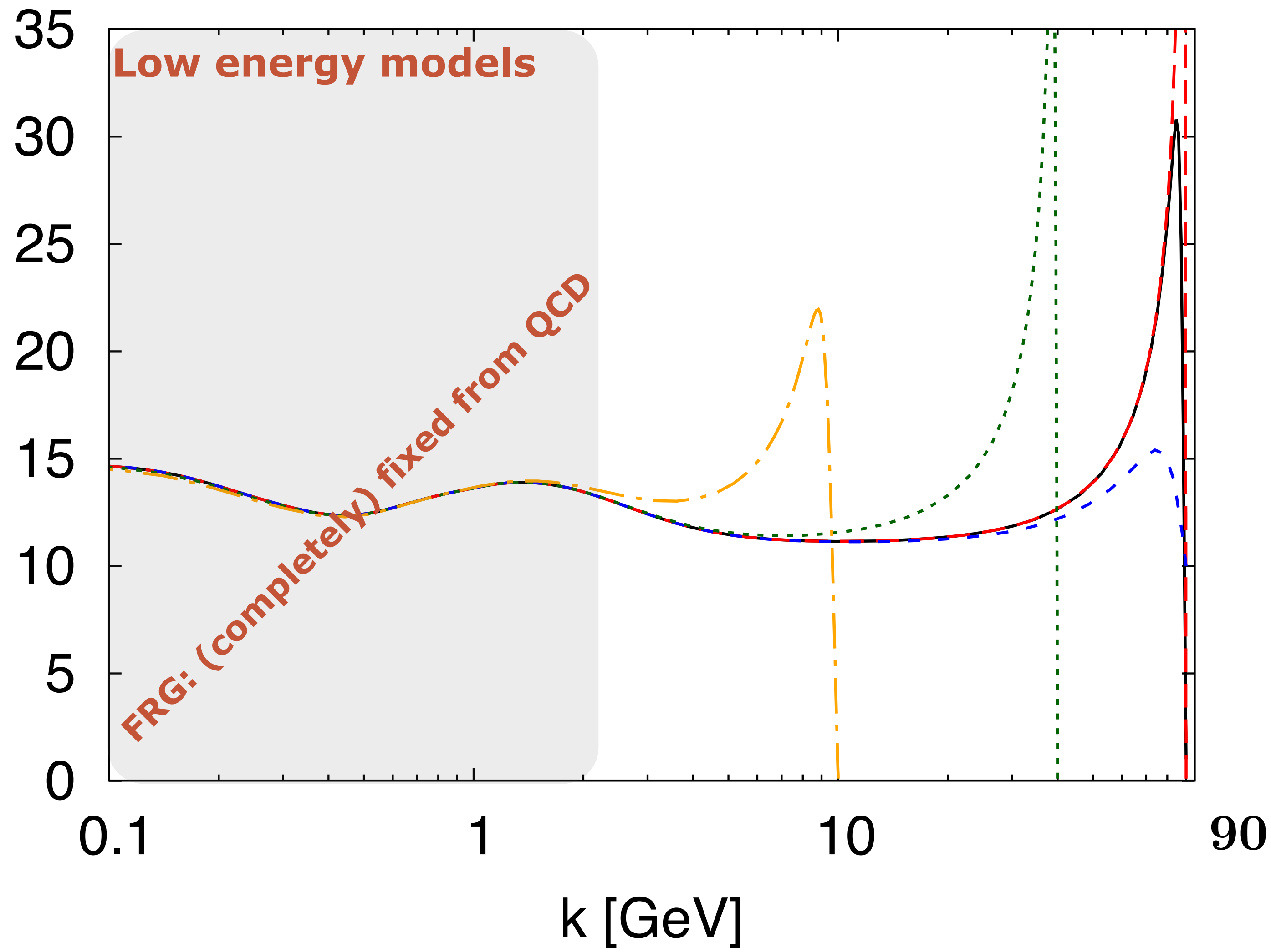

fQCD

PQM-model

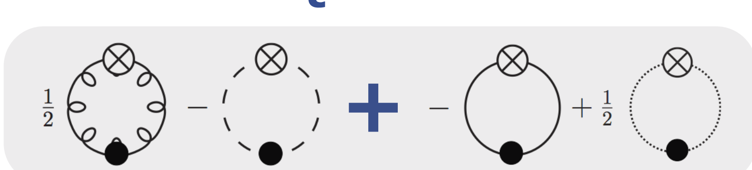

PNJL-model

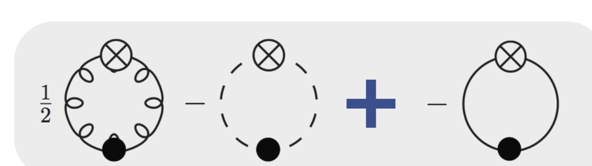

QM-model

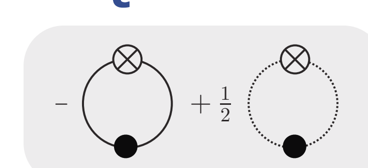

NJL-model

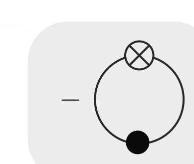

QCD

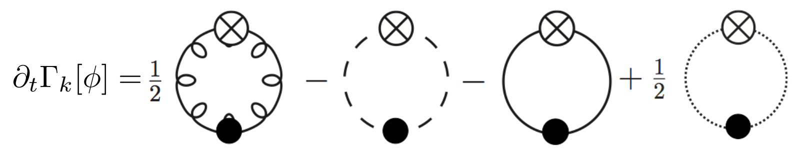

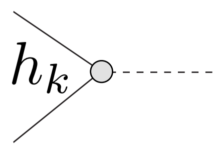

quark-meson coupling

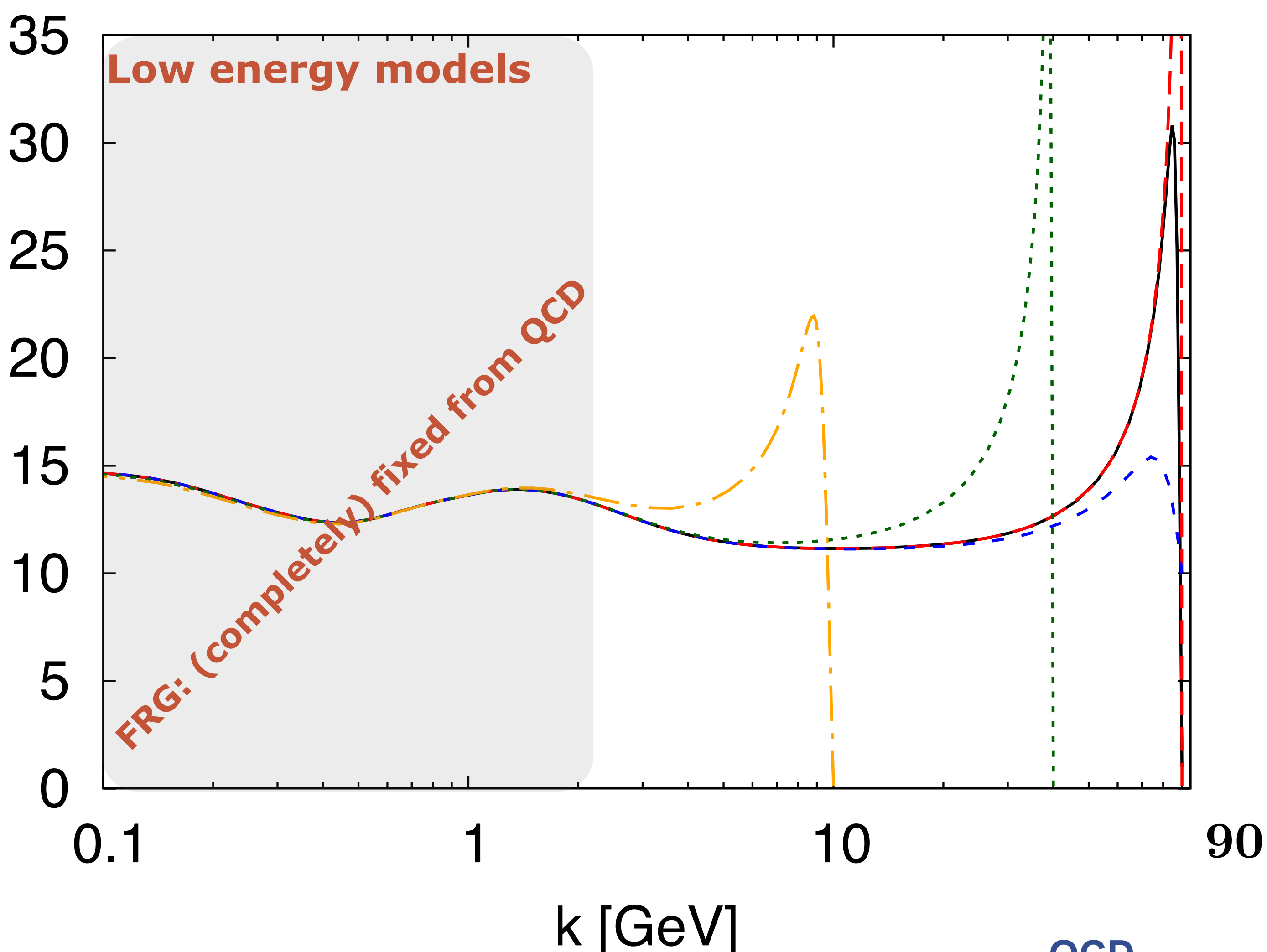

fQCD

PQM-model

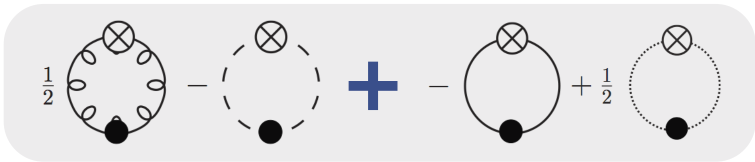

PNJL-model

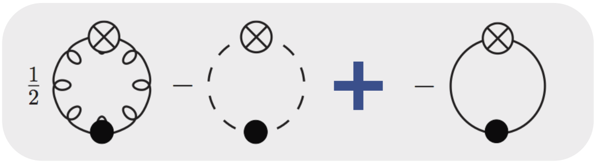

QM-model

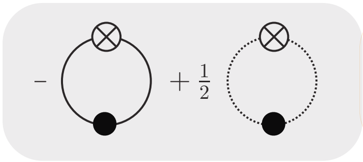

NJL-model

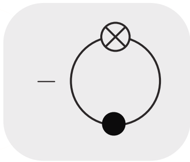

QCD

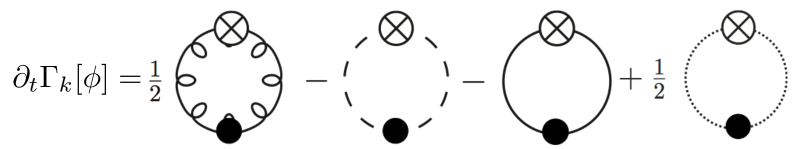

Polyakov loop potential in full QCD

Yang-Mills

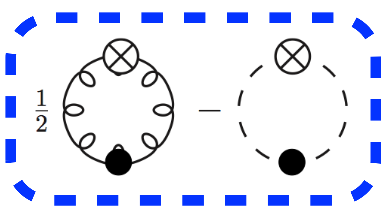

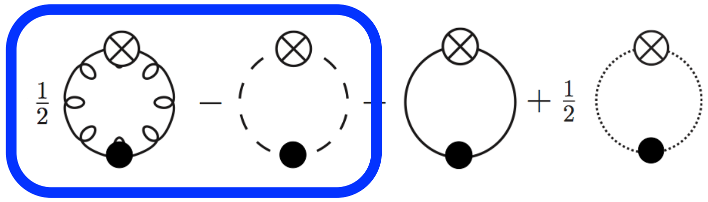

glue

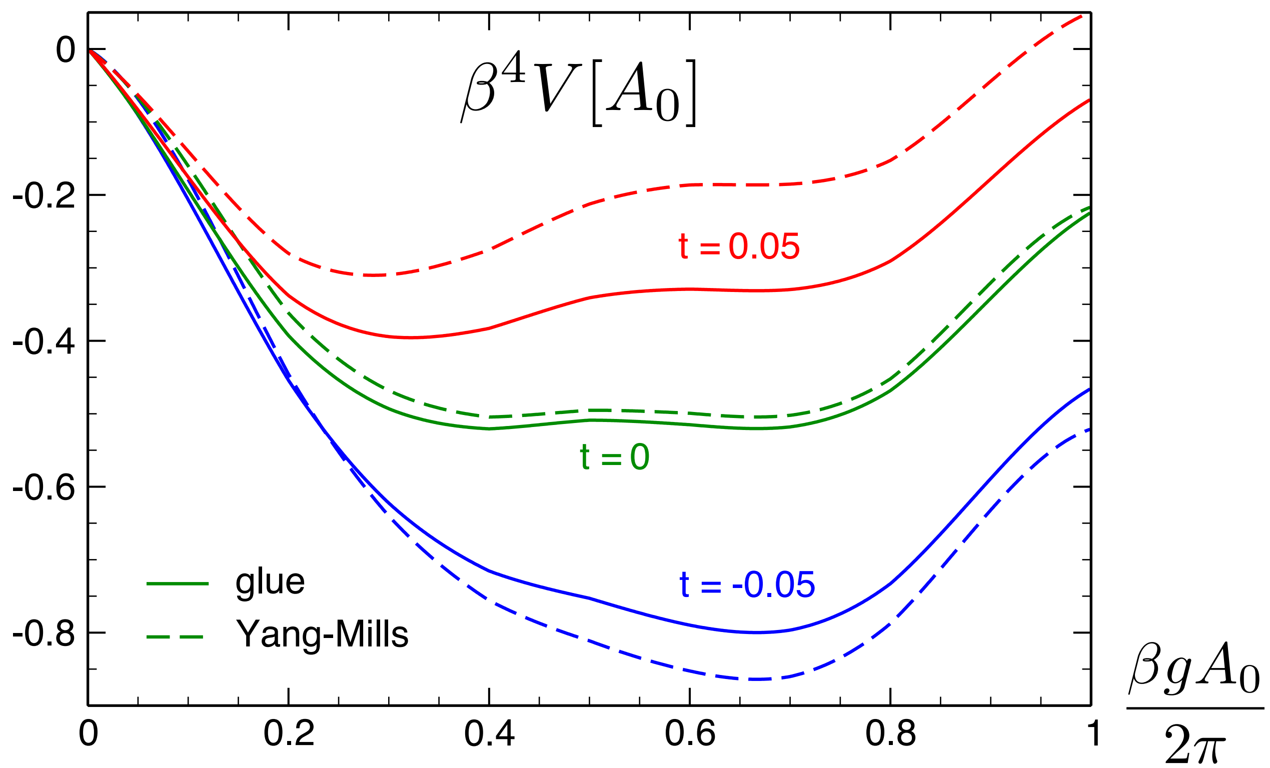

JMP, AIP Conf.Proc. 1343 (2011)

Haas, Stiele et al, PRD 87 (2013) 076004

PQM-model

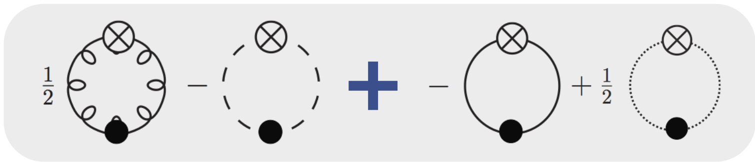

PNJL-model

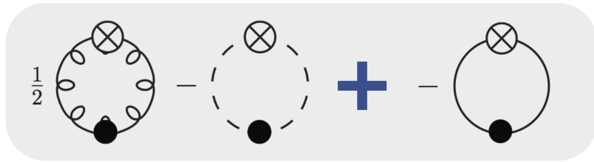

QM-model

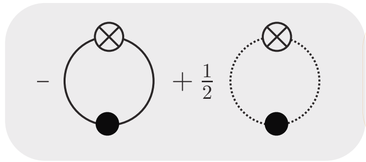

NJL-model

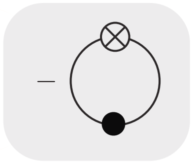

Thermodynamics

reduced chiral condensate

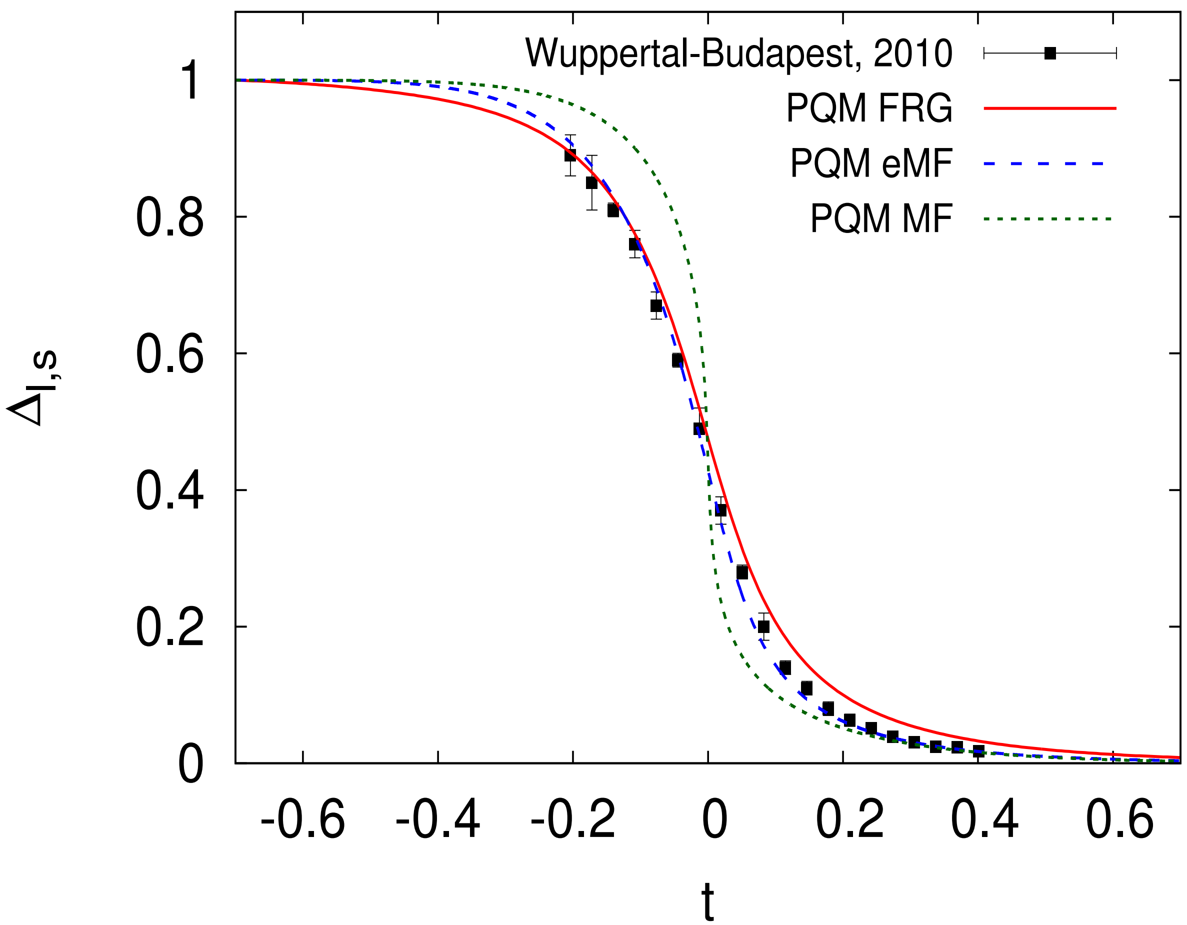

2+1 flavor QCD - enhanced PQM-model

Interaction measure

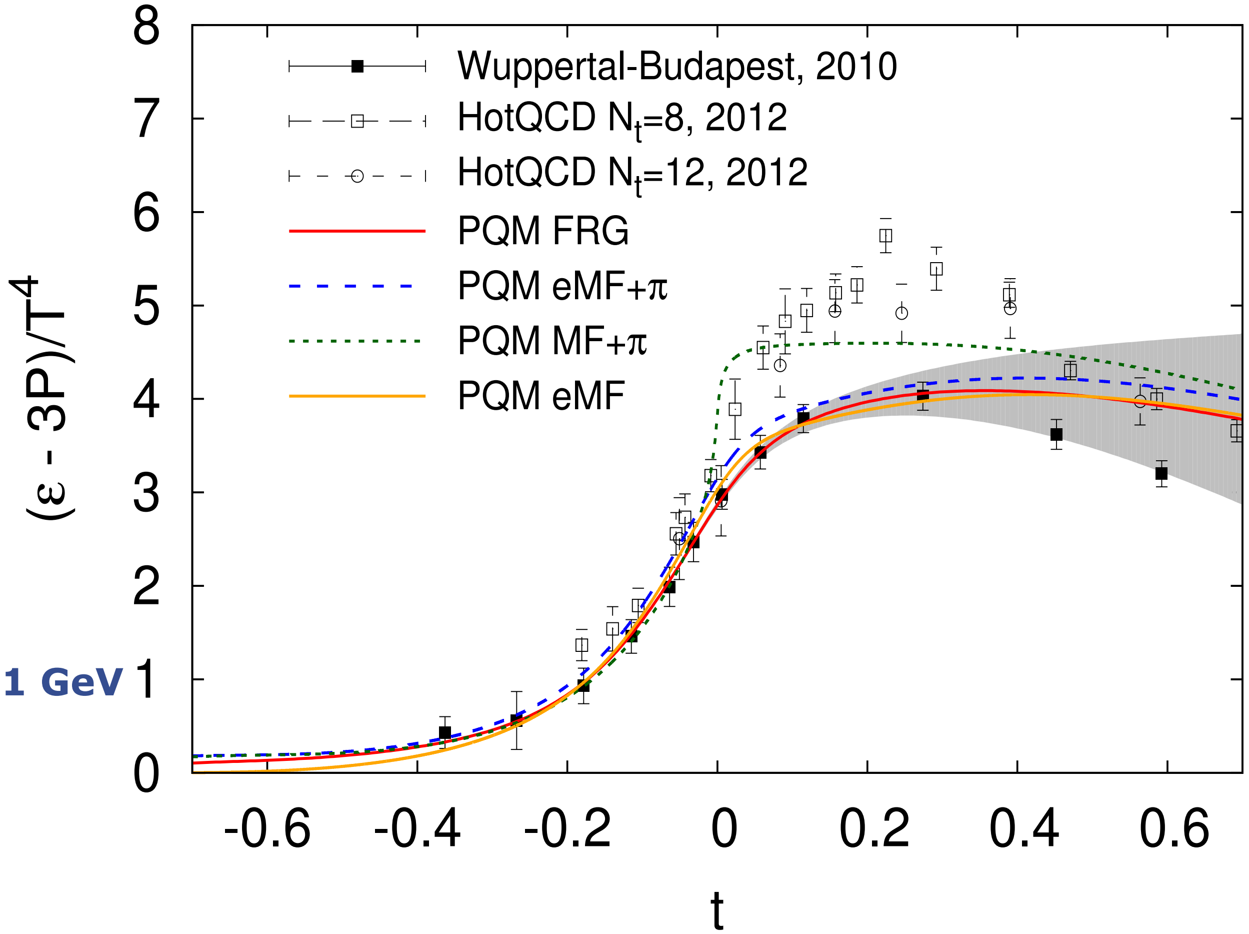

Yang-Mills pressure

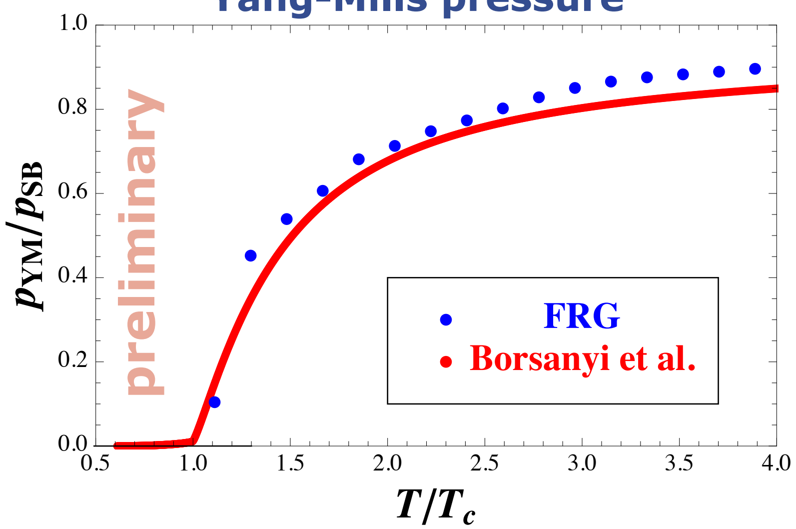

Shaded area:
systematic error estimate
due to low initial UV scale 1 GeV

Fister, JMP '11

Herbst, Mitter et al, PLB 731 (2014) 248-256

Phase structure at finite density

Phase diagram of quantised 2-flavor PQM-model

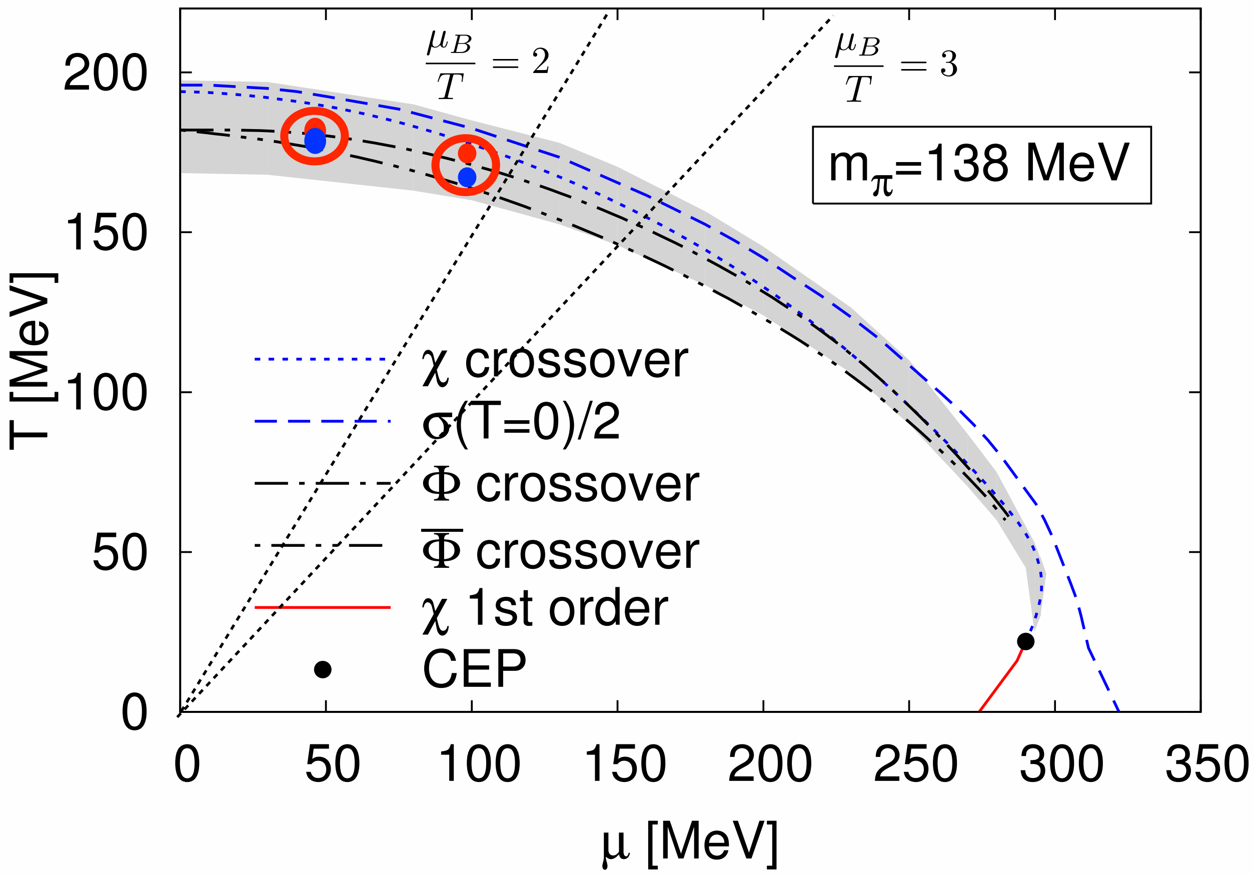

Herbst, JMP, Schaefer, PLB 696 (2011) 58-67
PRD 88 (2013) 1, 014007

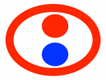

FRG QCD results at finite density
Haas, Braun, JMP '09, unpublished

Phase structure at finite density

Phase diagram of quantised 2-flavor PQM-model

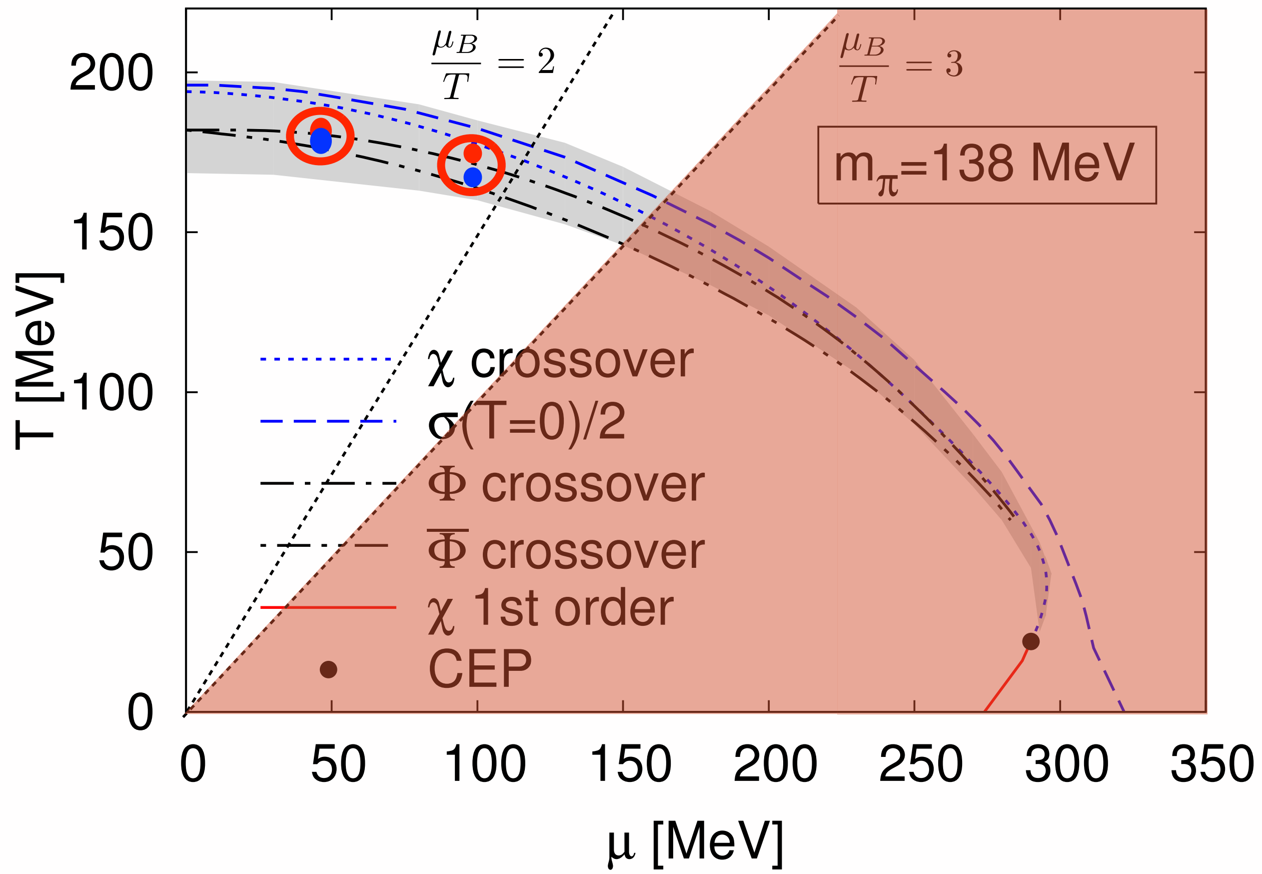

Herbst, JMP, Schaefer, PLB 696 (2011) 58-67
PRD 88 (2013) 1, 014007

FRG QCD results at finite density

Haas, Braun, JMP '09, unpublished

Phase structure at finite density

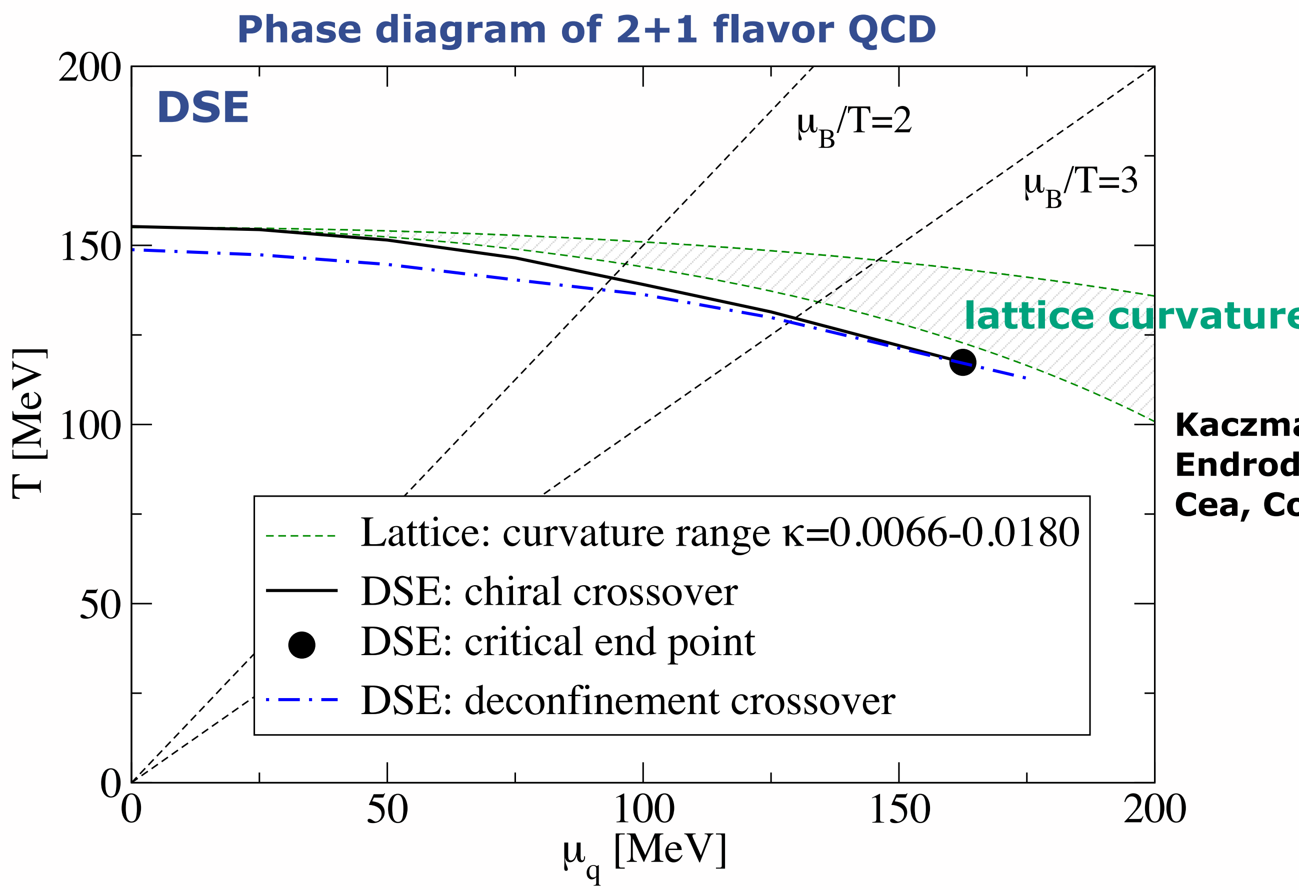

Kaczmarek at al. ’11
Endrodi, Fodor, Katz, Szabo ’11
Cea, Cosmai, Papa ’14

Fischer, Fister, Luecker, JMP, PLB732 (2014) 248

Fischer, Luecker, Welzbacher, PRD 90 (2014) 034022

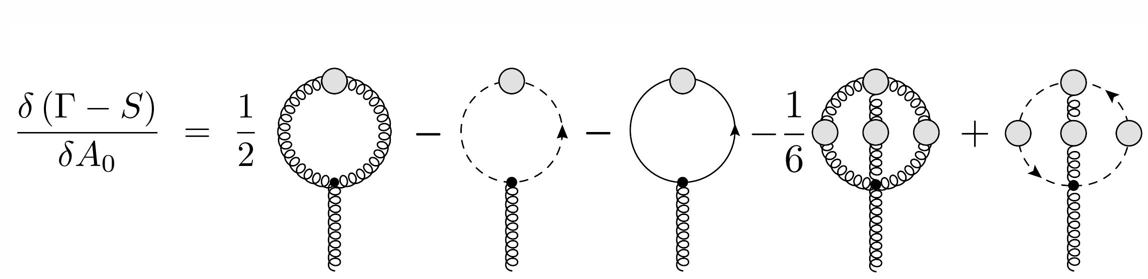

Fister, JMP, PRD 88 (2013) 045010

Phase structure at finite density

Phase diagram of 2+1 flavor QCD

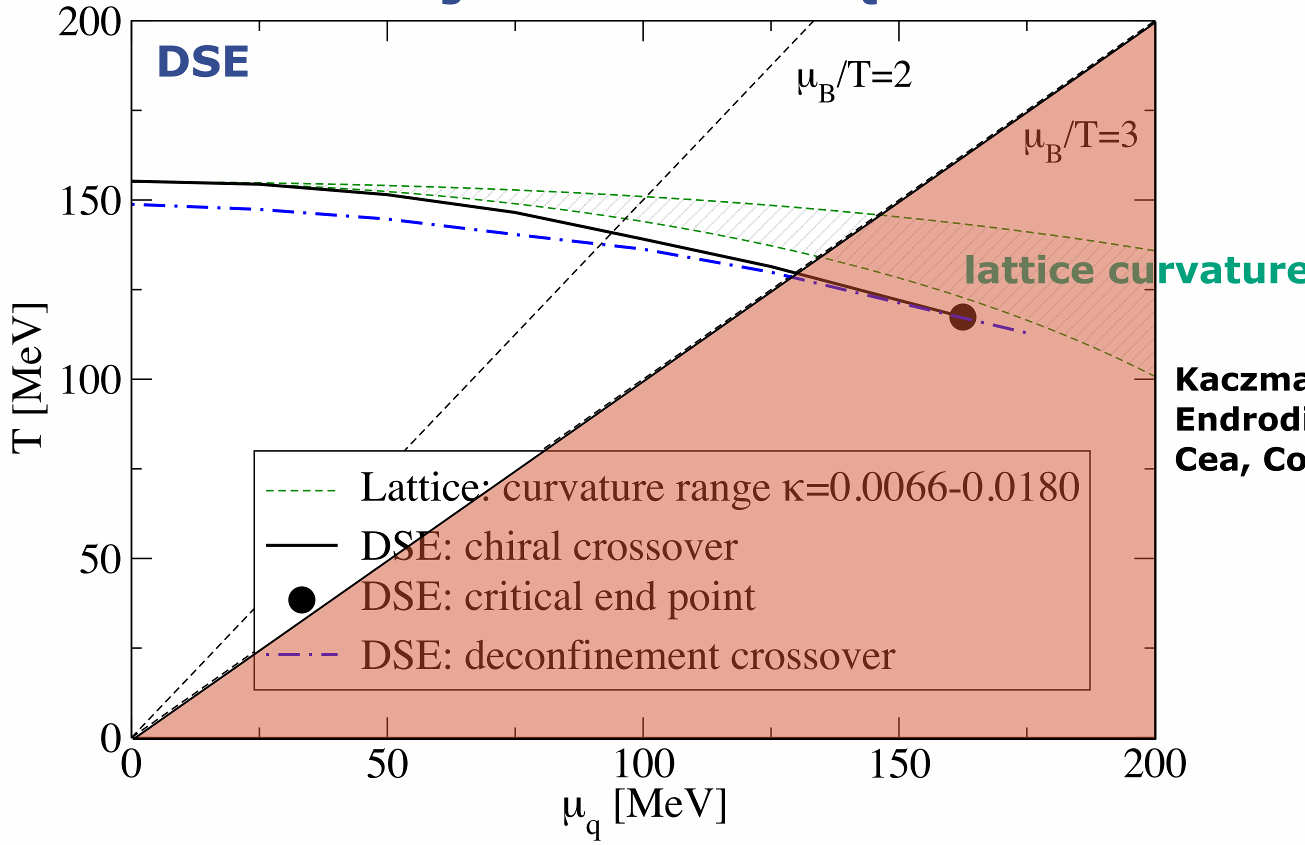

Kaczmarek at al. '11
Endrodi, Fodor, Katz, Szabo '11
Cea, Cosmai, Papa '14

Fischer, Fister, Luecker, JMP, PLB732 (2014) 248

Fischer, Luecker, Welzbacher, PRD 90 (2014) 034022

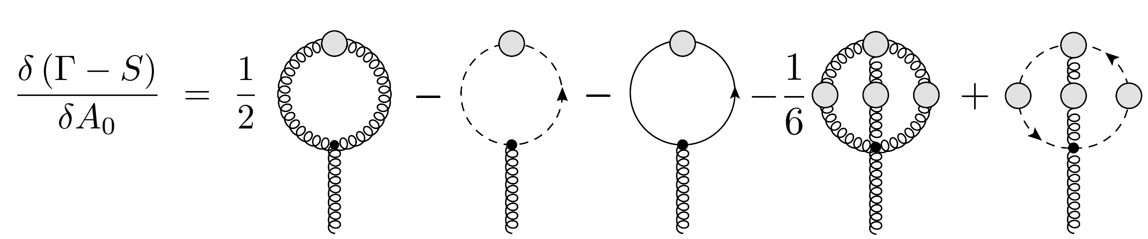

Fister, JMP, PRD 88 (2013) 045010

Phase structure at finite density

Phase diagram of 2+1 flavor QCD

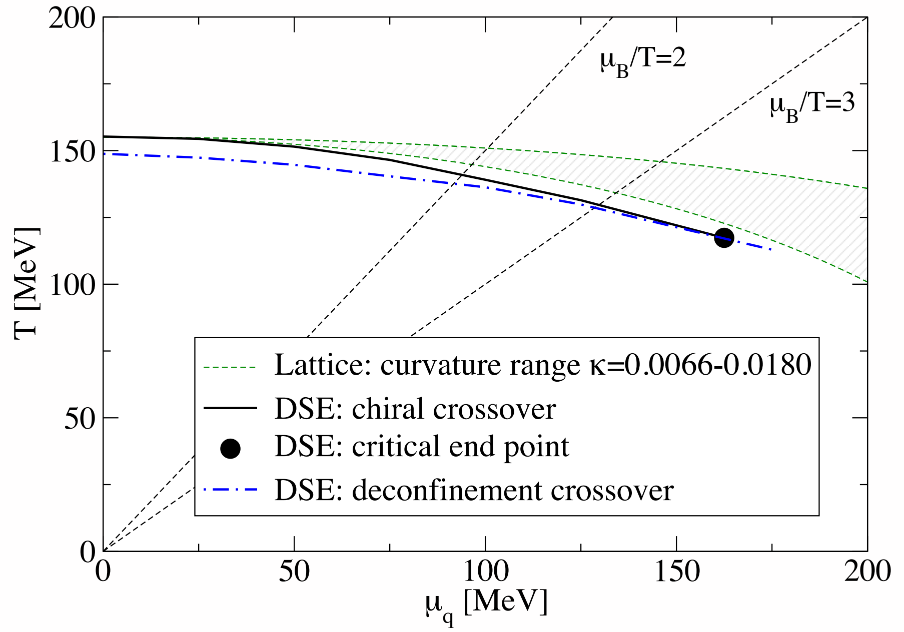

Phase diagram of quantised 2-flavor PQM-model

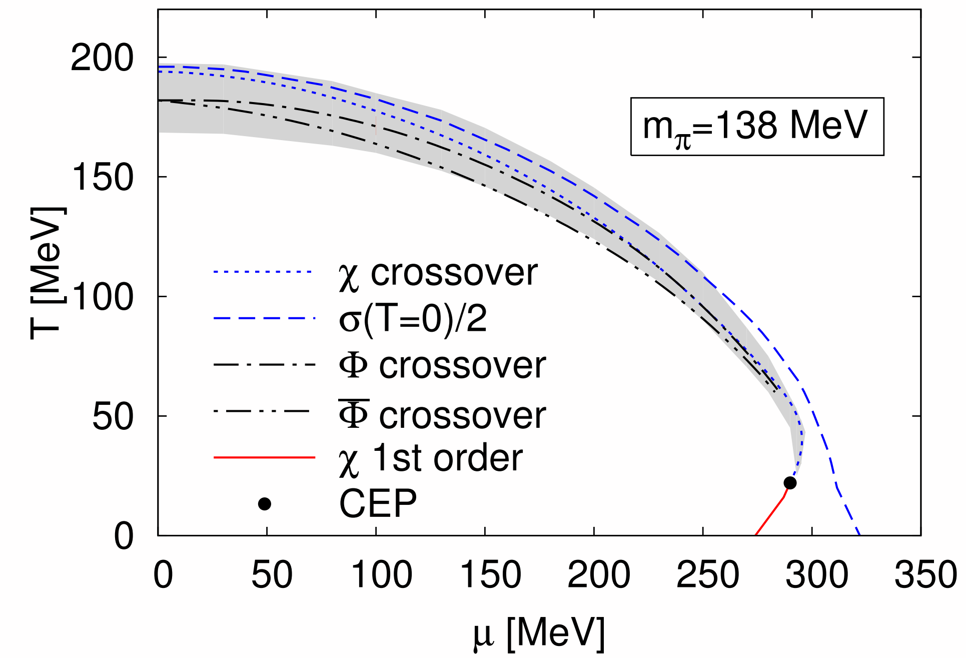

Comparison with 2 flavor vs 2+1 flavor scale matching of T_c

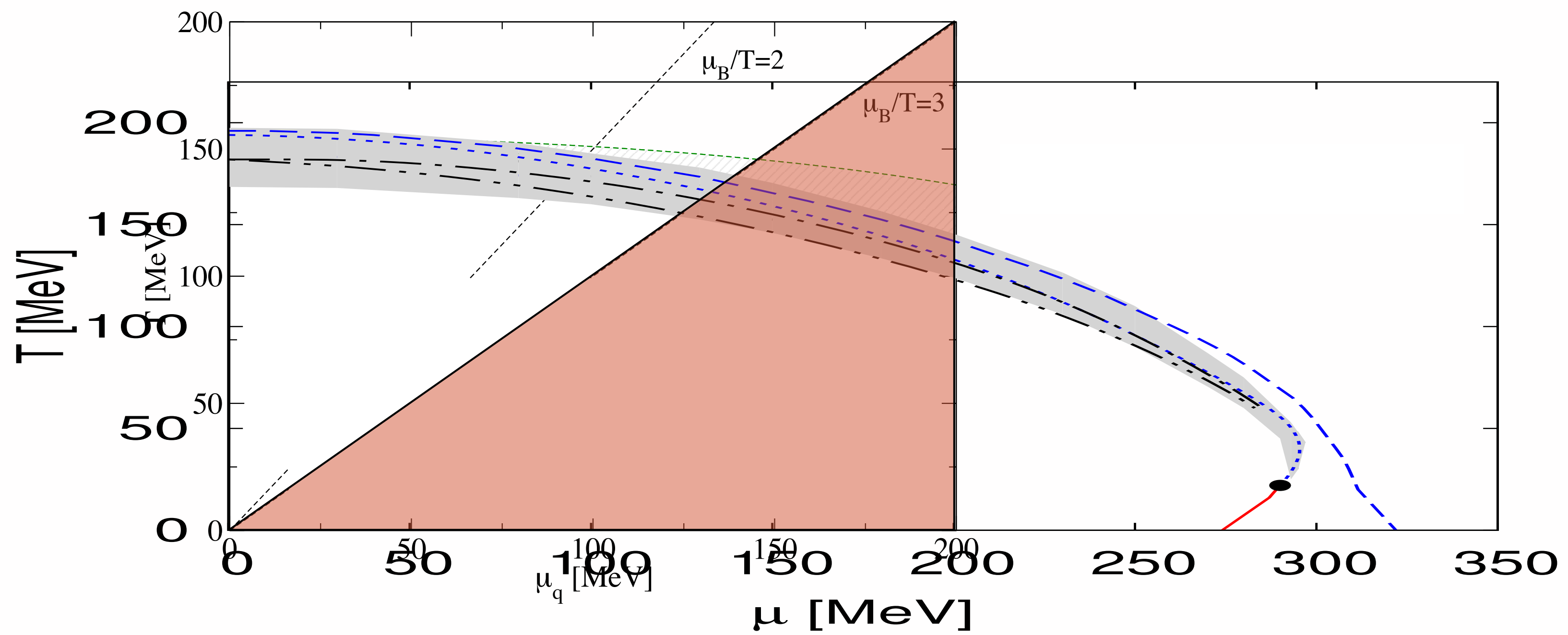

Phase structure at finite density for heavy quarks

Polyakov loop at finite density

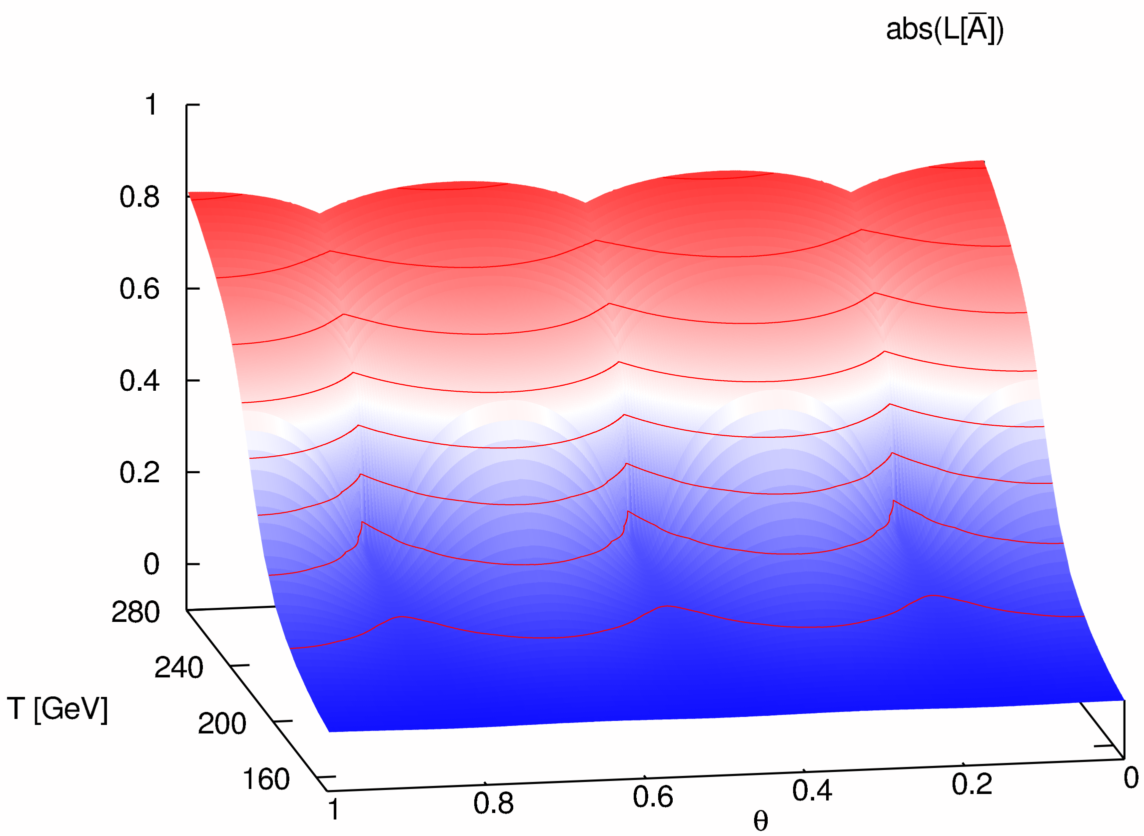

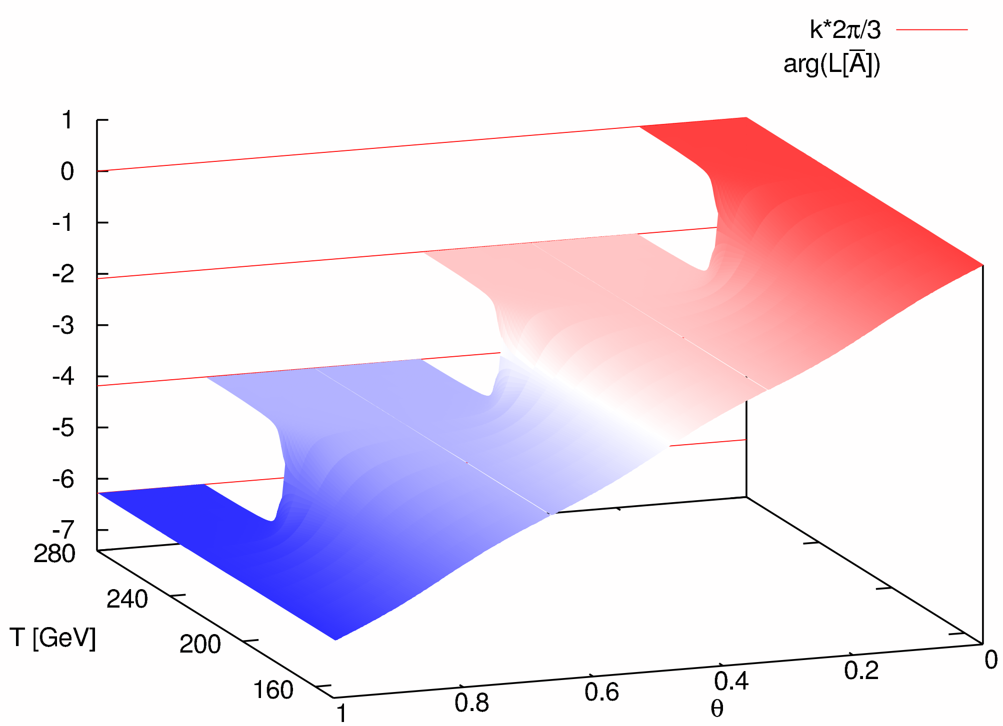

Critical surface at large masses

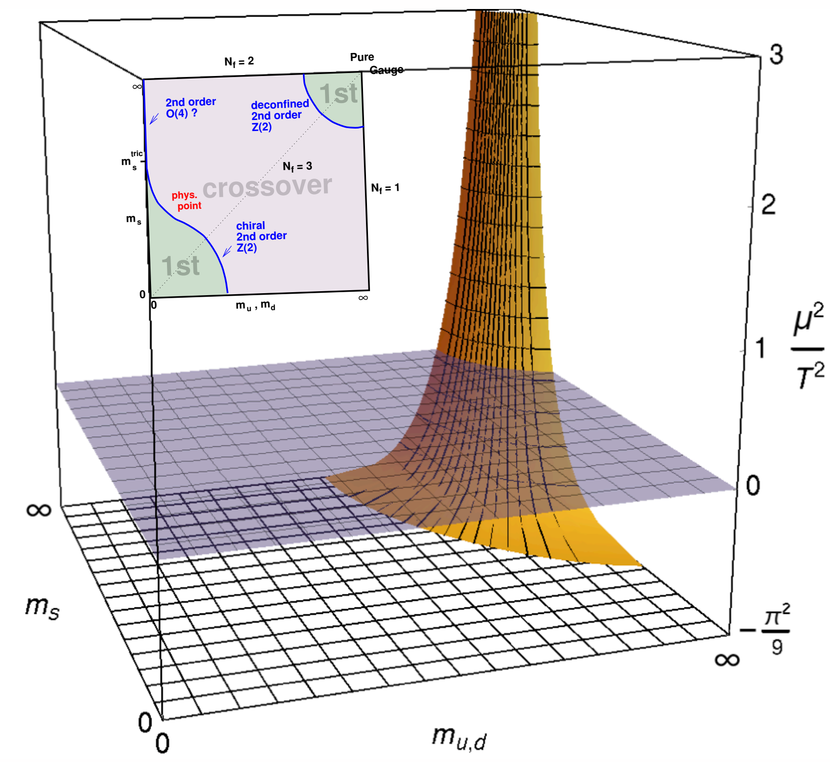

Tricritical scaling

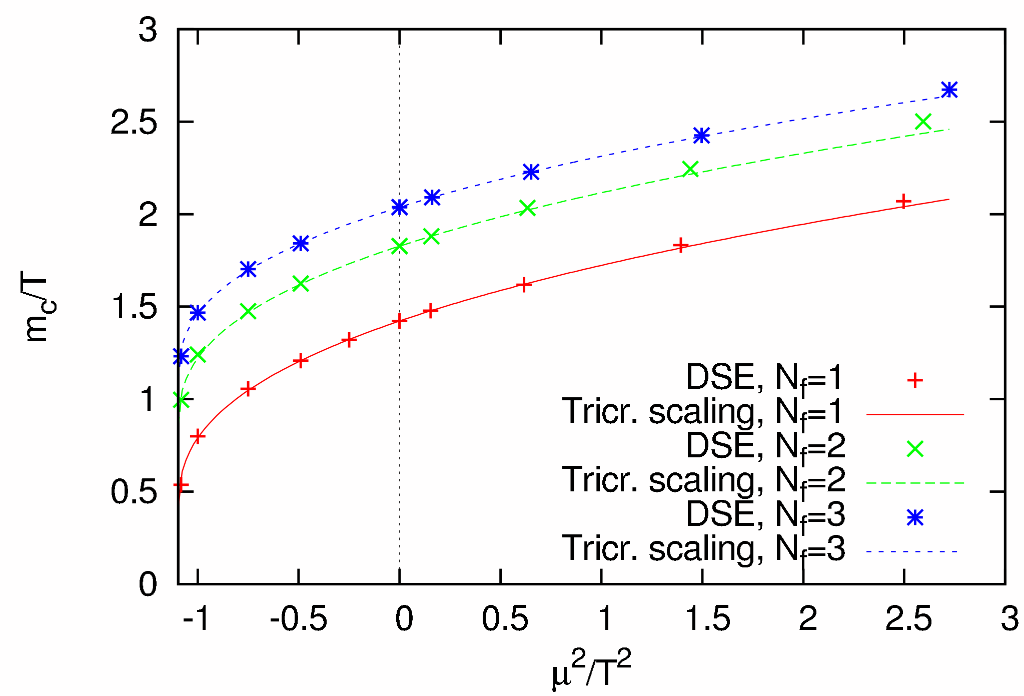

lattice see eg: Bonati, de Forcrand, D'Elia, Philipsen, Sanfilippo, PRD 90 (2014) 7, 074030

Fischer, Luecker, JMP, PRD 91 (2015) 1, 014024

Outline

- Vacuum QCD & the hadron spectrum
- Phase structure of QCD
- Spectral Functions & Transport Coefficients
- Outlook

Dynamics

Shooting the elephant

Proof of principle calculation:

Zhi Qiu and U. Heinz, to be published

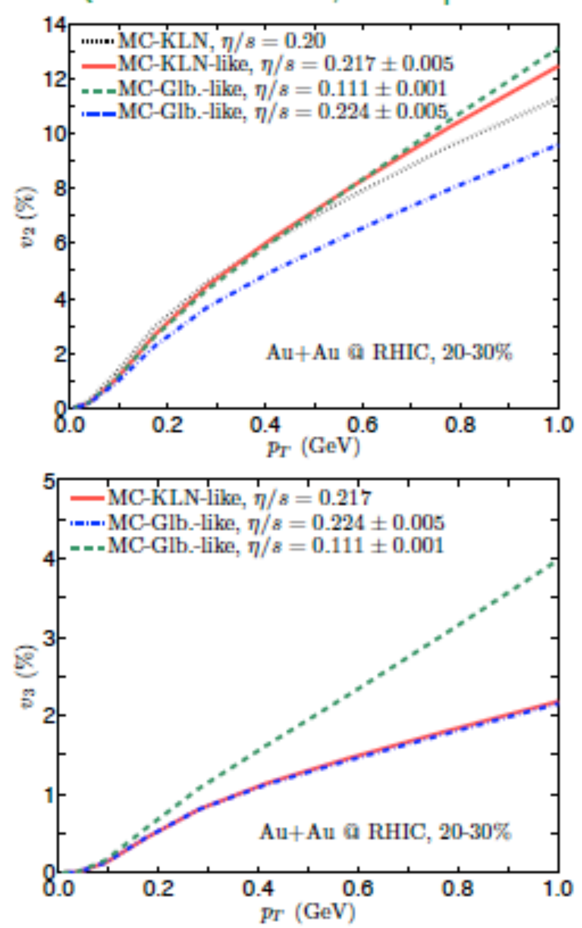

- Take ensemble of sum of deformed Gaussian profiles, $s(\boldsymbol{r}_\perp) = s_2(\boldsymbol{r}_\perp; \bar\varepsilon_2, \psi_2) + s_3(\boldsymbol{r}_\perp; \bar\varepsilon_3, \psi_3)$, with
  1. equal Gaussian radii $R_2^2 = R_3^2 = 8\,\mathrm{fm}^2$ to reproduce $\langle r_\perp^2 \rangle$ of MC-KLN source for 20-30% AuAu
  2. $\bar\varepsilon_2$ and $\bar\varepsilon_3$ adjusted such that
     - $\bar\varepsilon_{2,3} = \langle \varepsilon_{2,3} \rangle_{\mathrm{KLN}}^{20-30\%}$ ("MC-KLN-like")
     - $\bar\varepsilon_{2,3} = \langle \varepsilon_{2,3} \rangle_{\mathrm{Gl}}^{20-30\%}$ ("MC-Glauber-like")
  3. $\psi_2 = 0$, ψ_3 (direction of triangularity) distributed randomly
- Use $v_2^\pi(p_T)$ from VISH2+1 for $\eta/s = 0.20$ with MC-KLN initial conditions for 20-30% AuAu as "mock data"
- Fit mock $v_2^\pi(p_T)$ data with VISH2+1 for "MC-Glauber-like" or "MC-KLN-like" Gaussian initial conditions with both elliptic and triangular deformations by adjusting η/s
  $\Longrightarrow$ $(\eta/s)_{\mathrm{KLN}} = 0.217 \pm 0.005$ for "MC-KLN-like",
  $(\eta/s)_{\mathrm{Gl}} = 0.111 \pm 0.001$ for "MC-Glauber-like"
- Compute $v_3^\pi(p_T)$ for "MC-KLN-like" fit with $(\eta/s)_{\mathrm{Gl}}$=0.217 and reproduce it with "MC-Glauber-like" initial condition by readjusting η/s
  $\Longrightarrow$ $(\eta/s)_{\mathrm{Gl}}^{v_3} = 0.224 \pm 0.005$ for "MC-Glauber-like"
- Compute $v_2^\pi(p_T)$ for "MC-Glauber-like" initial profiles with readjusted $(\eta/s)_{\mathrm{Gl}}^{v_3} = 0.224$ and compare with "MC-Glauber-like" fit to original mock data $\Longrightarrow$ clearly visible (and measurable) difference!

This exercise proves: (i) Fitting $v_3(p_T)$ data with MC-Glauber and MC-KLN initial conditions yields the same η/s (within narrow error band); (ii) The corresponding $v_2(p_T)$ fits are quite different, and only one (more precisely: at most one!) of the models will fit the corresponding $v_2(p_T)$ data.

U. Heinz, talk at RETUNE '12

Dynamics

Computing the elephant

Proof of principle calculation:

Zhi Qiu and U. Heinz, to be published

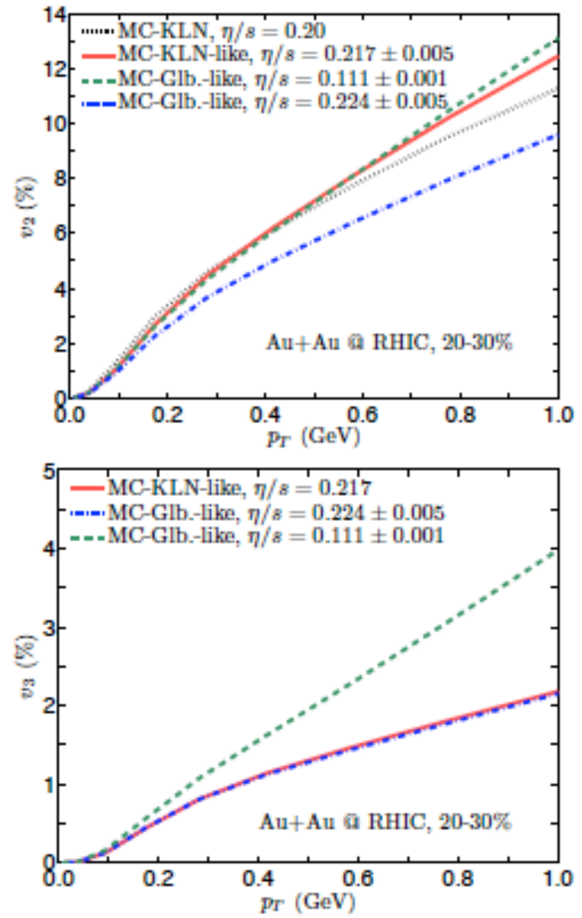

- Take ensemble of sum of deformed Gaussian profiles, $s(\boldsymbol{r}_\perp) = s_2(\boldsymbol{r}_\perp; \bar{\varepsilon}_2, \psi_2) + s_3(\boldsymbol{r}_\perp; \bar{\varepsilon}_3, \psi_3)$, with
  1. equal Gaussian radii $R_2^2 = R_3^2 = 8\,\mathrm{fm}^2$ to reproduce $\langle r_\perp^2 \rangle$ of MC-KLN source for 20-30% AuAu
  2. $\bar{\varepsilon}_2$ and $\bar{\varepsilon}_3$ adjusted such that
     - $\bar{\varepsilon}_{2,3} = \langle \varepsilon_{2,3} \rangle_{\mathrm{KLN}}^{20-30\%}$ ("MC-KLN-like")
     - $\bar{\varepsilon}_{2,3} = \langle \varepsilon_{2,3} \rangle_{\mathrm{Gl}}^{20-30\%}$ ("MC-Glauber-like")
  3. $\psi_2 = 0$, ψ_3 (direction of triangularity) distributed randomly
- Use $v_2^\pi(p_T)$ from VISH2+1 for $\eta/s = 0.20$ with MC-KLN initial conditions for 20-30% AuAu as "mock data"
- Fit mock $v_2^\pi(p_T)$ data with VISH2+1 for "MC-Glauber-like" or "MC-KLN-like" Gaussian initial conditions with both elliptic and triangular deformations by adjusting η/s
  $\Longrightarrow (\eta/s)_{\mathrm{KLN}} = 0.217 \pm 0.005$ for "MC-KLN-like",
  $(\eta/s)_{\mathrm{Gl}} = 0.111 \pm 0.001$ for "MC-Glauber-like"
- Compute $v_3^\pi(p_T)$ for "MC-KLN-like" fit with $(\eta/s)_{\mathrm{Gl}}$=0.217 and reproduce it with "MC-Glauber-like" initial condition by readjusting η/s
  $\Longrightarrow (\eta/s)_{\mathrm{Gl}}^{v3} = 0.224 \pm 0.005$ for "MC-Glauber-like"
- Compute $v_2^\pi(p_T)$ for "MC-Glauber-like" initial profiles with readjusted $(\eta/s)_{\mathrm{Gl}}^{v3} = 0.224$ and compare with "MC-Glauber-like" fit to original mock data $\Longrightarrow$ clearly visible (and measurable) difference!

This exercise proves: (i) Fitting $v_3(p_T)$ data with MC-Glauber and MC-KLN initial conditions yields the same η/s (within narrow error band); (ii) The corresponding $v_2(p_T)$ fits are quite different, and only one (more precisely: at most one!) of the models will fit the corresponding $v_2(p_T)$ data.

computing transport coefficients

Dynamics

gluon spectral function at finite T

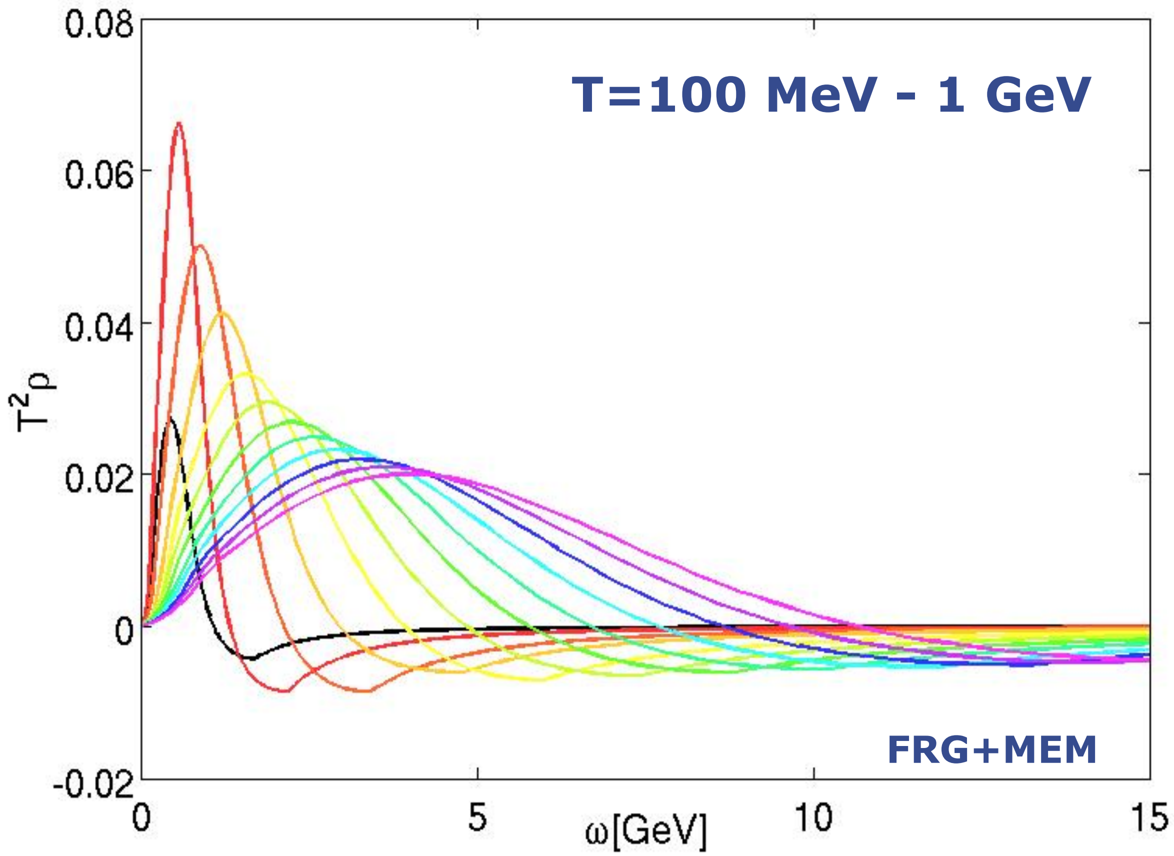

transversal

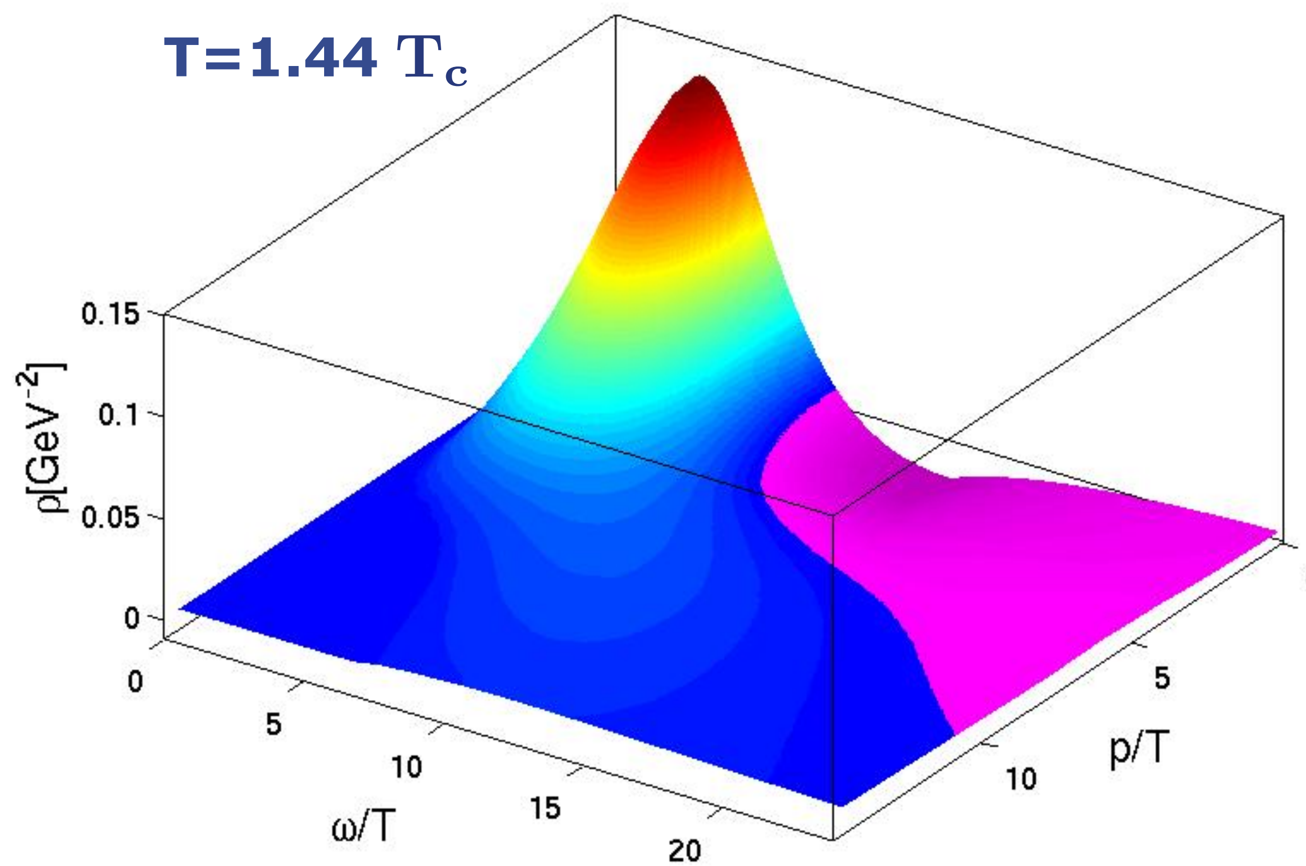

MEM

Haas, Fister, JMP, PRD 90 (2014) 9, 091501

Dynamics

gluon spectral function at finite T

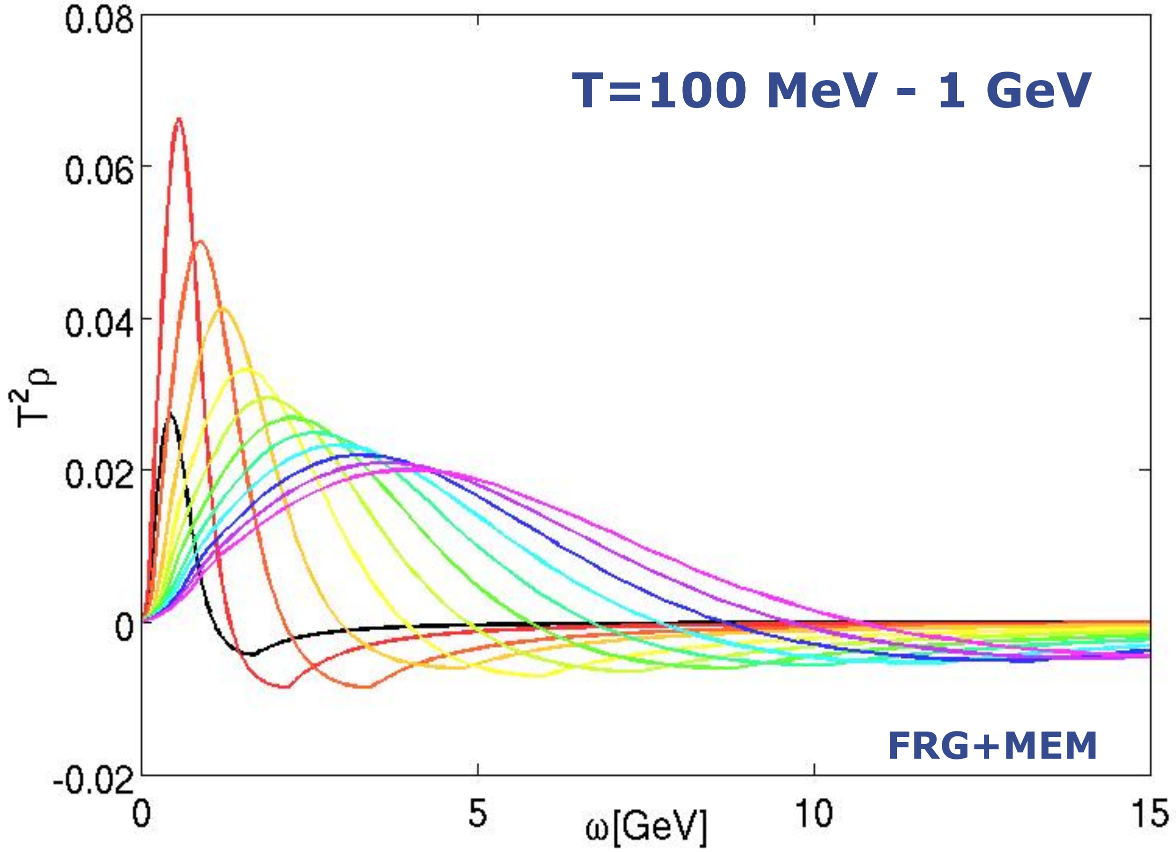

transversal

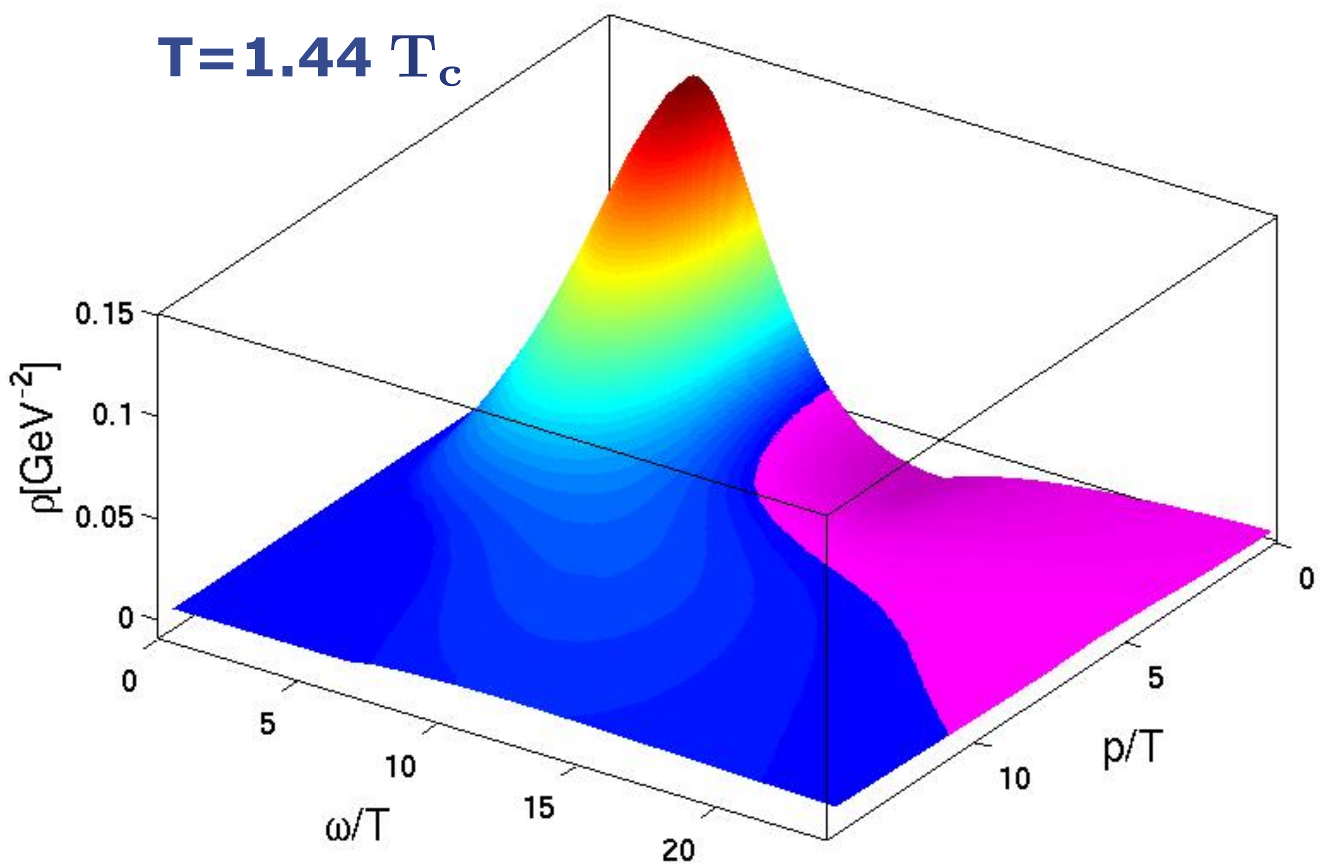

'Those are my methods (principles), and if you don't like them…well, I have others'

direct computation **Groucho Marx**

Haas, Fister, JMP, PRD 90 (2014) 9, 091501

Dynamics

gluon spectral functions

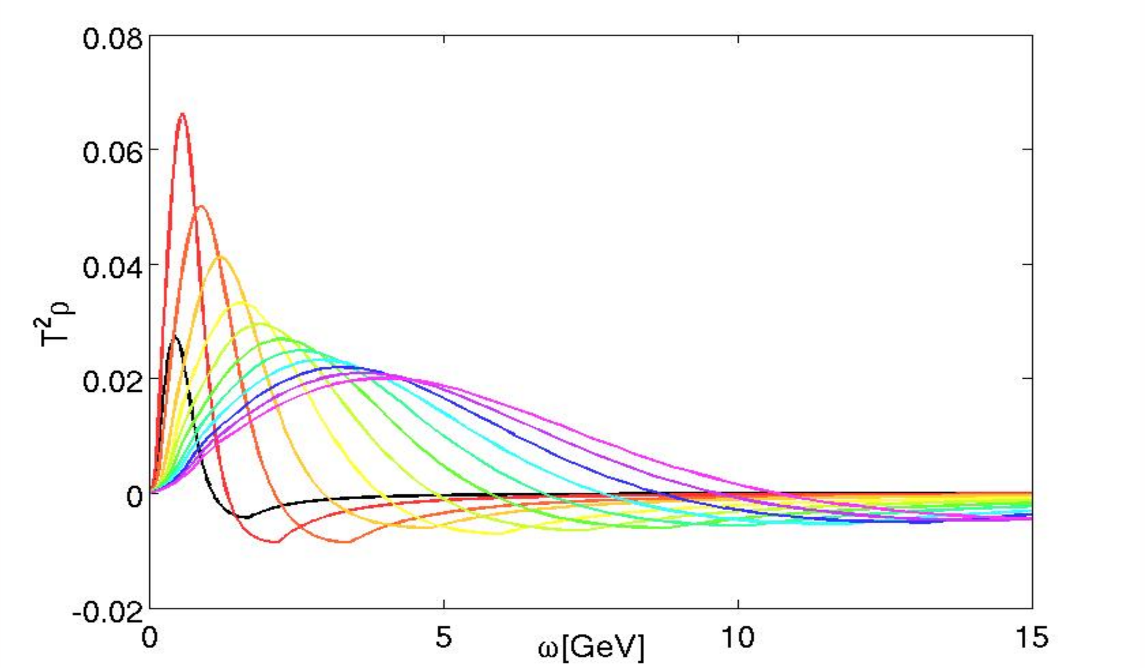

Haas, Fister, JMP, PRD 90 (2014) 9, 091501

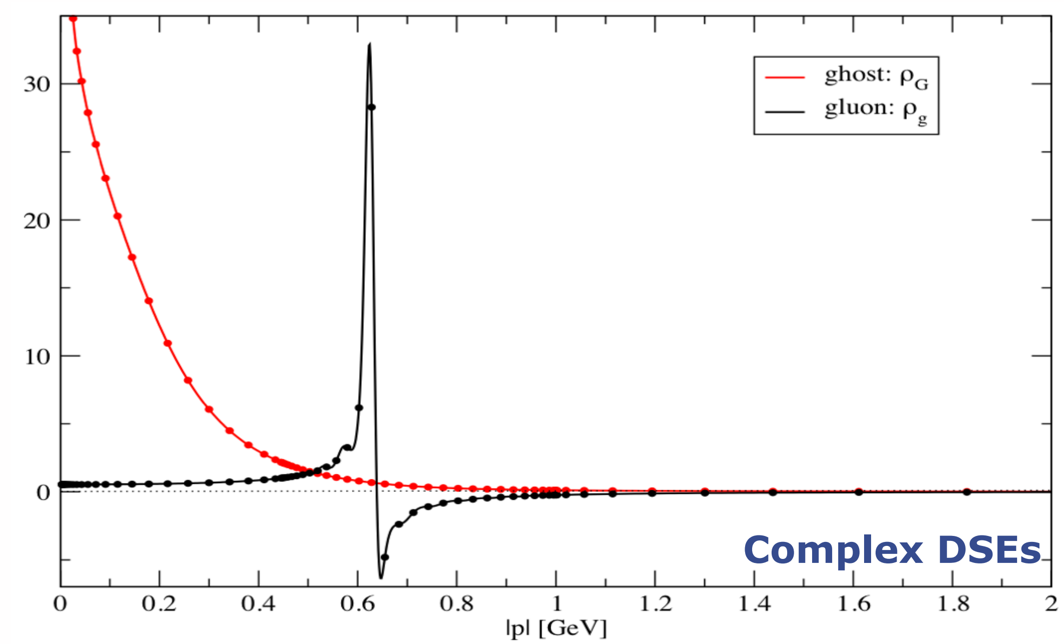

Strauss, Fischer, Kellermann, PRL 109 (2012) 252001

pion and sigma spectral functions

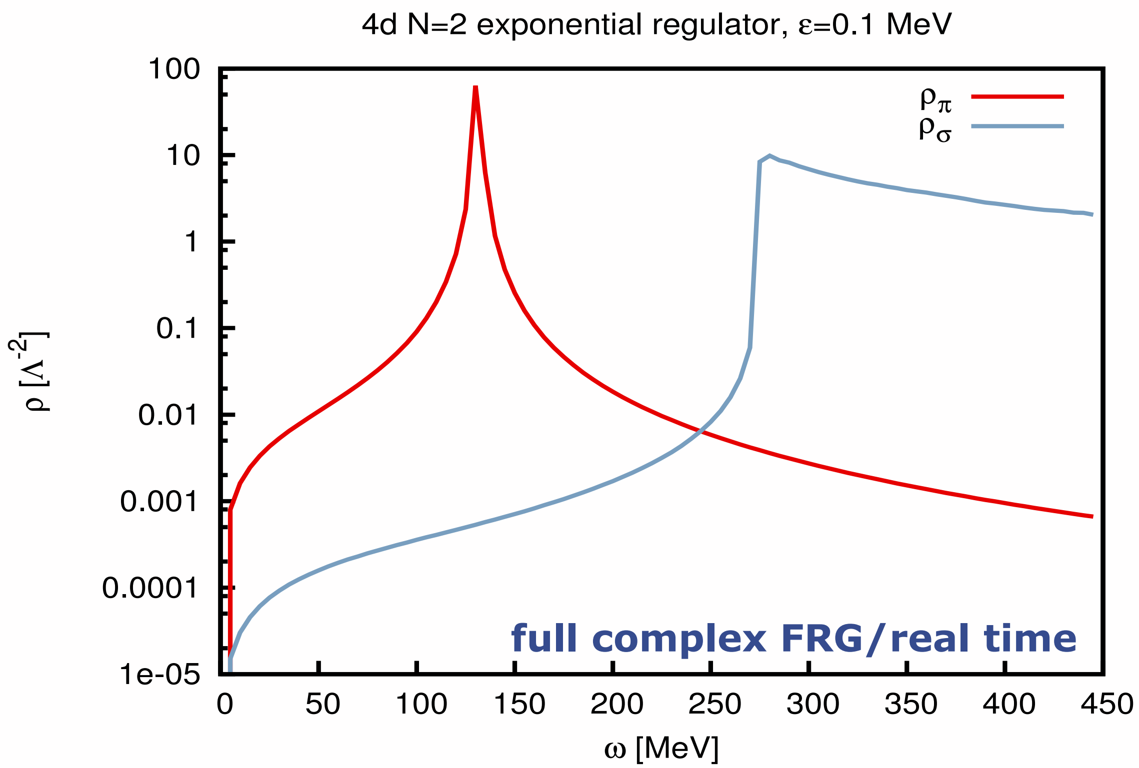

JMP, Strodthoff, in preparation

analytic complex FRG

Tripolt, Strodthoff, von Smekal, Wamach, PRD 89 (2014) 034010
Kamikado, Strodthoff, von Smekal, Wambach, EPJ C74 (2014) 2806

Dynamics

gluon spectral functions

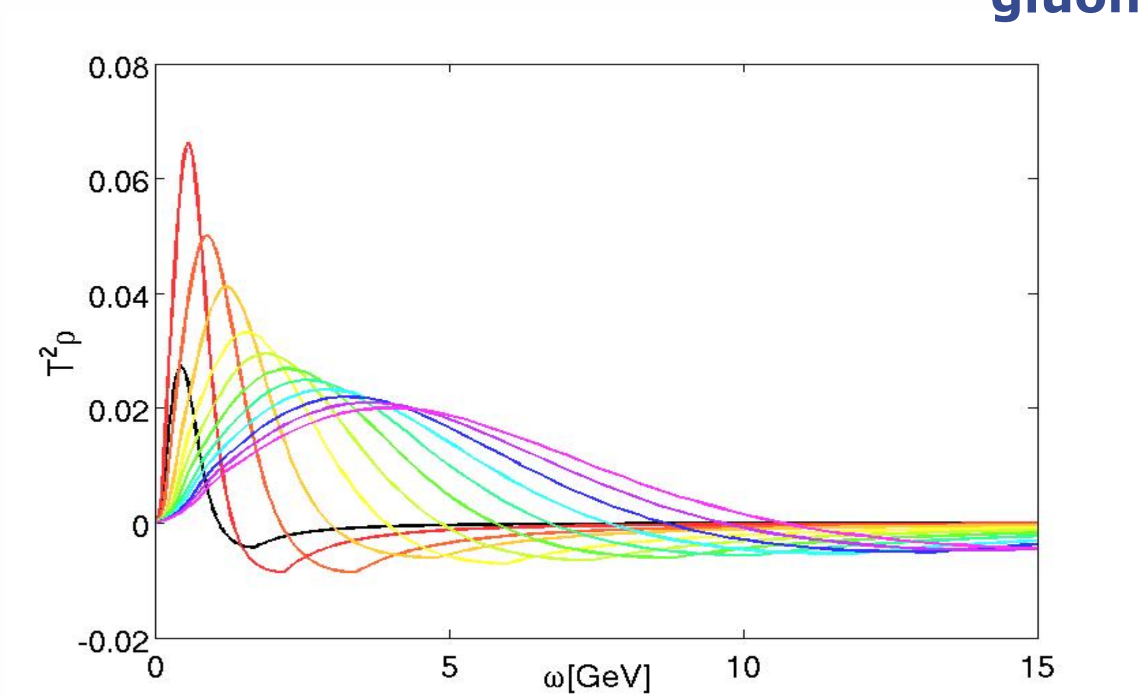

Haas, Fister, JMP, PRD 90 (2014) 9, 091501

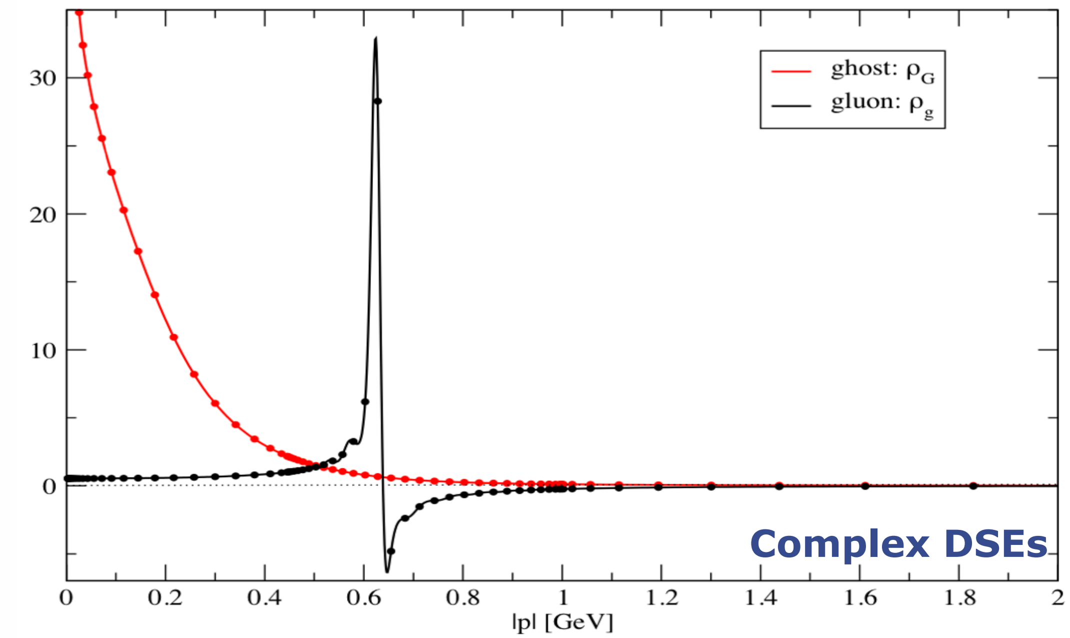

Strauss, Fischer, Kellermann, PRL 109 (2012) 252001

pion and sigma spectral functions

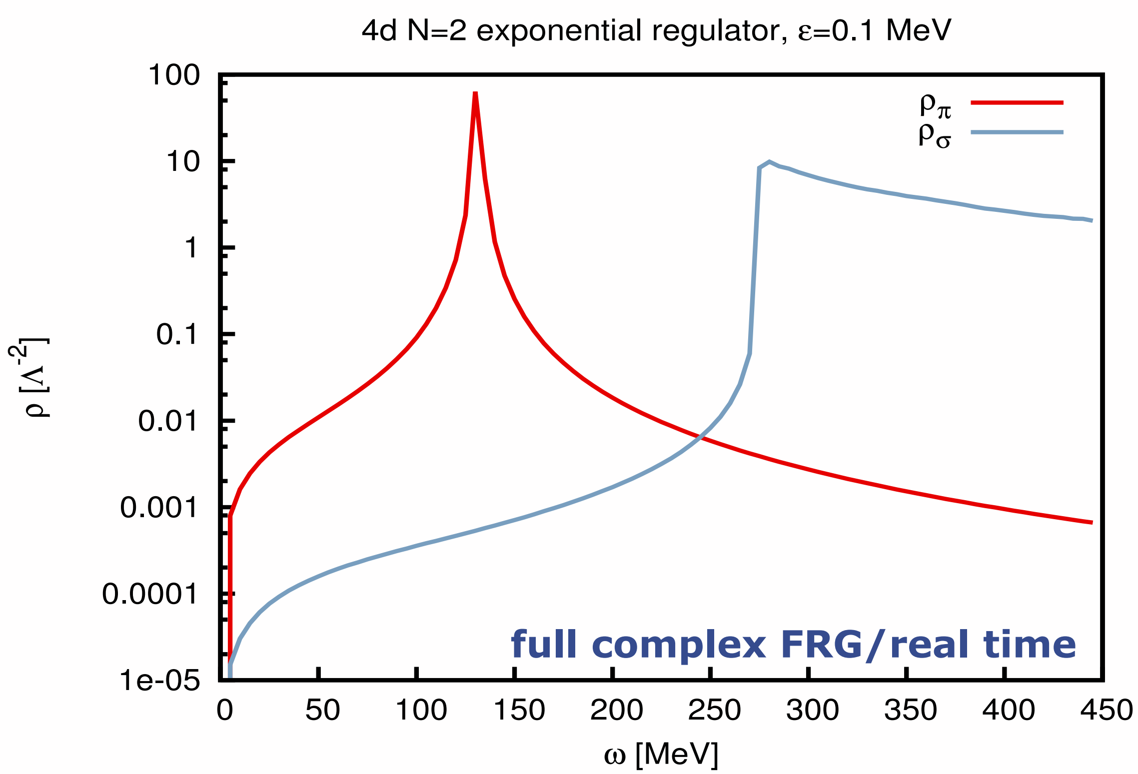

JMP, Strodthoff, in preparation

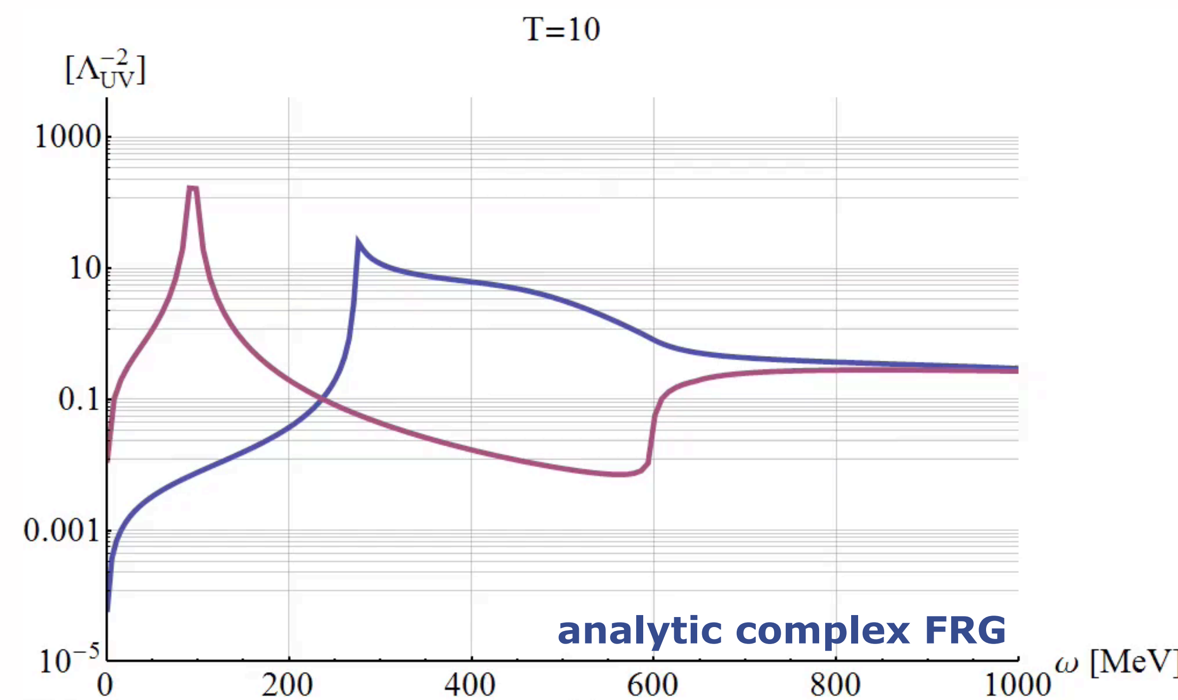

Tripolt, Strodthoff, von Smekal, Wamach, PRD 89 (2014) 034010
Kamikado, Strodthoff, von Smekal, Wambach, EPJ C74 (2014) 2806

Dynamics

gluon spectral functions

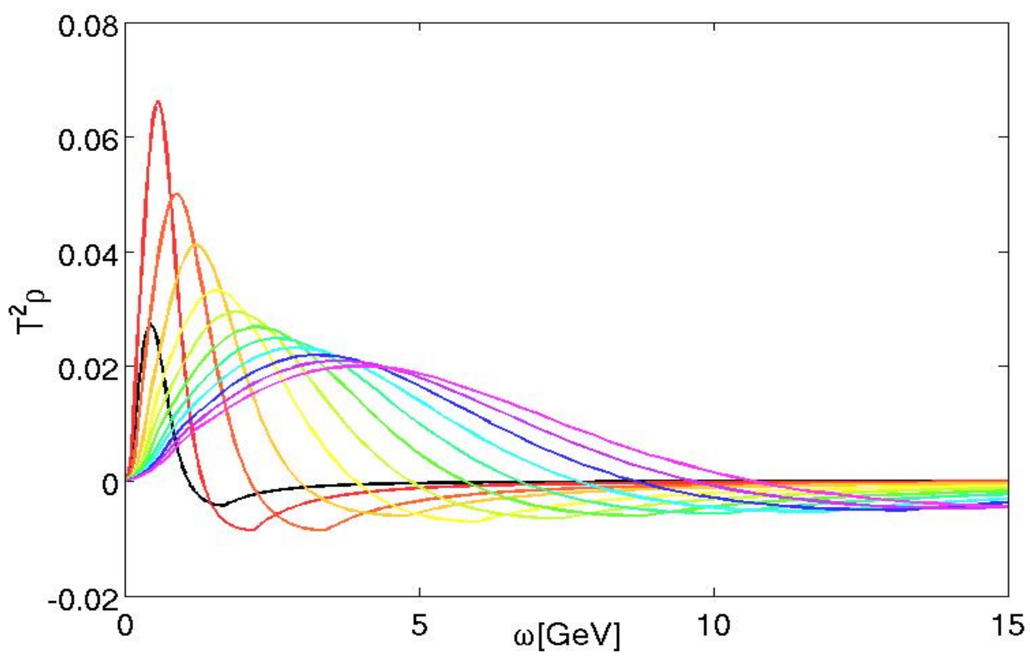

Haas, Fister, JMP, PRD 90 (2014) 9, 091501

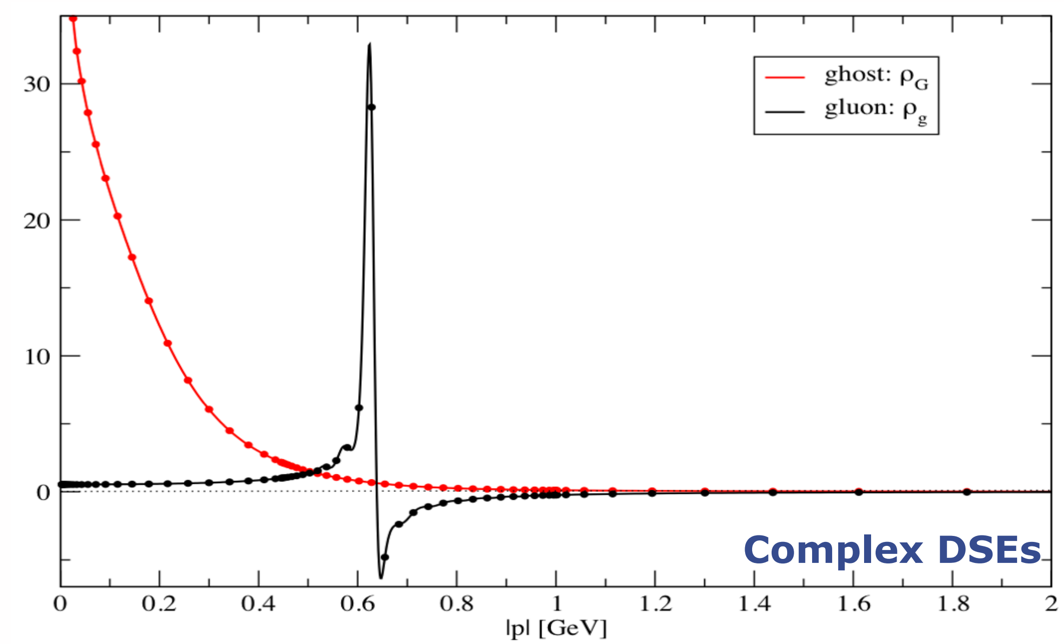

Strauss, Fischer, Kellermann, PRL 109 (2012) 252001

pion and sigma spectral functions

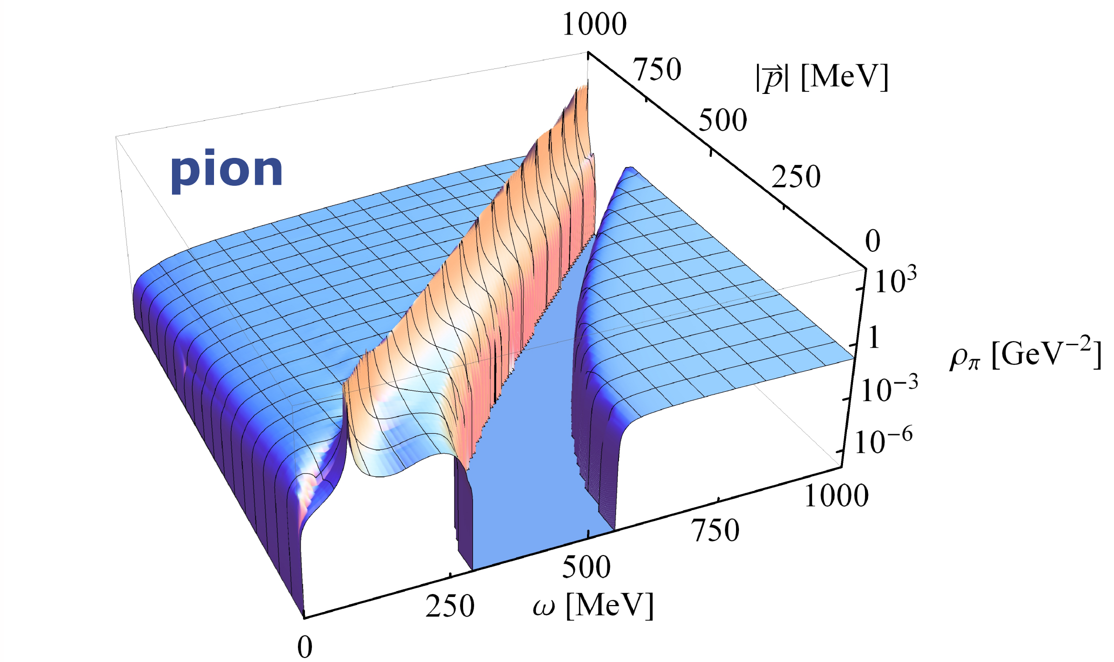

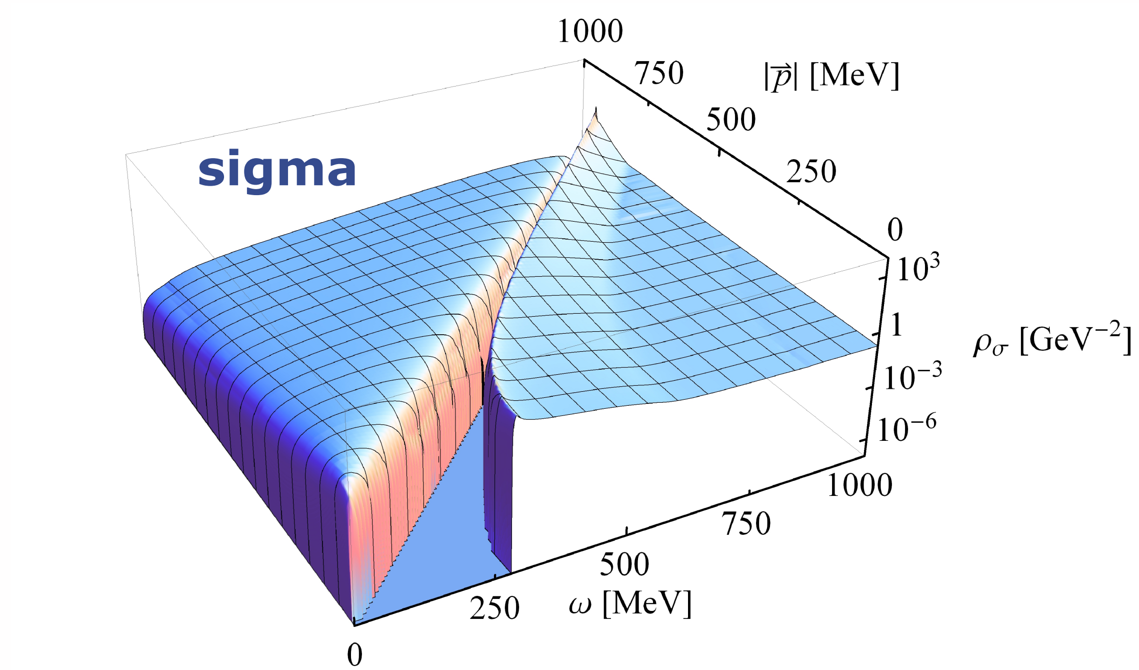

Tripolt, von Smekal, Wambach, Phys.Rev. D90 (2014) 7, 074031
Tripolt, PhD-thesis

Dynamics

transport coefficients

viscosity over entropy ratio

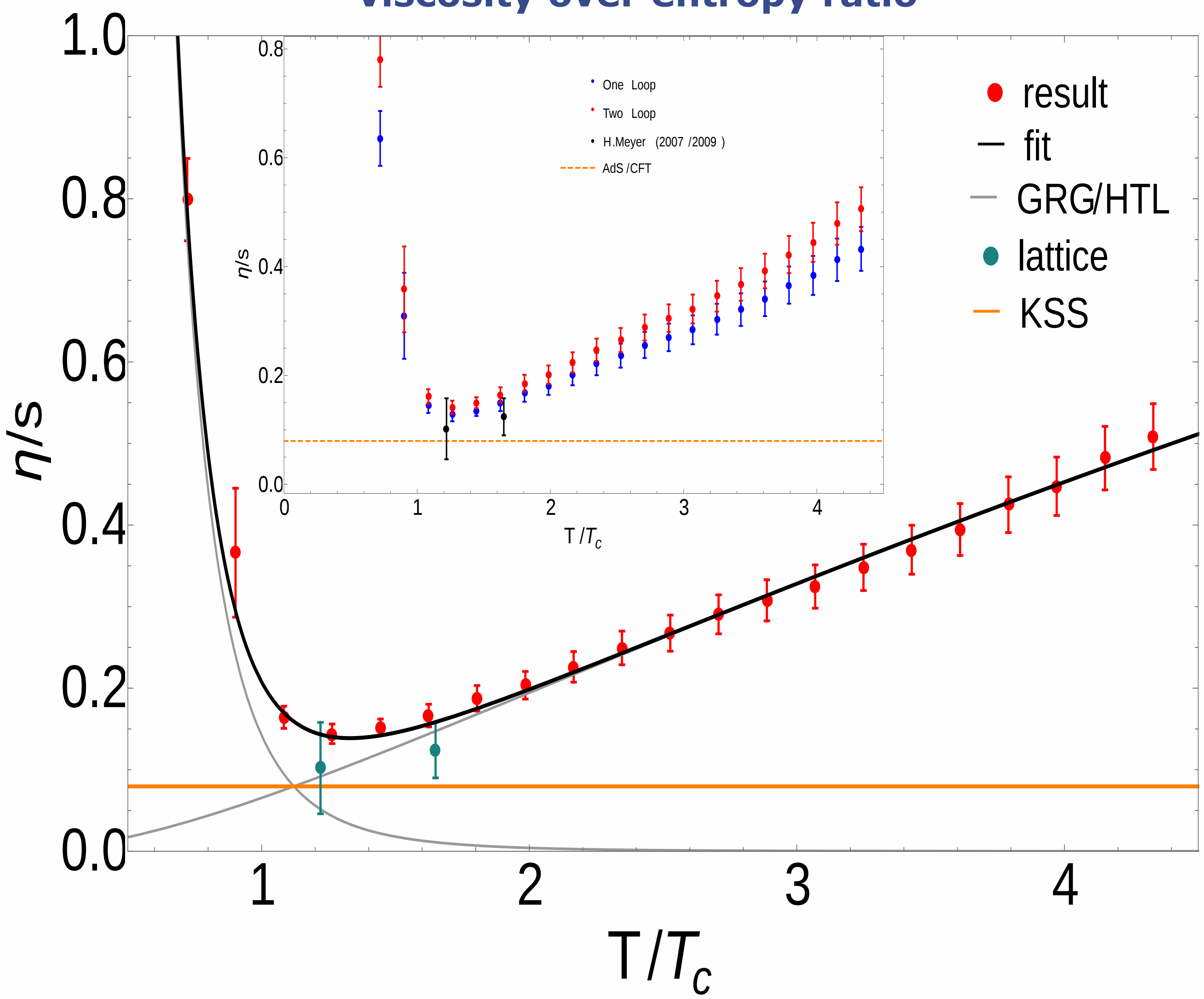

Kubo relation

$$\eta = \frac{1}{20}\,\frac{d}{d\omega}\bigg|_{\omega=0} \rho_{\pi\pi}(\omega, 0)$$

'3-loop' exact functional relation for $\rho_{\pi\pi}$

1 & 2-loop terms

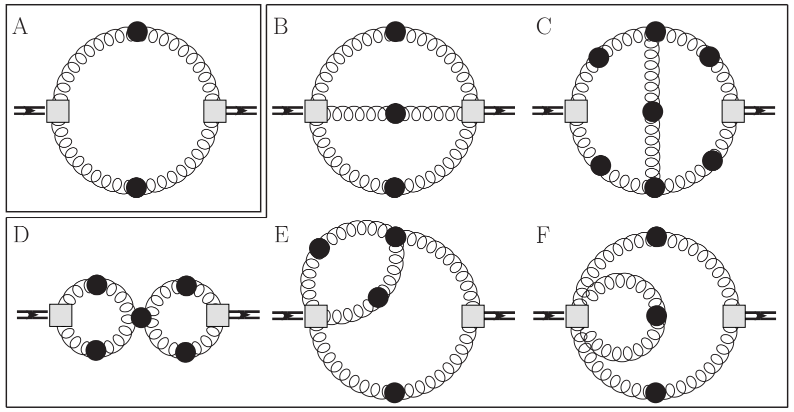

Haas, Fister, JMP, PRD 90 (2014) 9, 091501

Christiansen, Haas, JMP, Strodthoff, arXiv:1411.7986

Dynamics

QCD - estimate for viscosity over entropy ratio

viscosity over entropy ratio

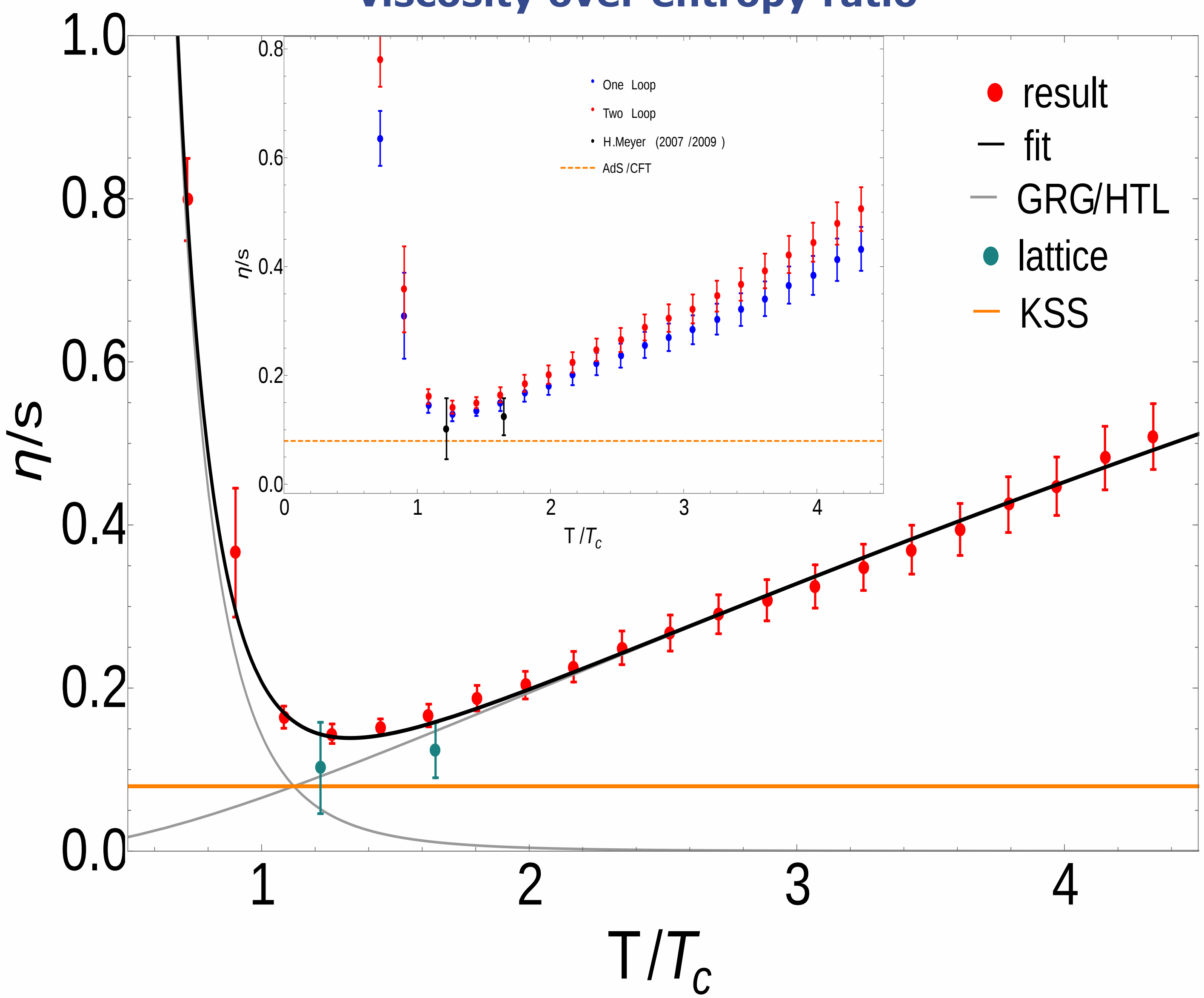

$$\frac{\eta}{s}(T) = \frac{a_{\rm qgp}}{\alpha_s^{\gamma_{\rm qgp}}(c\,T/T_c)} + \frac{a_{\rm grg}}{(T/T_c)^{\gamma_{\rm grg}}}$$

$$\gamma_{\rm grg} \approx 5$$

$$\gamma_{\rm qgp} \approx 1.6$$

pure glue

$$a_{\rm qgp} \approx 0.15$$

$$a_{\rm hrg} \approx 0.14$$

$$c \approx 0.66$$

Christiansen, Haas, JMP, Strodthoff, arXiv:1411.7986

Dynamics

QCD - estimate for viscosity over entropy ratio

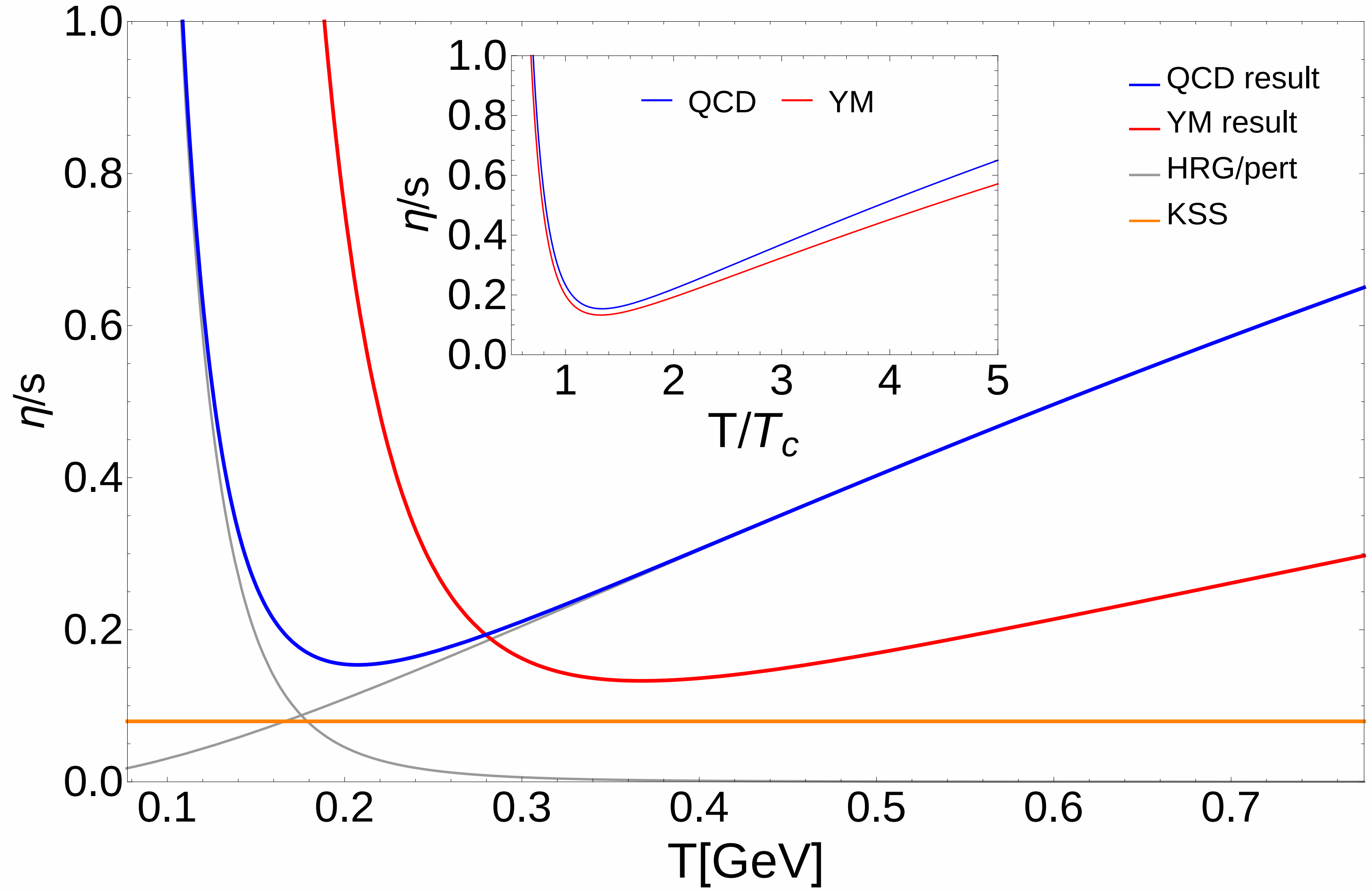

$$\frac{\eta}{s}(T) = \frac{a_{\rm qgp}}{\alpha_s^{\gamma_{\rm qgp}}(cT/T_c)} + \frac{a_{\rm grg}}{(T/T_c)^{\gamma_{\rm grg}}}$$

$$a_{\rm qgp} \approx 0.2$$
$$a_{\rm hrg} \approx 0.16$$
$$c \approx 0.79$$

QCD

$$\gamma_{\rm grg} \approx 5$$
$$\gamma_{\rm qgp} \approx 1.6$$

pure glue

$$a_{\rm qgp} \approx 0.15$$
$$a_{\rm hrg} \approx 0.14$$
$$c \approx 0.66$$

Christiansen, Haas, JMP, Strodthoff, arXiv:1411.7986

Summary & Outlook

Summary & Outlook

- **Chiral Symmetry Breaking and Confinement**

$$\frac{f_{\pi,\mathrm{FRG}}}{f_{\pi,\mathrm{lattice}}} = 0.99$$

quark propagator

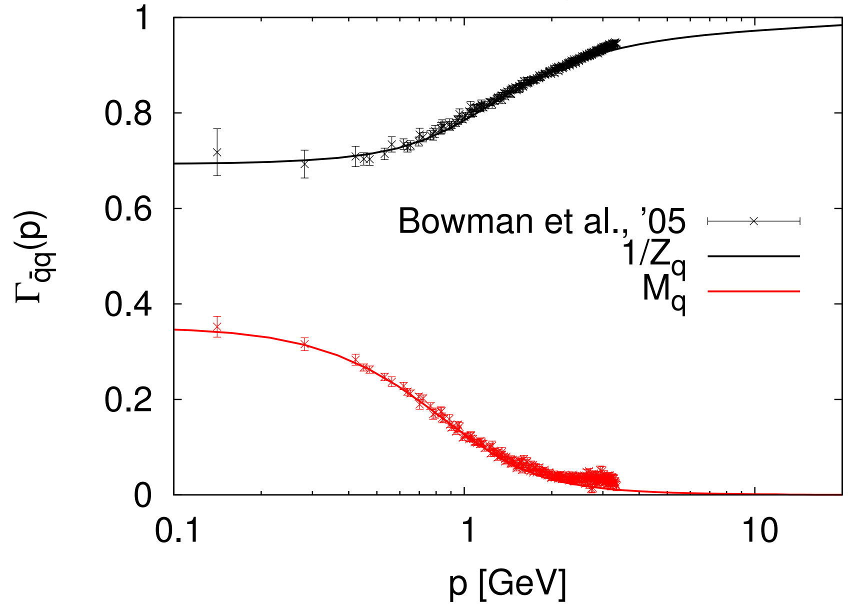

meson masses & decoupling

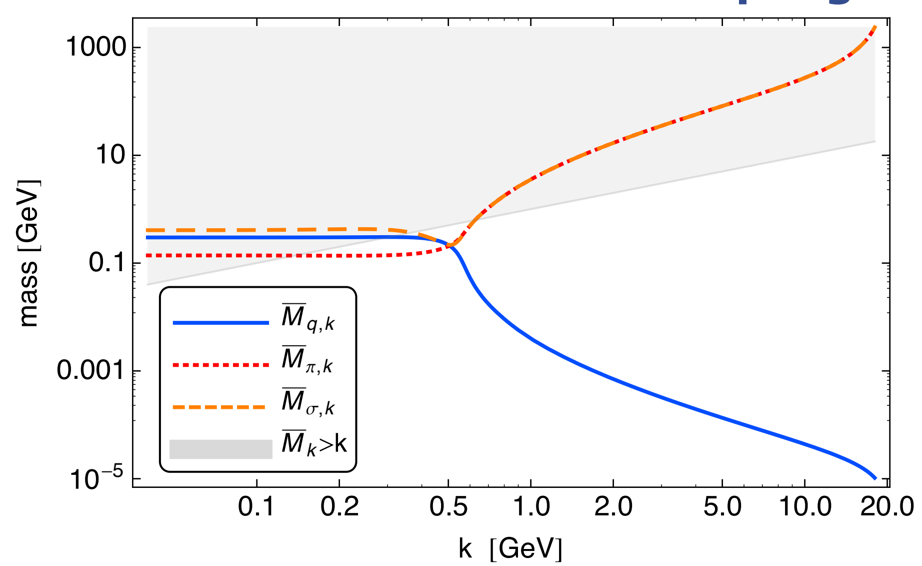

fQCD

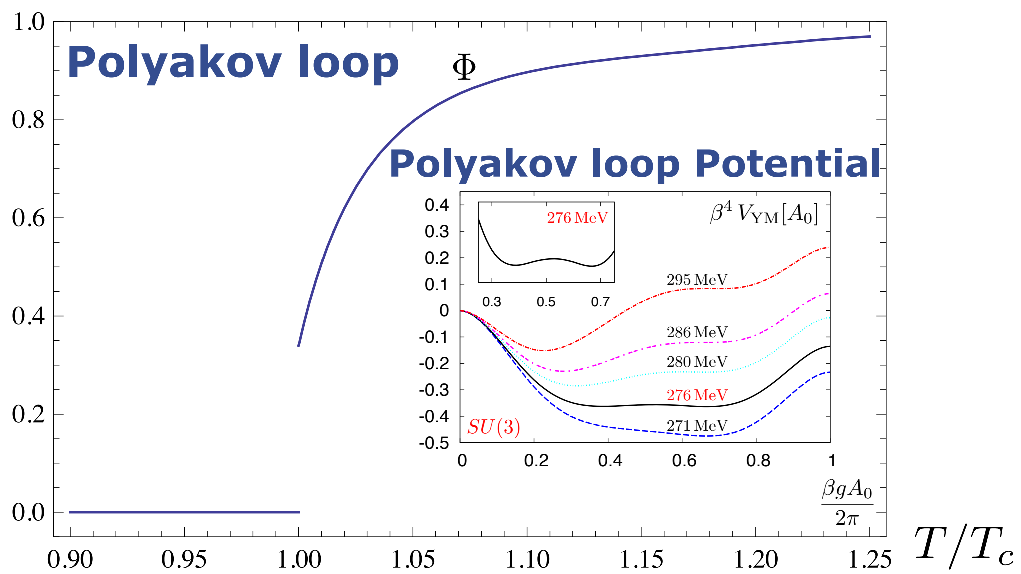

gluon propagator

no confinement without chiral symmetry breaking

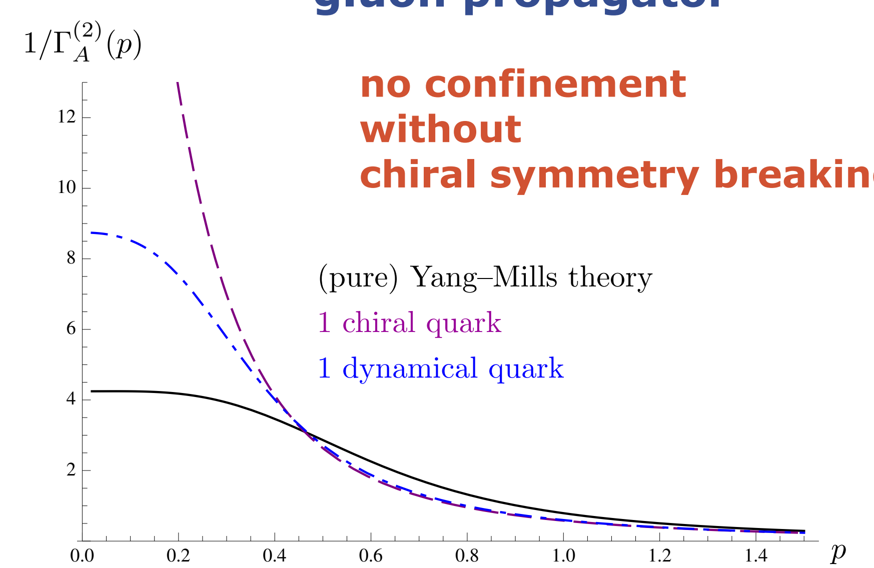

Summary & Outlook

- **Phase structure and Transport**

Phase structure at $\mu \in i\mathbb{R}$

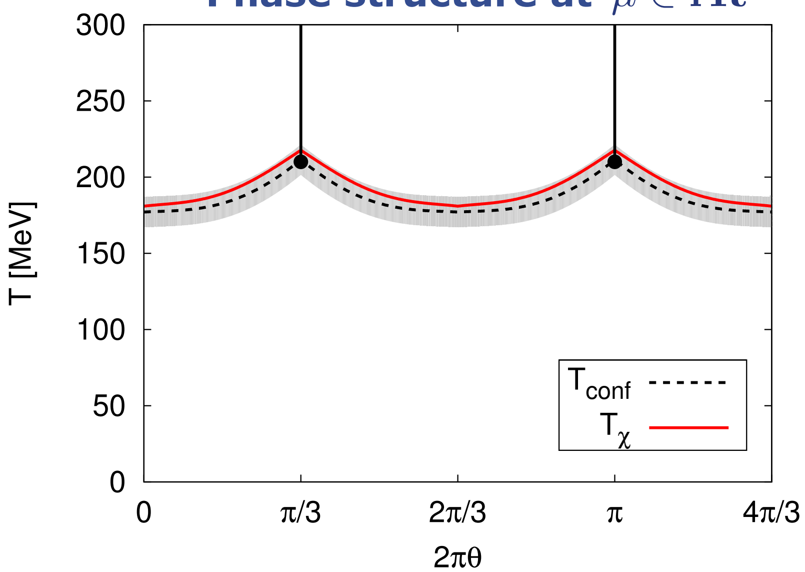

Interaction measure

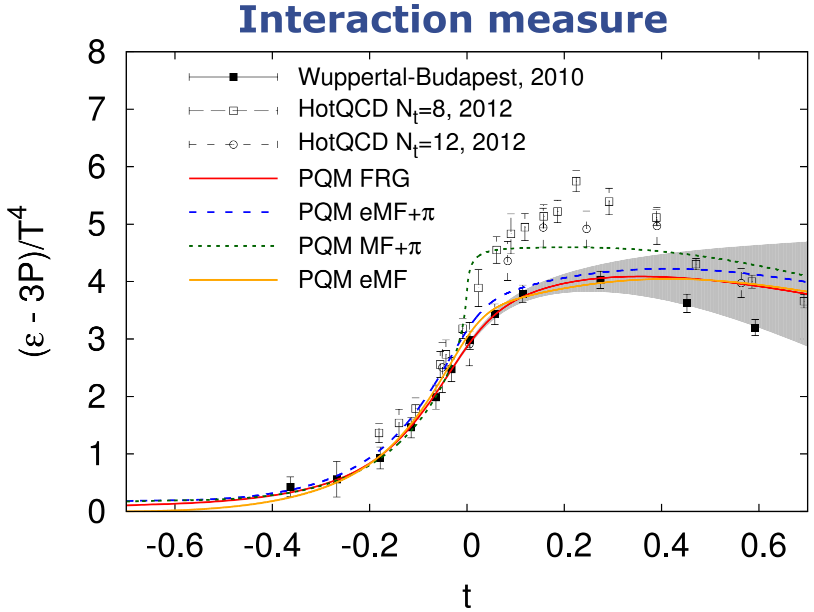

Phase structure at finite density

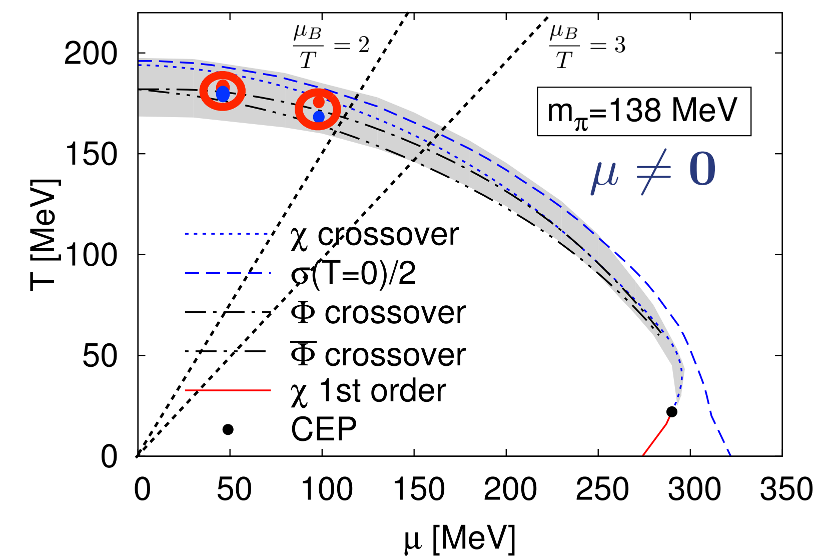

meson spectral fcts.

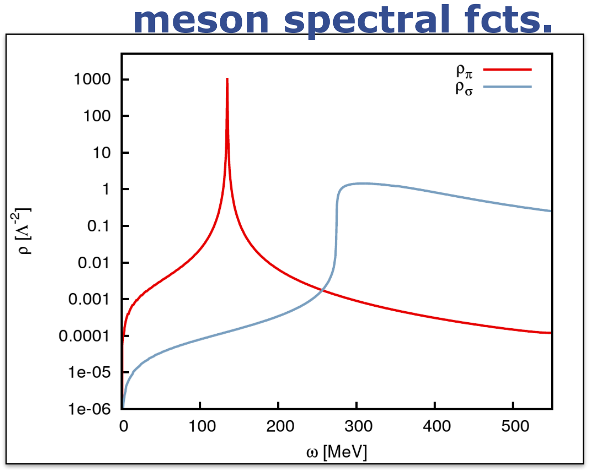

gluon spectral fcts.

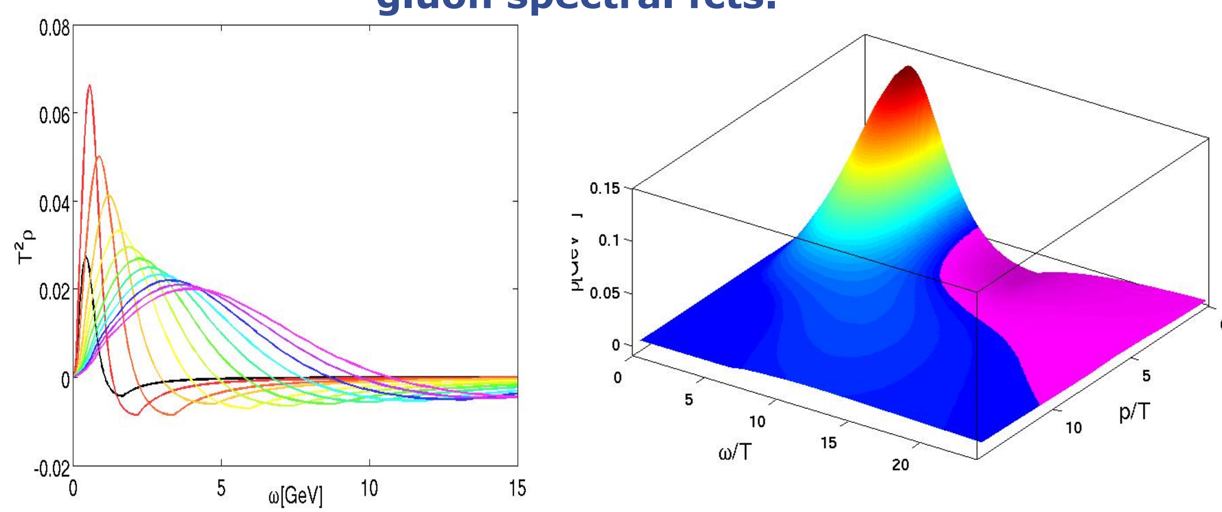

glue viscosity/entropy

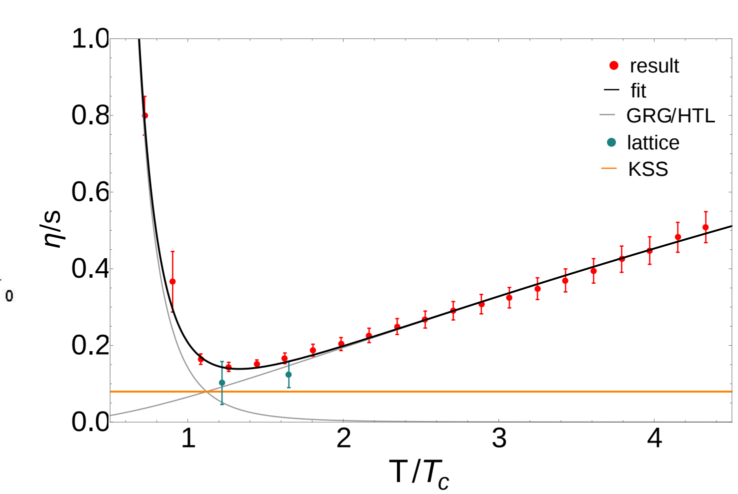

Summary & Outlook

- **Chiral Symmetry Breaking and Confinement**

- **Phase Structure and Transport**

- **Towards quantitative precision**

- **Baryons, high density regime & CEP, dynamics**

- **Hadronic properties**
  - **hadron spectrum & in medium modifications**
  - **low energy constants**

Additional material

Confinement & symmetry breaking

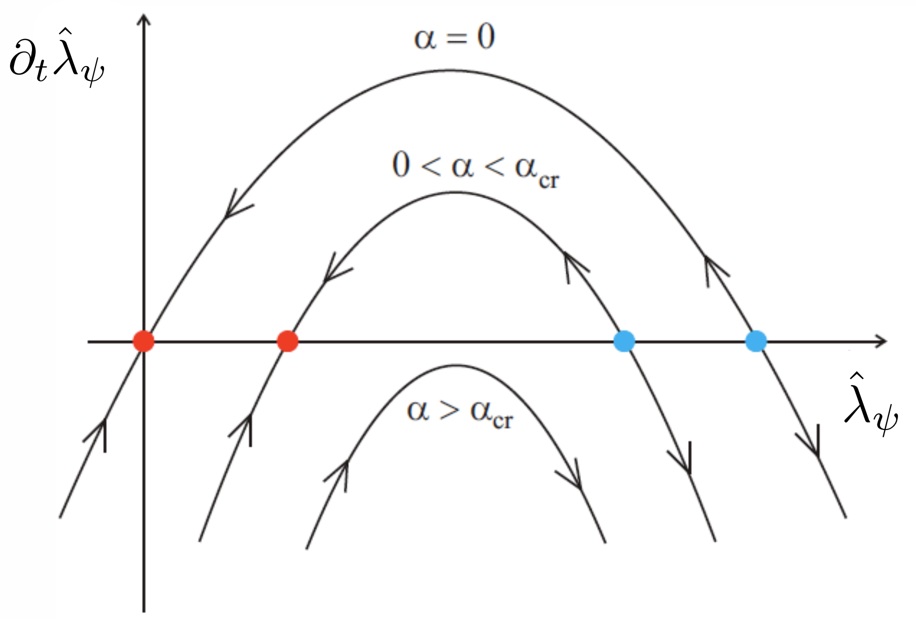

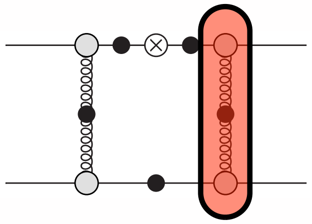

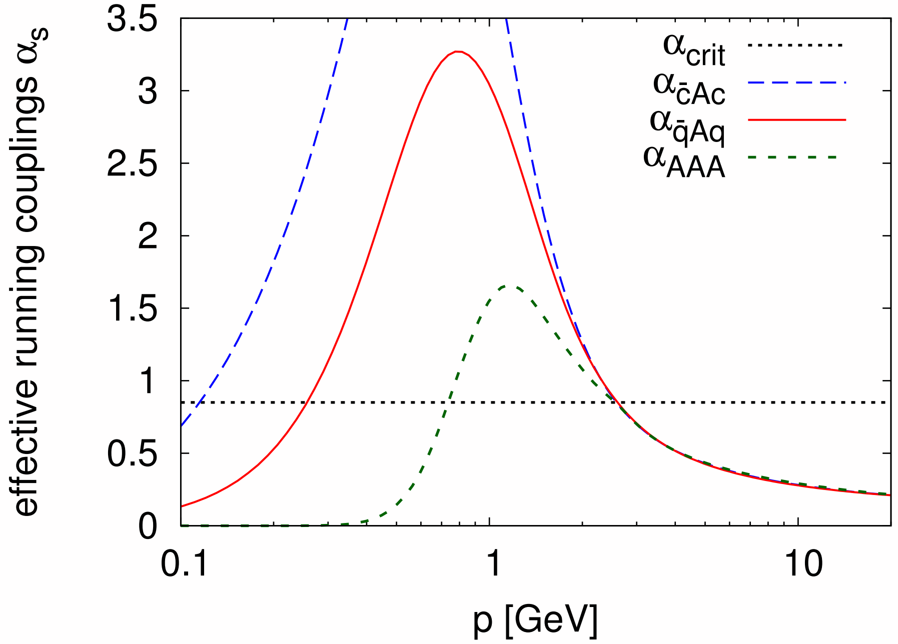

Mitter, JMP, Strodthoff '14

Braun, Fister, Haas, JMP, Rennecke '14

Confinement & symmetry breaking

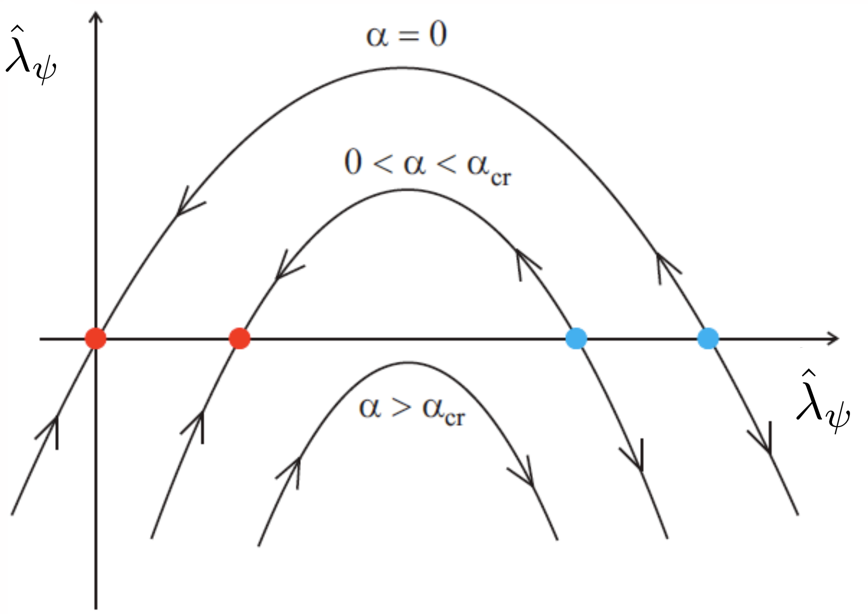

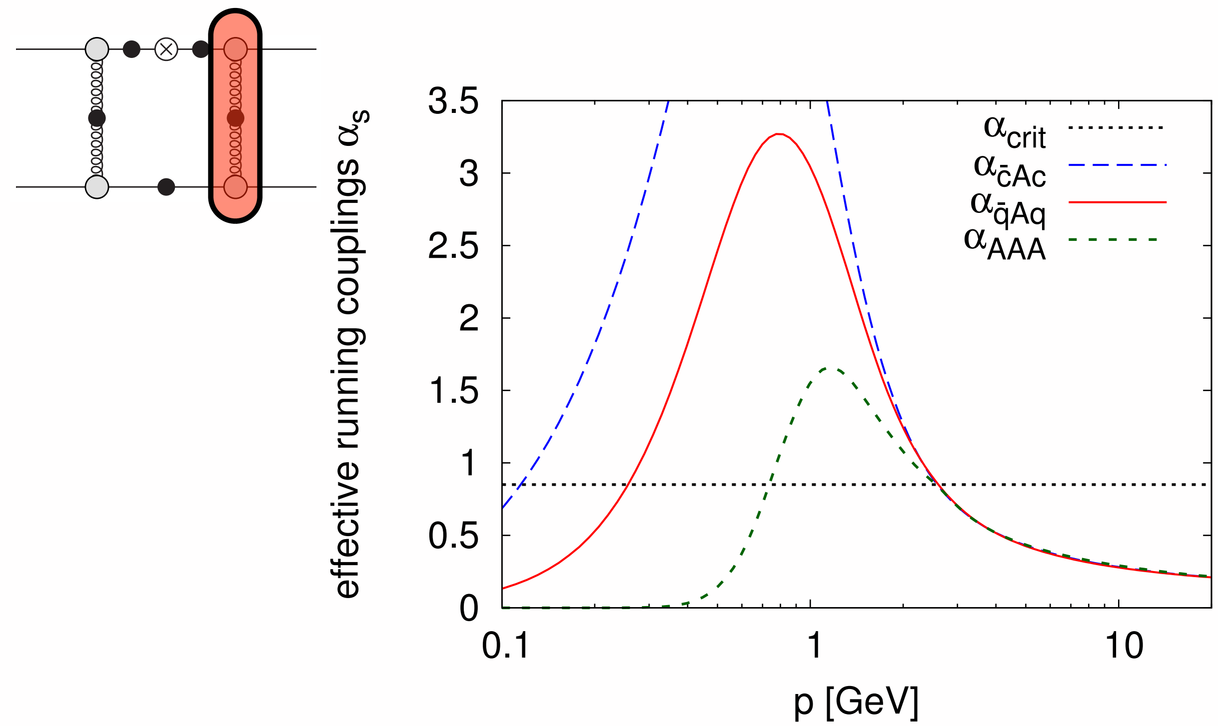

Mitter, JMP, Strodthoff '14

Braun, Fister, Haas, JMP, Rennecke '14

dynamical correlation of confinement
and
chiral symmetry breaking

confinement	**chiral symmetry breaking**
gluon propagator **gapped relative to** **ghost propagator**	**gluon propagator** **not gapped too much**

Fister, Mitter, JMP, Strodthoff '14

Confinement

FRG: Braun, Gies, JMP, PLB 684 (2010) 262

FRG, DSE, 2PI: Fister, JMP, PRD 88 (2013) 045010

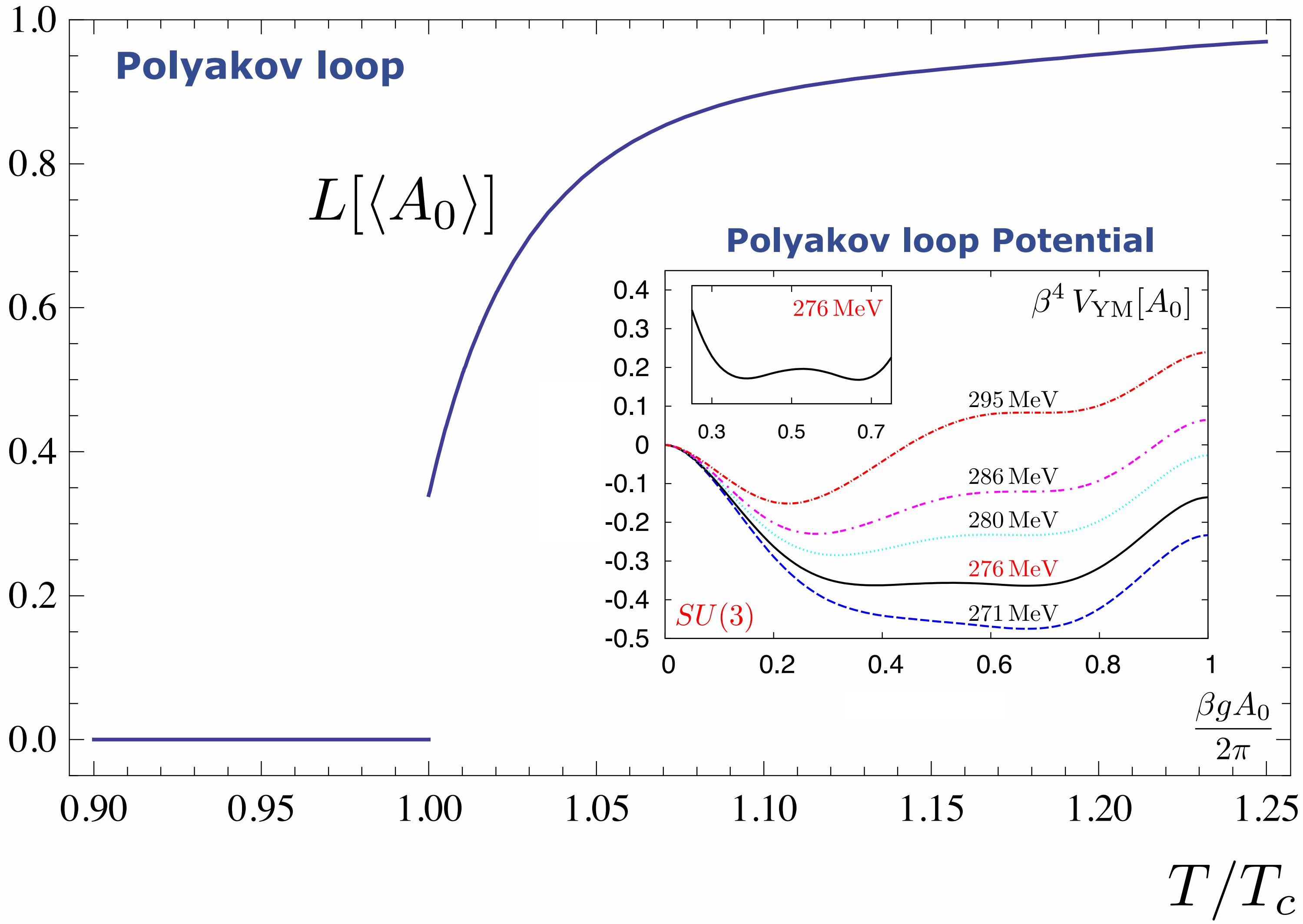

$$T_c/\sqrt{\sigma} = 0.658 \pm 0.023$$

$$\text{lattice}: T_c/\sqrt{\sigma} = 0.646$$

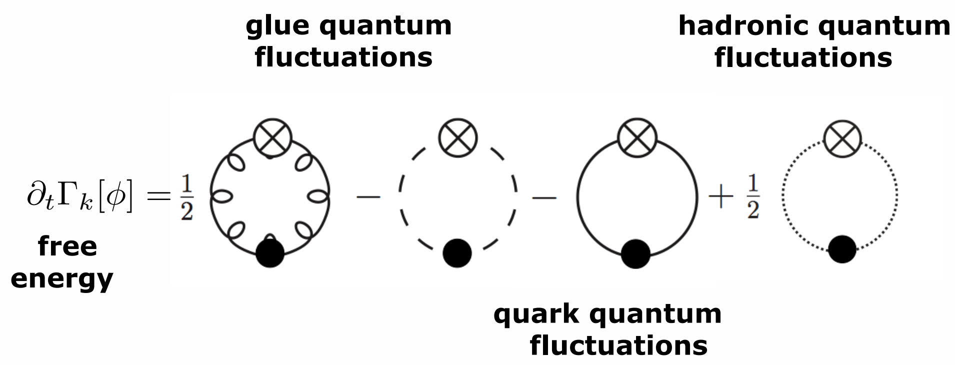

Confinement

FRG: Braun, Gies, JMP, PLB 684 (2010) 262

FRG, DSE, 2PI: Fister, JMP, PRD 88 (2013) 045010

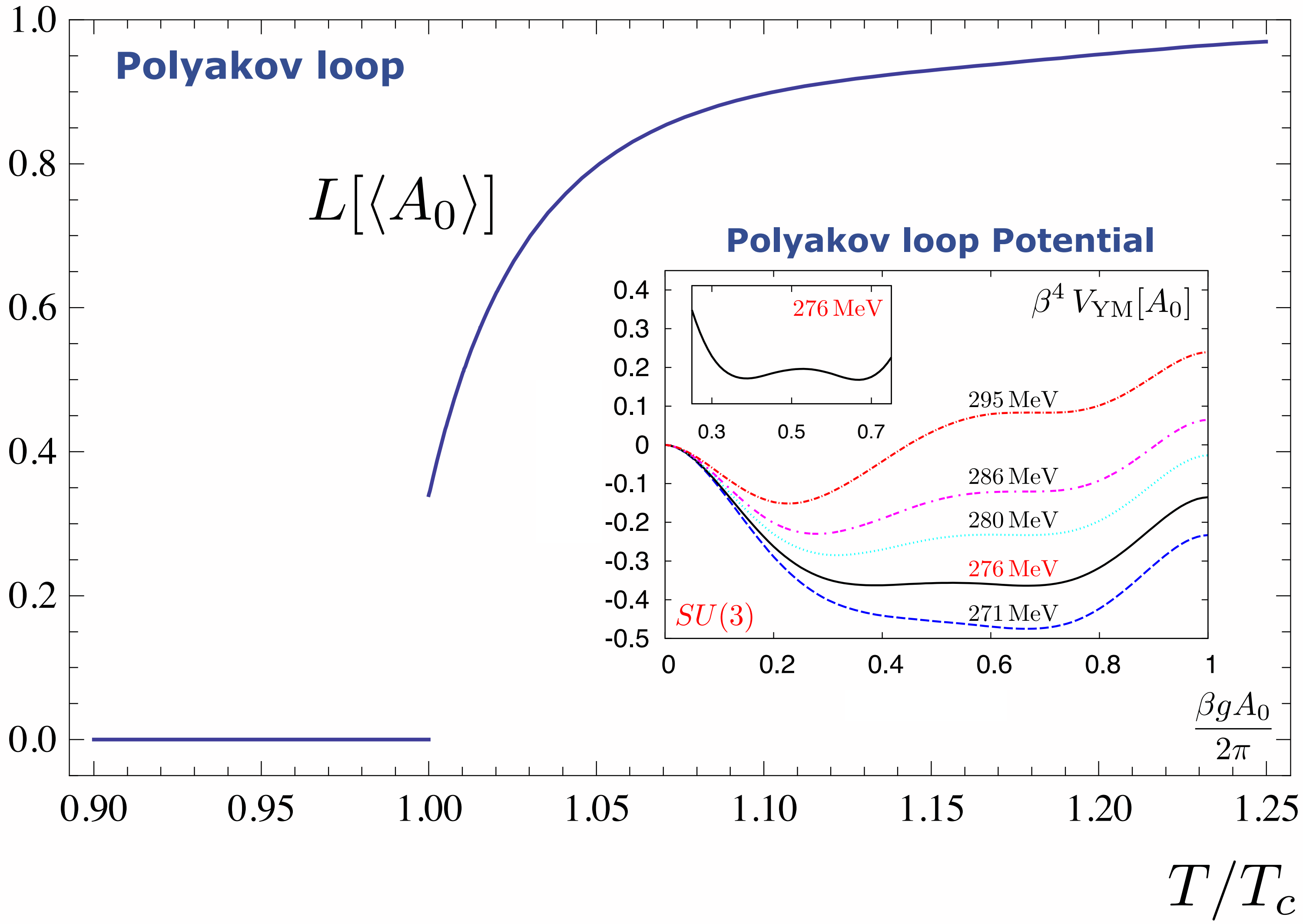

$$T_c/\sqrt{\sigma} = 0.658 \pm 0.023$$

$$\text{lattice}: T_c/\sqrt{\sigma} = 0.646$$

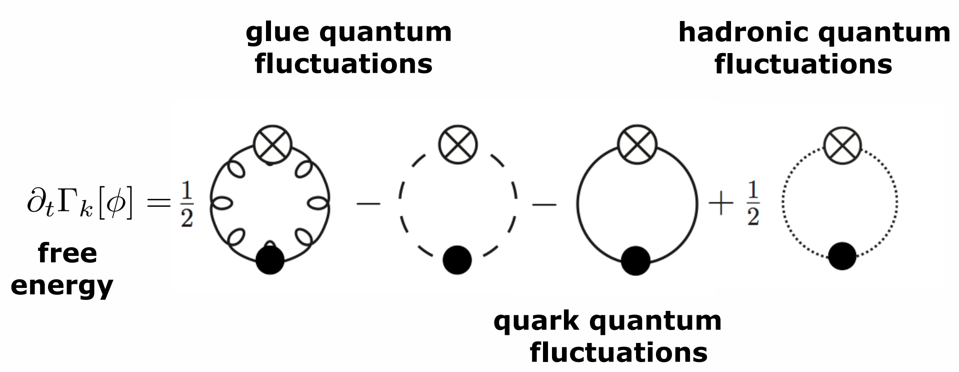

confinement

gluon propagator
gapped relative to
ghost propagator

Braun, Gies, JMP '07
Marhauser, JMP '08
Fister, JMP '13

Confinement

FRG: Braun, Gies, JMP, PLB 684 (2010) 262

FRG, DSE, 2PI: Fister, JMP, PRD 88 (2013) 045010

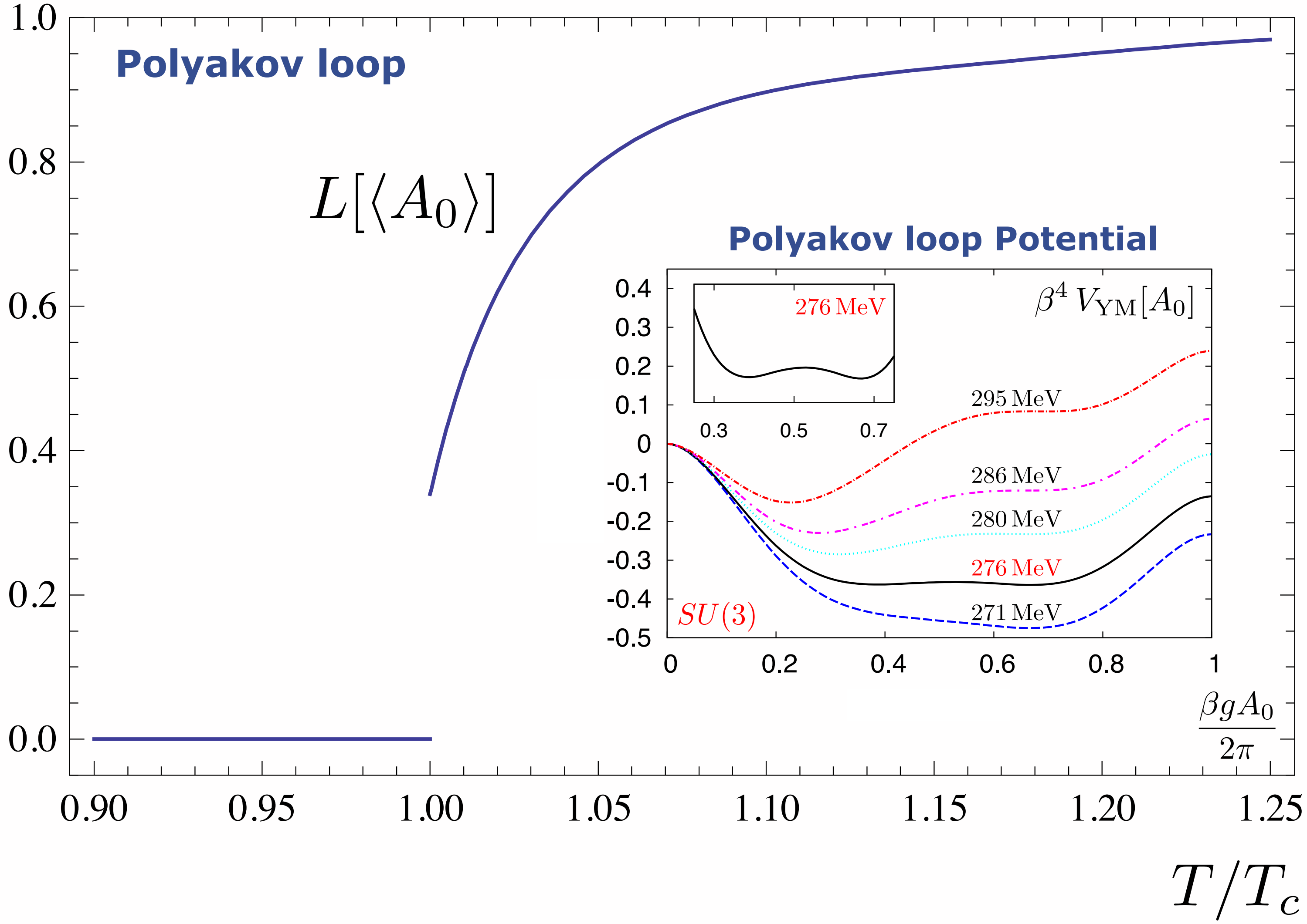

$$T_c/\sqrt{\sigma} = 0.658 \pm 0.023$$

$$\text{lattice}: T_c/\sqrt{\sigma} = 0.646$$

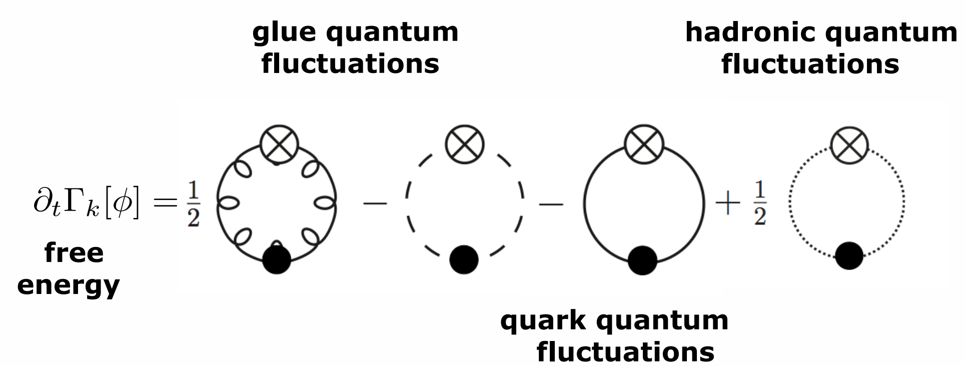

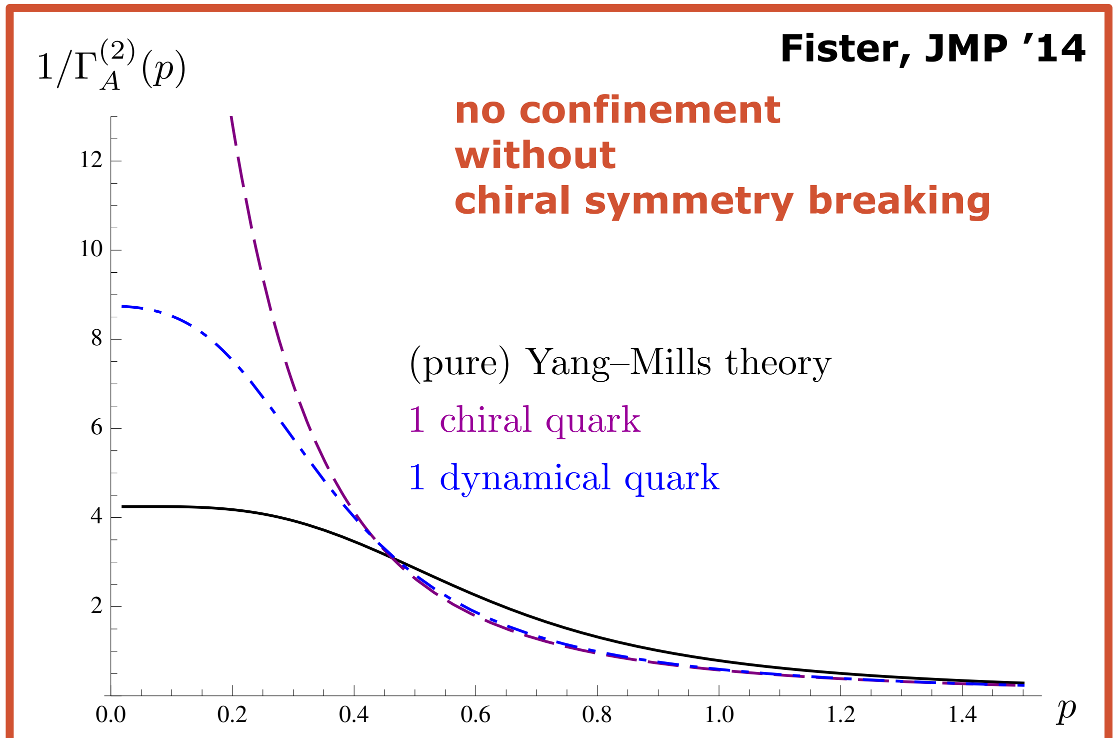

QCD

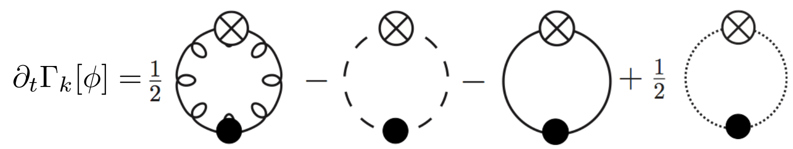

2 flavors & chiral limit

vanishing density

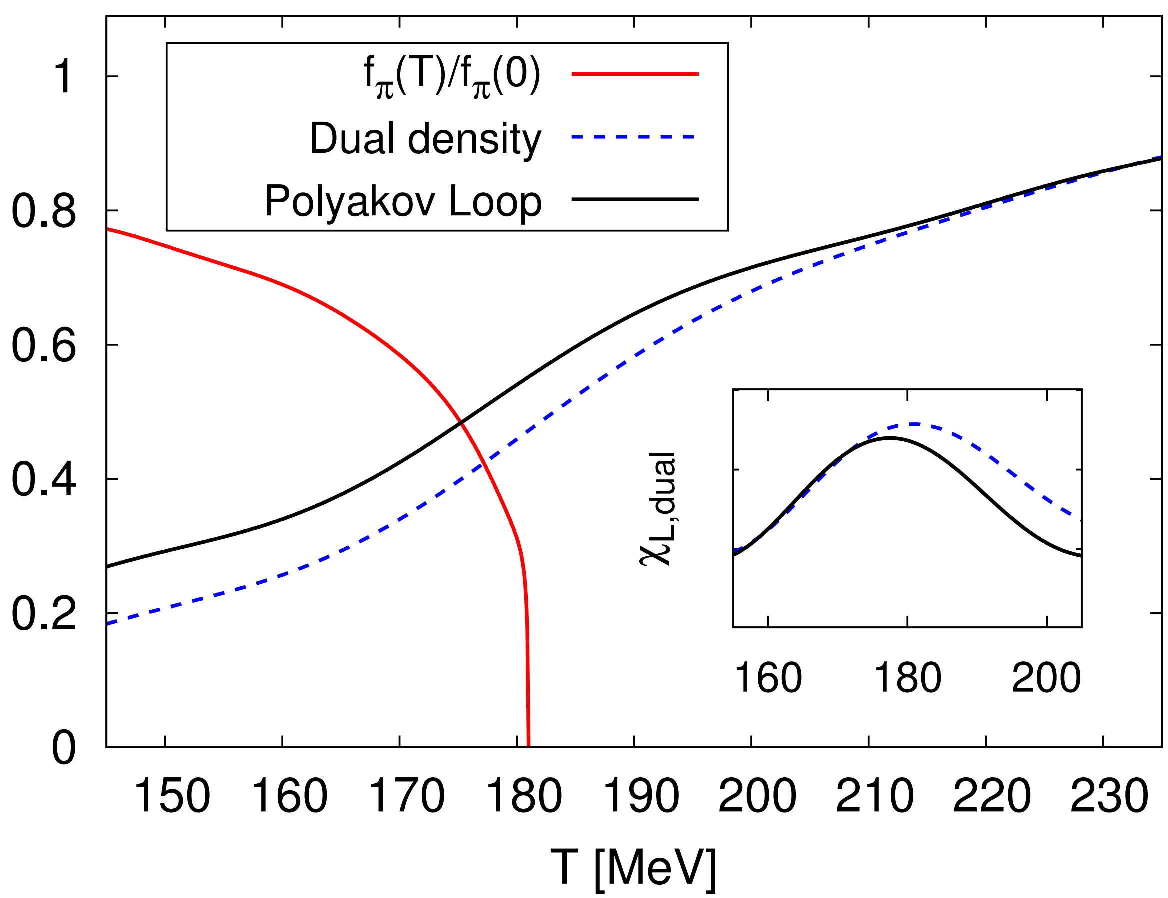

imaginary chemical potential

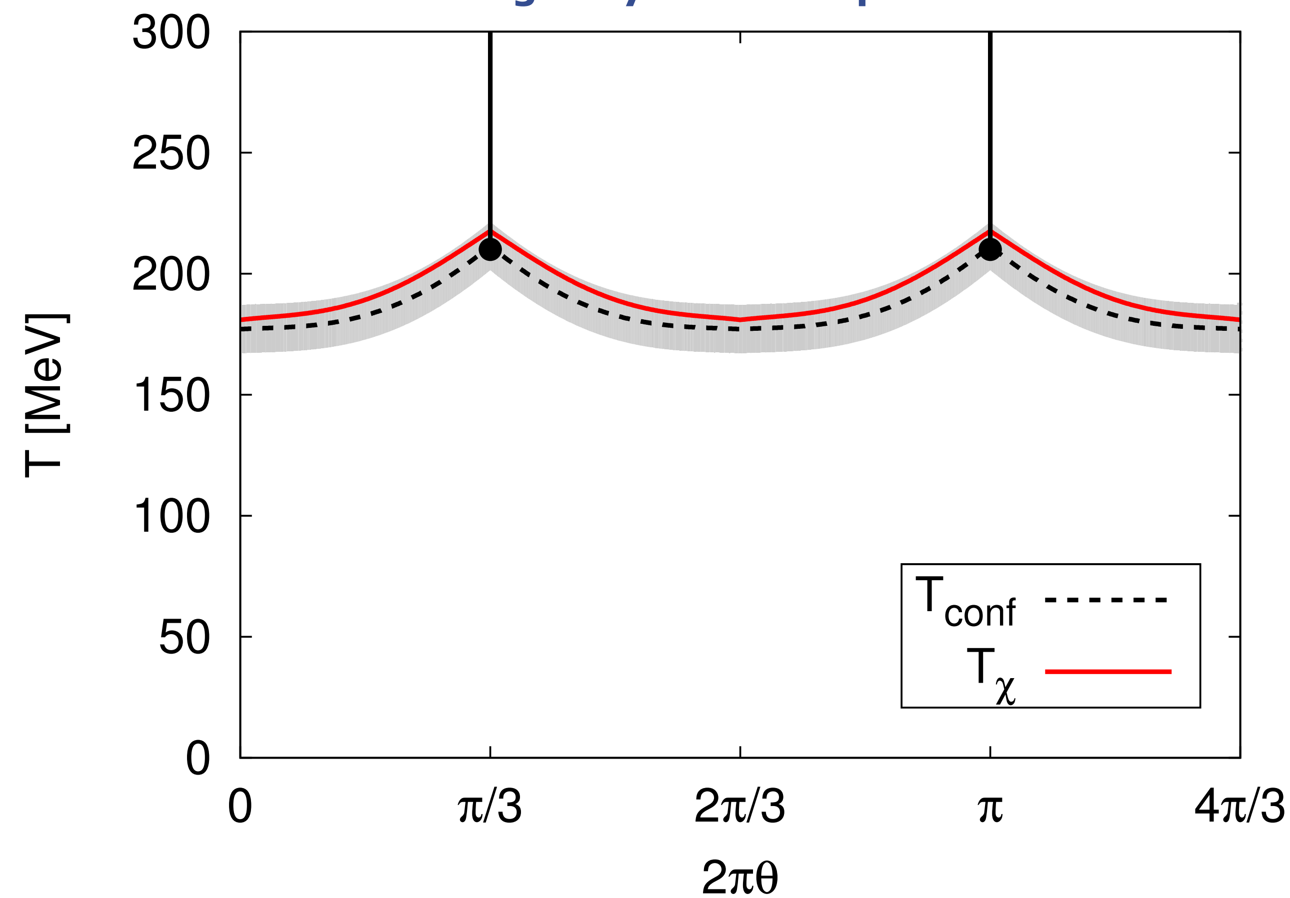

Braun, Haas, Marhauser, JMP, PRL 106 (2011) 022002